CHARACTERISATION OF THE MURINE IMMUNE RESPONSE TO SELF-AMPLIFYING MRNA SEQUENCES ENCODING HEPATITIS B VIRUS SURFACE PROTEINS

Nazia Samudh

A dissertation submitted to the Faculty of Health Sciences, University of the Witwatersrand, Johannesburg, in fulfilment of the requirements for the degree of Master of Science in Medicine (Haematology and Molecular Medicine)

Johannesburg, 2024.

DECLARATION

I, Nazia Samudh, declare that this dissertation is my own, unaided work. It is being submitted for the degree of Master of Science in Medicine (Haematology and Molecular Medicine) at the University of the Witwatersrand, Johannesburg. It has not been submitted before for any degree or examination at any other university.

_____

(Signature of candidate)

5th day of March 2024 in Johannesburg

PRESENTATIONS ARISING FROM THIS RESEARCH PROJECT

1. **'*In vitro* expression and innate immune response-stimulating capabilities of self-amplifying mRNA'.** Poster presented at the South African Immunology Society conference (September 2022) and Molecular Biosciences Research Thrust research day (December 2022) held in Johannesburg, South Africa.

2. **'Exploring self-amplifying mRNA:delivery, expression, and interferon responses'.** Poster presented by Dr. Kristie Bloom (supervisor), at the mRNA Process Development and Manufacturing summit (September 2022) held in Boston, USA.

PUBLICATIONS ARISING FROM THIS RESEARCH PROJECT

1. Kairuz, D., Samudh, N., Ely, A., Arbuthnot, P., Bloom, K., 2023. Production, Characterization, and Assessment of Permanently Cationic and Ionizable Lipid Nanoparticles for Use in the Delivery of Self-Amplifying RNA Vaccines. Pharmaceutics 15, 1173.

2. Kairuz, D., Samudh, N., Ely, A., Arbuthnot, P., Bloom, K., 2022. Advancing mRNA technologies for therapies and vaccines: An African context. Front. Immunol. 13, 1018961.

ABSTRACT

Vaccination against Hepatitis B virus (HBV) remains the most effective means of preventing infection. However, approximately 10% of vaccinated individuals fail to develop neutralising antibodies necessitating the development of improved vaccines which target the more immunogenic large HBV surface antigen (L-HBsAg) and can elicit cell-mediated immunity. Although Africa bears a high burden of HBV infections, placing many individuals at risk of contracting the disease, we rely on imported vaccines for prophylactic vaccination programmes. The COVID-19 pandemic was a stark reminder of Africa's vaccine dependence and since then great interest has been generated in establishing vaccine manufacturing capabilities on the African continent. Herein, we explored the Alphavirus-based self-amplifying RNA (saRNA) vaccine platform to produce dose-sparing HBV vaccines which could contribute to vaccine independence. saRNAs encoding reporter proteins, small HBV surface antigen (S-HBsAg) or L-HBsAg were synthesised by optimised *in vitro* transcription. Expression of reporter proteins from saRNAs was achieved even at low concentrations and was observed for extended periods of time *in vitro*. saRNAs encoding S-HBsAg were able to trigger the interferon response in a dose-response manner *in vitro*, however, this did not hamper antigen expression. Expression of L-HBsAg was achieved but restricted to the intracellular space and will require sequence modification to facilitate secretion. *In vivo* delivery of saRNAs by electroporation or commercially available cationic liposomes was found to be unsuccessful, and further optimisation of *in vivo* saRNA delivery is required before determining the prophylactic potential of candidate vaccines. This preliminary study has produced promising results demonstrating the dose-sparing properties and self-adjuvanting nature of the saRNA vaccine platform.

ACKNOWLEDGEMENTS

1. I would like to thank my supervisors Dr. Kristie Bloom, Dr. Kubendran Naidoo, and Prof. Patrick Arbuthnot from the Antiviral Gene Therapy Research Unit (AGTRU) for their invaluable insight, guidance, and support.
2. I would also like to acknowledge the support and advice from other members of the AGTRU team.
3. Finally, many thanks to the following providers of funding which made this research possible: University of the Witwatersrand Medical Faculty Research Endowment Fund and Postgraduate Merit Award, Poliomyelitis Research Foundation, and the South African Medical Research Foundation.

TABLE OF CONTENTS

LIST OF FIGURES

LIST OF APPENDIX FIGURES

APPENDIX A

APPENDIX B

APPENDIX C

LIST OF TABLES

LIST OF APPENDIX TABLES

Appendix B

Appendix C

LIST OF ABBREVIATIONS

APC	Antigen presenting cell
cccDNA	Covalently closed circular deoxyribonucleic acid
CSEs	Conserved sequence elements
DNA	Deoxyribonucleic acid
DOE	Design of experiments
dsRNA	Double-stranded ribonucleic acid
eGFP	Enhanced green fluorescent protein
ELISA	Enzyme-linked immunosorbent assay
EMCV	Encephalomyocarditis Virus
ER	Endoplasmic reticulum
Fluc	Firefly luciferase
GAPDH	Glyceraldehyde 3-phosphate dehydrogenase
HBV	Hepatitis B virus
HEK	Human Embryonic kidney
IFIT1	Interferon-induced proteins with tetratricopeptide repeats 1
IFN	Interferon
IL	Interleukin
IRES	Internal ribosome entry site
ISGs	Interferon-stimulated genes
IU	International units
IVT	*In vitro* transcription
L-HBsAg	Large Hepatitis B surface antigen
Luc2	Luciferase 2
MDA5	Melanoma-associated differentiation antigen 5
MERS CoV	Middle East respiratory syndrome coronavirus
M-HBsAg	Medium Hepatitis B surface antigen
MHC	Major histocompatibility complex
mRNA	Messenger ribonucleic acid
NMRI	Naval medical research institute
nsPs	Non-structural proteins
NTCP	Sodium taurocholate co-transporting peptide
NTP	Nucleotide triphosphate
OAS1	2’-5’- oligoadenylate synthetase 1

ORF	Open Reading Frame
PCR	Polymerase chain reaction
PDI	Polydispersity index
PKR	Protein kinase R
Poly I:C	Polyinosinic:polycytidylic acid
PRR	Pattern recognition receptor
qRT-PCR	Quantitative reverse transcription PCR
RIG-I	Retinoic-acid inducible gene I product
RNA	Ribonucleic acid
RPRP	RNA dependent RNA polymerase
rRNA	Ribosomal RNA
saRNA	Self-amplifying RNA
SARS-CoV-2	Severe acute respiratory syndrome coronavirus 2
S-HBsAg	Small Hepatitis B surface antigen
ssRNA	Single-stranded RNA
TLR	Toll-like receptor
TM	Transmembrane
VEEV	Venezuelan equine encephalitis virus

1. INTRODUCTION

1.1 Epidemiology and transmission of Hepatitis B Virus (HBV)

HBV is the aetiological agent responsible for most virus-associated hepatitis mortalities worldwide (World Health Organisation, 2021). Infection with HBV occurs in most areas in the world with Asia and Africa being the most affected regions (World Health Organisation, 2021). Globally there are approximately 296 million chronically infected individuals who may benefit from curative treatment (World Health Organisation, 2021). However, currently available treatments for chronic infections are non-curative and aim to achieve viral suppression and prevent disease progression (reviewed in Zoulim and Durantel, 2015). Late diagnosis and limited access to treatment in certain endemic regions are factors that contribute to development of HBV-associated complications, such as cirrhosis and hepatocellular carcinoma, for which the prognosis is poor (reviewed in Nayagam and Thursz, 2019). In addition, individuals chronically infected with HBV are at risk for superinfections with hepatitis D virus, which accelerates progression of the disease (Smedile et al., 1981). As such, HBV-associated mortality has steadily increased over the past years, even surpassing the mortality rates of TB, HIV and malaria (World Health Organisation, 2017). In 2019 alone 820 000 individuals died because of HBV-related illnesses (World Health Organisation, 2021). This highlights the need for improved therapeutic treatments as well as measures aimed at preventing transmission of HBV.

HBV is transmitted through contact with infected bodily fluids. In highly endemic areas, perinatal transmission from infected mothers to their newborns, and horizontal transmission from infected to uninfected children under the age of five are the predominant modes of transmission (World Health Organisation et al., 2017). HBV infection in early childhood is associated with a 90% risk of developing chronic hepatitis by adulthood (Edmunds et al., 1993). Individuals in endemic regions and healthcare workers are also at high risk of infection as a result of increased exposure to infected bodily fluids (reviewed in Franco et al., 2012). Transfusion of contaminated blood products and the use of contaminated needles also account for new infections in low-income countries with high endemicity.

1.2 Molecular biology of HBV

HBV is a partially double-stranded DNA virus belonging to the *Hepadnaviridae* family of hepatotropic viruses (reviewed in Datta et al., 2012). The viral particle, also known as a Dane particle, is spherical, and 42 nm in diameter (Dane et al., 1970). Its relatively small 3.2 kilobase (kb) genome is efficiently organised into four overlapping open reading frames (ORFs) i.e.,

Core, Polymerase, Surface, and X ORFs (reviewed in Datta et al., 2012). Its DNA is contained within an icosahedral nucleocapsid which is surrounded by an envelope that is derived from host cell lipids in which three related viral surface antigens are embedded. These surface antigens are encoded by a single ORF (Surface ORF) containing three in-frame translation initiation codons from which translation of large (L-HBsAg), medium (M-HBsAg) and small (S-HBsAg) surface antigen is initiated. Initial attachment of virions to target cells is mediated by electrostatic interactions between surface antigens and heparan sulphate proteoglycans found on hepatocytes (Sureau and Salisse, 2013). Subsequently, the virus is endocytosed following highly specific interactions between L-HBsAg and the sodium taurocholate co-transporting polypeptide (NTCP), which is a bile acid transporter expressed by hepatocytes (Yan et al., 2012). These surface antigens, which mediate infectivity, have thus been the target of many prophylactic vaccines which successfully prevent infection in most individuals.

Upon entry into hepatocytes, the nucleocapsid is uncoated and transported to the nucleus (reviewed in Datta et al., 2012). Synthesis of the partial DNA strand is completed within the nucleus and episomal viral DNA with a covalently closed circular DNA (cccDNA) conformation is established. This viral replication intermediate drives production of progeny virus which are subsequently assembled and secreted from the host cell. In addition to infectious virions, subviral particles consisting mainly of S-HBsAg with trace amounts of L-HBsAg and devoid of the nucleocapsid are also produced during HBV infection (Heermann et al., 1984). These particles are initially filamentous in nature and formed by oligomerisation of surface antigens in the endoplasmic reticulum (ER) (Patient et al., 2007). Filaments are thereafter reduced to 20 nm spherical particles which are secreted into the bloodstream in excessive amounts compared to infectious virions. Secretion of such large amounts of S-HBsAg is thought to be a decoy mechanism employed by the virus to inundate the adaptive immune system allowing infectious virions to escape neutralisation (Rydell et al., 2017). Interestingly, S-HBsAg is the primary immunogen included in current HBV prophylactic vaccines.

1.3 HBV surface antigen structure and immunogenicity

All three HBV surface antigens are encoded by the same ORF with translation initiating at different in-frame start codons (Figure 1A) (reviewed in Ho et al., 2020). Thus, all three proteins share a common C-terminal domain with different N-termini (Figure 1B). S-HBsAg is the smallest of the three surface antigens and consists of 226 amino acids and four transmembrane (TM) domains. This entire amino acid sequence, also known as the S domain, is also present in M-HBsAg and L-HBsAg. Co-translational insertion of S-HBsAg into the ER results in a

complex topological arrangement of the protein which plays an important part in antigenicity, viral particle formation and infectivity (Figure 1C). Insertion of TM1, which includes a signal sequence, results in translocation of a short upstream N-terminal sequence into the ER lumen. Insertion of TM2 and TM3 produces a short internal cytosolic loop followed by a larger external loop. The external loop contains eight cysteine residues which form disulphide bonds, maintaining the loop in a specific configuration to produce the highly immunogenic conformational epitope known as the 'a' determinant. The 'a' determinant also forms part of a heparan binding site which is necessary for attachment to hepatocytes and thus, vital to infectivity (Sureau and Salisse, 2013). An asparagine residue located in the external loop (N146) serves as a glycosylation site for approximately half of all S-HBsAg monomers found on viral particles. This glycosylation is essential for maturation and release of infectious viral particles (Lu et al., 1995). Viral particle formation is mediated by dimerisation of surface antigen monomers which are held together by intermolecular disulphide bridges formed between the S-domains of individual monomers (Wounderlich and Bruss, 1996; Suffner et al., 2018). The expression of S-HBsAg alone is sufficient for subviral particle formation and is not dependent on glycosylation (Lu et al., 1995).

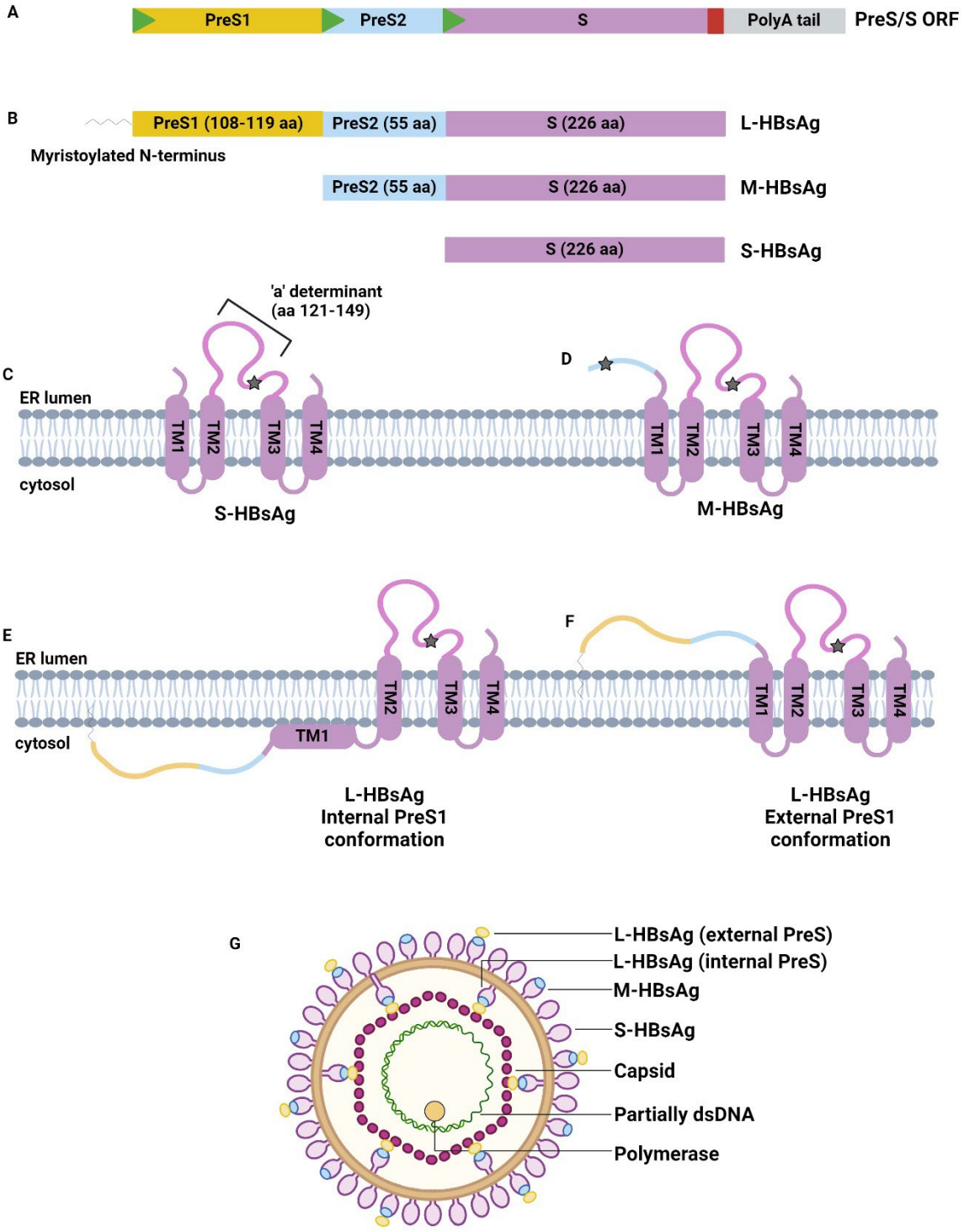

Figure 1. Comparison of HBV surface antigen domains and conformation.

(A) The open reading frame (ORF) for HBV surface antigens contains three in-frame start codons (green triangles), a common stop codon (red rectangle), and poly-A tail. This results in three different surface antigens (L-HBsAg, M-HBsAg and S-HBsAg) which share the same C-

terminal domain but differ in their N-termini. **(B)** Comparison of HBV surface antigen domains and amino acid (aa) length. **(C and D)** Topological conformations of S-HBsAg and M-HBsAg following synthesis at the endoplasmic reticulum (ER). The highly immunogenic 'a' determinant is formed by aa 121-149. N-glycosylation sites are indicated by black stars. **(E)** Retention of PreS1, PreS2 and part of the S domain in the cytosol. **(F)** Post-translational translocation of PreS1, PreS2 and part of the N-terminus into the ER lumen and insertion of TM1 into the ER membrane resulting in external presentation of PreS domains. **(G)** Structure of assembled virion depicting surface antigens, L-HBsAg interaction with capsid, viral polymerase and DNA. Created using BioRender.com.

M-HBsAg is identical to S-HBsAg except for an additional N-terminal sequence known as the PreS2 domain (Figure 1D). The PreS2 domain consists of 55 amino acids which are also translocated into the ER lumen and contains a conserved glycosylated asparagine residue (N4) required for M-HBsAg secretion (Werr and Prange, 1998). Like S-HBsAg, M-HBsAg is also capable of subviral particle formation and secretion as well as immune stimulation to produce neutralising antibodies directed against PreS2 epitopes (Cheng and Moss, 1987).

L-HBsAg is the perhaps the most complex of the three surface antigens displaying dual topology with distinct functions (Bruss et al., 1994). In addition to the PreS2 and S domains, an additional 108, 118, or 119 (genotype dependent) N-terminal amino acids make up the PreS1 domain specific to L-HBsAg. An important feature of the PreS1 domain is myristoylation of glycine-2 which is essential for infectivity (Gripon et al., 1995; Persing et al., 1987). This lipid modification occurs in the cytosol and enables interaction with the ER membrane. Translation of the PreS1 domain prevents insertion of TM1 into the ER (Bruss et al., 1994). Instead, L-HBsAg is anchored in the membrane by TM2-4 resulting in the cytosolic disposition of the PreS1, PreS2 and a portion of the S domain (Figure 1E). This conformation is necessary for binding to the capsid and promotes virion formation (Bruss and Vieluf, 1995). Half of L-HBsAg monomers synthesised will subsequently undergo a conformational change resulting in insertion of TM1 into the lipid membrane and post-translational translocation of PreS1, PreS2 and the first seven amino acids of the S domain to the surface of the mature virion (Figures 1F and G). This topological change is necessary to mediate binding to NTCP and entry into hepatocytes. When expressed on its own, L-HBsAg monomers oligomerise forming 20 nm particles with the PreS1, PreS2 domain in the external conformation (Xu et al., 1997). However, unlike S-HBsAg and M-HBsAg subviral particles, L-HBsAg particles are not secreted but rather retained in a pre-Golgi compartment. The PreS1 domain contains multiple highly

immunogenic epitopes capable of eliciting broad neutralising B-cell responses and well as strong T-cell responses (Ferrari et al., 1992, 1989; Maeng et al., 2000; Milich et al., 1987; Yato et al., 2021).

1.4 Prophylactic vaccines against HBV

Since the 1980s, global efforts to curb the transmission of HBV by implementation of immunisation programs have averted an estimated 210 million infections amongst children (reviewed in Nayagam and Thursz, 2019). A sombre testament to the success of HBV immunisation programs is the fact that 93% of individuals succumbing to the disease are older than the age of 30 and thus were infected prior to the wide-spread availability of HBV vaccines (World Health Organisation et al., 2017). Despite being a vaccine preventable disease, approximately 1.5 million new HBV infections were reported in 2019, with the WHO African region accounting for 66% of these new infections (World Health Organisation, 2021). Although vaccine coverage has increased in children under the age of five, birth dose immunisations which can reduce mother-to-child transmission, remains unacceptably low.

1.4.1 Protein-based vaccines

First generation HBV vaccines were composed of non-infectious sub-viral particles extracted from plasma of asymptomatic HBV-carriers (reviewed in Stephenne, 1990). Safety concerns over the use of blood-derived products for prophylactic vaccination, limitations in supply of plasma, and increased costs associated with extraction and purification of blood-derived subviral particles led to the rapid development of second-generation vaccines which were developed using recombinant DNA technology and yeast expression systems (reviewed in Stephenne, 1990; McAleer et al., 1984). Most currently licensed HBV vaccines, such as Engerix-B (GlaxoSmithKline Biologicals, UK) and Recombivax HB (Merck & Co, USA), are second-generation vaccines composed of recombinant S-HBsAg particles similar to blood-derived subviral particles. Following immunisation, S-HBsAg particles are phagocytosed by antigen presenting cells (APCs), processed into antigen fragments, and presented in association with the Major Histocompatibility Complex II (MHC II) to induce a humoral immune response against the antigen. These protein-based vaccines require formulation with adjuvants, such as aluminium hydroxide, to stimulate antigen-specific helper T cells into producing Th2 type cytokines, such as interleukin (IL) 4 and 5 (Brewer et al., 1999). These cytokines, when present in high concentrations, support the development of a humoral immune response mediated by potent neutralising antibodies against S-HBsAg (reviewed in Shouval, 2003). Seroprotection conferred by these vaccines is considered optimal at antibody titres in excess of 100 IU/L and

is observed in approximately 90-95% of healthy vaccinees following a 3-dose (20 µg each) intramuscularly administered regimen (reviewed in Roukens and Visser, 2011). This type of HBV vaccine has been in use for almost four decades and contributed immensely to the decrease in new infections (reviewed in Nayagam and Thursz, 2019).

Although second-generation HBV vaccines are safe, efficient, and widely accepted, there are some limitations and thus room for improvement. From a manufacturing perspective, S-HBsAg is not capable of forming subviral particles following translation within the yeast cell and is thus retained intracellularly (Lünsdorf et al., 2011). This necessitates lysis of cells and extensive downstream processing to obtain immunogenic subviral particles. In addition, native glycosylation patterns, which enhance uptake and presentation of surface antigen by APCs, are absent in yeast-derived HBV vaccines (reviewed in Dobrica et al., 2020; Hyakumura et al., 2015). A concerning shortcoming of second-generation vaccines is that approximately 10% of vaccinees fail to develop protective antibody titres following the primary series of immunisations (reviewed in Roukens and Visser, 2011). These individuals, referred to as non-responders, remain at high risk of contracting HBV. Reasons behind vaccine non-responsiveness are thought to be related to age, chronic conditions, genetic predisposition, immunodeficiencies or immunosuppressive treatments (reviewed in Walayat et al., 2015). Increasing the antigen concentration (40 µg), immunising via the intradermal route, or including more immune-stimulatory adjuvants in vaccine formulations have shown promise in seroconverting a fraction of non-responders (reviewed in Walayat et al., 2015). However, to achieve seroconversion in individuals who are incapable of MHC II presentation of S-HBsAg as a result of their genetic predisposition, will require immune stimulation by alternative HBV surface epitopes found on L-HBsAg and M-HBsAg.

More recently, a new and improved yeast-expressed recombinant S-HBsAg vaccine, Heplisav-B® (Dynavax Technologies, USA), entered the market. This vaccine takes advantage of the innate immune system-stimulating properties of the single-stranded synthetic DNA oligonucleotide cytidine-phosphate-guanosine oligodeoxynucleotide, to activate toll-like receptor (TLR) 9 and elicit a cell-mediated or Th1-type immune response (Halperin et al., 2012). This cellular immune response is characterised by the production of interferon gamma (IFN-γ), tumour necrosis factor-beta and IL-2, and is effective against intracellular pathogens (reviewed in Romagnani, 1999). In addition to cell-mediated immunity, two-doses (20 µg/dose) of Heplisav-B® elicited earlier and greater seroprotection in individuals compared to three-dose Engerix-B vaccine.

Mammalian cell expression systems have also been explored to produce HBV subviral particles and address the limitations posed by yeast-derived vaccines. This platform ensures that antigens are folded in their native conformation bearing the correct post-translational modifications. These characteristics are difficult to achieve using yeast expression systems but are vital to the development of robust and protective immune responses. The licensed third-generation vaccine, Prehevbrio™ (VBI Vaccines, USA), is produced in Chinese Hamster Ovarian cells and consists of antigenic particles predominantly composed of S-HBsAg, as well as small quantities of L-HBsAg and M-HBsAg, with native glycosylation patterns (Shouval et al., 1994). These particles are adsorbed to the adjuvant aluminium hydroxide which promotes a Th2-biased immune response. Compared to yeast-derived vaccines, Prehevbrio™ has been shown to elicit rapid and higher seroconversion rates following a single 10 μg priming dose (Shapira et al., 2001). In addition, Prehevbrio™ has demonstrated remarkable capability in circumventing vaccine non-responsiveness (reviewed in Shouval et al., 2015). A similar candidate vaccine incorporating all three HBV surface antigens and produced in Chinese Hamster Ovarian cells is CVI-HBV-002 (NCT04289987). In contrast to Prehevbrio™, this candidate vaccine is formulated with the Th1-stimulating adjuvant L-PAMPO which is composed of a lipopeptide and synthetic double-stranded RNA (dsRNA) to elicit a cell-mediated immune response (Yum et al., 2012).

1.4.2 DNA and conventional mRNA-based vaccines

Improvements to HBV vaccines by increasing the breadth of immune protection and recruiting cell-mediated immunity have been explored and achieved by the above-mentioned platforms. While yeast expression systems are cost-effective and easy to upscale, they lack the ability to mediate post-translational modifications to the antigen and require additional processing to extract the antigen. Mammalian cell expression systems overcome these drawbacks, however, it can be difficult to establish the platform, as well as costly to upscale vaccine production. Nucleic acid-based vaccines provide an alternative approach by enabling *in vivo* translation of viral antigens following delivery of antigen-encoding nucleic acids into target cells. Thus, the requirement for costly protein expression systems, cell culture, extraction and purification of the antigen is circumvented, while correct post-translational modifications and folding of the antigen is achieved (reviewed in Leitner et al., 1999). In addition to whole antigens, multiple immunogenic epitopes from different proteins, immune-stimulatory molecules or sequences can be encoded in nucleic acid vaccine constructs which makes it a highly versatile platform. *In vivo* expression of antigens also results in proteasomal processing and presentation of antigenic peptides by MHC I and II (professional APCs only) to promote both humoral and

cell-mediated immune responses. Early efforts to develop nucleic acid vaccines and therapies focused mainly on DNA strategies, however difficulties in achieving nuclear delivery, safety concerns, and poor efficacy in early human clinical trials hampered this approach (reviewed in Ferraro et al., 2011). The development of *in vivo* electroporation techniques for DNA vaccine delivery provided a much-needed breakthrough to the field. This improved DNA uptake, antigen expression, antigen-specific immune responses, and localised inflammatory responses (Luxembourg et al., 2006; Babiuk et al., 2007; De Pooter et al., 2021).

Recently, advances in mRNA synthesis, stabilisation, immune modulation and delivery have brought the mRNA vaccine platform to the forefront of vaccine development (reviewed in Kairuz et al., 2022). mRNAs are produced from antigen-encoding plasmid DNA templates using a simple and efficient cell-free *in vitro* transcription (IVT) technique. Synthetic mRNAs are complexed with lipid-based delivery systems to facilitate uptake by target cells which then produce the encoded antigen to elicit an immune response. The advantages of using mRNA over DNA are immediate with transient expression of the antigen in the cytosol without the need to cross the nuclear envelope. Importantly, there is no risk of mRNA integration into the host genome. mRNAs can also be produced rapidly in response to disease outbreaks and manufacturing is scalable.

The benefits and efficacy of this platform have been showcased with the rapid development of multiple, highly effective vaccines against SARS-CoV-2 during the Covid-19 pandemic. While both mRNA and recombinant protein SARS-CoV-2 vaccines can elicit high levels of neutralising antibodies, mRNA vaccines are able to induce a significantly greater cellular immune response which is important in eliminating intracellular pathogens (Wu et al., 2022). Thus, mRNA-based HBV vaccines could provide both prophylactic and therapeutic benefits and could be used to treat chronically infected individuals. Currently, the mRNA platform is being used to develop vaccines against a variety of infectious diseases and cancers, including personalised cancer vaccines (reviewed in Kairuz et al., 2022). mRNA technology is not restricted to vaccine development. This versatile platform is also being used to develop immunotherapies, gene editing tools and protein replacement therapies, many of which are already in clinical trials.

1.4.3 Alphavirus-based saRNA vaccines

Production of mRNA vaccines requires expensive raw materials such as modified nucleotides, cap analogues or capping enzymes, and purification under stringent processes. Considering that transient antigen expression requires large amounts of mRNA per dose to elicit an effective

immune response, manufacturing costs can be high and thus, represents a bottleneck for developing African countries when trying to achieve vaccine independence. In this regard, self-amplifying RNA (saRNA) vaccines provide an attractive alternative to conventional mRNA vaccines. This highly sophisticated next generation vaccine platform exploits the self-replicating properties of alphaviruses, such as Venezuelan Equine Encephalitis viruses (VEEV), to enable *in situ* replication of mRNA sequences encoding vaccine antigens. This allows for delivery of lower amounts of mRNAs to achieve protective immune responses (Vogel et al., 2018).

Alphaviral genomes are single-stranded positive sense RNAs, which contain two ORFs that are separated by a sub-genomic promoter sequence (Figure 2A) (reviewed in Leung et al., 2011). The upstream ORF encodes a polyprotein that is cleaved to produce four non-structural proteins (nsPs 1-4). These proteins form an RNA-dependent RNA polymerase (RDRP) complex, which mediates self-replication and capping of genomic and sub-genomic RNAs. The downstream ORF is under transcriptional control of the sub-genomic promoter and encodes another polyprotein which is cleaved to produce viral structural proteins. The ORFs are flanked by untranslated conserved sequence elements (CSEs) which, together with nsPs 1-4, are indispensable for *in situ* self-propagation of viral RNAs. Both genomic and sub-genomic RNAs are capped at the 5'end with a cap 0 structure and polyadenylated at the 3' end (reviewed in Hyde et al., 2015). A cap 0 structure is an N7-methyl guanosine that is attached to the 5' end of nascent eukaryotic mRNAs in a reverse orientation through a 5'-5' triphosphate link to prevent degradation by 5'-3' exonucleases, and to recruit translation machinery (reviewed in Ramanathan et al., 2016). Eukaryotic mRNAs also have a 3' homopolymeric stretch of adenine nucleotides known as a poly-A tail, which is required for increasing the longevity of mRNA transcripts and ensuring efficient translation (reviewed in Passmore and Coller, 2022). These structural similarities of Alphaviral RNAs to endogenous eukaryotic mRNAs contribute to the efficient translation of viral RNAs. saRNA vaccine constructs based on Alphaviral genomes contain the same sequences, except genes that code for the viral structural proteins are replaced by sequences encoding the antigen of interest (Figure 2B) (Fleeton et al., 2001). Synthesis of saRNAs is achieved using the same IVT techniques employed in conventional mRNA synthesis without the requirement for costly modified nucleotides as well as the stringent purification methods to eliminate immunogenic dsRNA contaminants (reviewed in Kairuz et al., 2022). Transcripts can be capped co-transcriptionally or post-translationally with either a cap 0 or cap 1 structure. Methylation of the 2'-O site of the first nucleotide adjacent to the cap 0 structure produces a cap 1 structure to distinguish between mature endogenous mRNAs and viral mRNAs

(reviewed in Ramanathan et al., 2016). Upon delivery into the cytosol, nsPs are translated and complementary negative sense RNAs are transcribed (Figure 2C) (reviewed in Leung et al., 2011). This serves as a template from which positive sense RNAs and exponential amounts of subgenomic RNA encoding the antigen of interest is subsequently transcribed. Translated antigen is thereafter secreted for uptake by immune cells or can be designed for display on the surface of cells by inclusion of a C-terminal transmembrane domain sequence. Antigens can also be processed by the proteasome and the resulting peptides presented on MHC I molecules for recognition by T cells. saRNA vaccines, targeting a number of infectious diseases and cancers, have successfully elicited both humoral and cell-mediated immunity against the encoded antigen (reviewed in Kairuz et al., 2022). However, T-cell immune responses against nsPs1-4, which could potentially elicit anti-vector immunity and reduce efficacy of Alphaviral-based saRNA vaccines administered subsequently, have not yet been explored.

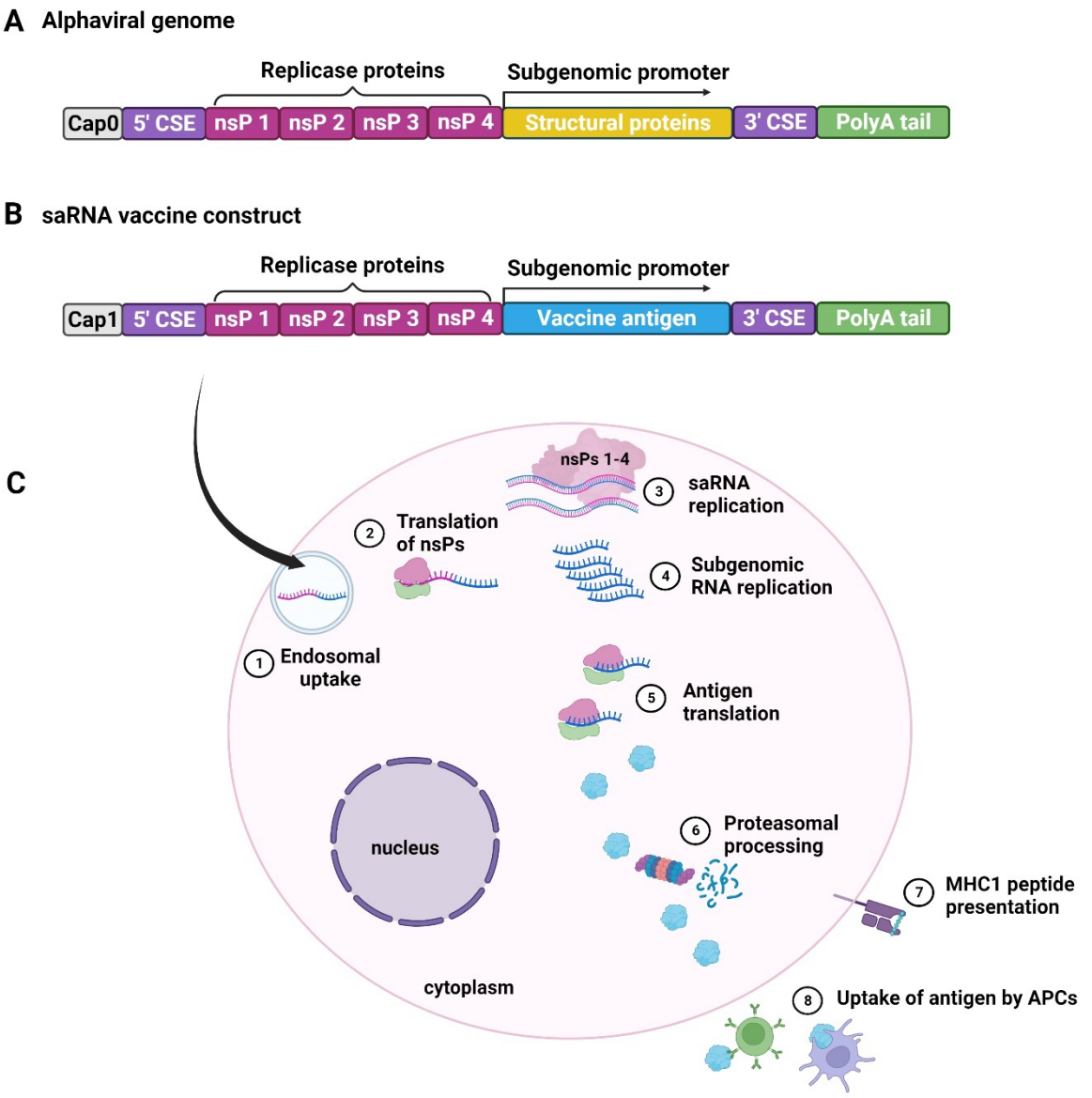

Figure 2. The self-amplifying RNA vaccine platform.

(A) Sequence elements of Alphaviral genome: 5'cap 0 structure and conserved sequence element (CSE), non-structural proteins 1-4 (nsPs 1-4), subgenomic promoter, viral structural proteins, 3' CSE and poly-A tail. **(B)** Sequence elements of saRNA vaccine construct: 5'cap 0 or cap 1 structure, CSE, nsPs 1-4, subgenomic promoter, antigen, 3' CSE and poly-A tail. **(C)** Antigen production and adaptive immune system stimulation by saRNAs: **(1)** saRNAs are endocytosed and released into cytosol. **(2)** saRNAs are translated to form nsPs1-4. **(3 and 4)** nsPs1-4 mediate replication of genomic and subgenomic RNAs. **(5)** Vaccine antigen is translated. **(6 and 7)** Antigen is degraded by the proteasome and peptides are presented in association with Major Compatibility Complex I molecules for T-cell recognition. **(8)** Whole

antigen is secreted for uptake by professional antigen presenting cells (APCs). Created using BioRender.com.

1.5 Innate immune system response to saRNAs

As part of mammalian cell antiviral defence mechanisms, cells are equipped with a variety of pattern recognition receptors (PRRs) to detect the presence of invading viruses and initiate innate immune system responses (reviewed in Jensen and Thomsen, 2012). saRNAs and unmodified mRNAs, like viral RNAs, can trigger the innate immune response and thus, unlike protein-based vaccines, do not require co-formulation with adjuvants to enhance the immune response (Figure 3) (reviewed in Kairuz et al., 2022). Uridine-rich single-stranded RNAs (ssRNAs) and dsRNAs are recognised by endosomal PRRs, such as TLRs 3, 7, and 8, that are present in plasmacytoid dendritic cells and B-cells. In most cell types, ssRNAs and dsRNAs are recognised by cytosolic PRRs such as retinoic-acid inducible gene I product (RIG-I) and melanoma-associated differentiation antigen 5 (MDA 5). Recognition of exogenous RNAs by these PRRs results in a cascade of events which culminates in secretion of type 1 interferons and pro-inflammatory cytokines to create an extracellular milieu conducive to the development of a Th1 immune response. Secreted interferons also act in an autocrine and paracrine manner to upregulate expression of interferon-stimulated genes (ISGs).

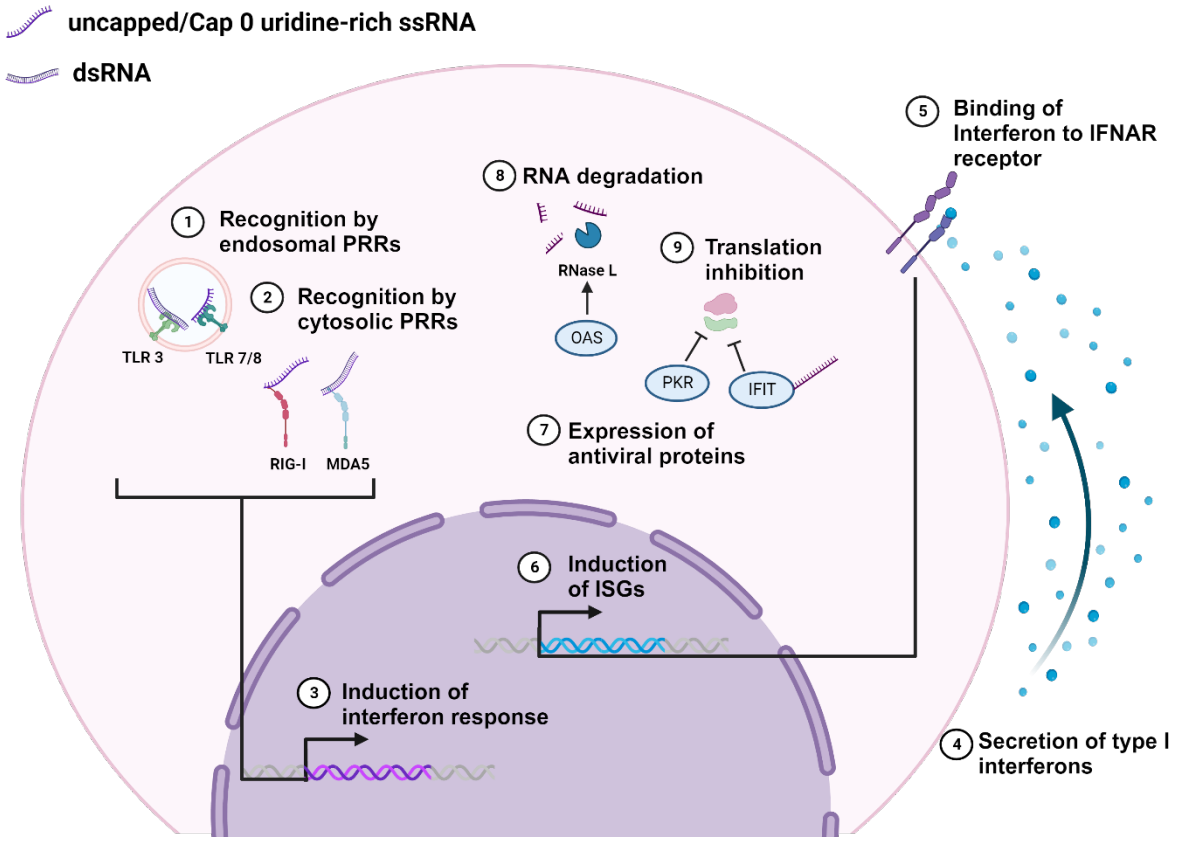

Figure 3. Innate immune system response to exogenous RNAs.

(1) Uridine-rich single-stranded RNA (ssRNA) and double-stranded RNA (dsRNA) taken up by professional antigen presenting cells trigger endosomal pattern recognition receptors (PRRs) called Toll-like receptors (TLRs). **(2)** ssRNA and dsRNA present in the cytosol are recognised by the cytosolic PRRs retinoic-acid inducible gene I product (RIG-I) and melanoma-associated differentiation antigen 5 (MDA 5) present in most cells. **(3 and 4)** Activation of PRRs induces expression and secretion of type I interferons. **(5 and 6)** Secreted interferon binds to IFNAR receptors and upregulates expression of interferon-stimulated genes (ISGs). **(7)** Proteins with antiviral properties are translated. **(8)** 2'-5'- oligoadenylate synthetase 1 (OAS1) mediates activation of RNase L which cleaves RNAs. **(9)** Protein kinase R (PKR) and interferon-induced proteins with tetratricopeptide repeats 1 (IFIT1) inhibit translation of mRNAs. Adapted from Kairuz et al., 2022. Created using BioRender.com.

ISGs encode numerous proteins which act in a multi-pronged approach to inhibit various stages of viral replication (reviewed in Schneider et al., 2014). The antiviral proteins most pertinent to RNA-based vaccines are 2'-5'- oligoadenylate synthetase 1 (OAS1), protein kinase R (PKR) and interferon-induced proteins with tetratricopeptide repeats 1 (IFIT1). These proteins possess

pattern recognition capabilities and are expressed at basal levels in an inactive form (reviewed in Fensterl and Sen, 2015; reviewed in Sadler and Williams, 2008). Upon binding to exogenous RNAs, these proteins are activated, and expression is further upregulated by type I interferon signalling. OAS1 mediates the synthesis of 2'-5'- oligoadenylates when activated by cytosolic dsRNA. These oligomers then activate latent cytosolic RNase L which cleaves RNAs to prevent its translation. PKR is a kinase which mediates phosphorylation of eukaryotic translation initiation factor 2α resulting in inhibition of translation. IFIT1 contains two domains which mediate translation inhibition. Its N-terminus can bind to uncapped or cap 0 mRNAs to prevent association with the ribosome, whereas its C-terminal domain binds to eukaryotic initiation factor 3 to prevent formation of the pre-initiation complex required for translation.

While type I interferon signalling is important for the development of a robust immune response against invading pathogens in the context of RNA-based vaccines, a strong innate immune system response may prematurely inhibit translation of the antigen, thus diminishing vaccine efficacy. The conventional mRNA vaccine and therapeutic platform has undergone numerous iterations to reduce innate immune system stimulation however those modifications are not amenable to the saRNA vaccine platform (reviewed in Kairuz et al., 2022). saRNAs are delivered as ssRNAs, replicate to produce dsRNA replication intermediates, and contain polyuridine motifs, all of which have the potential to activate a multitude of PRRs and limit translation of antigen. saRNAs can be capped with a cap 1 structure to avoid recognition by IFIT1 but this advantage is only available to the delivered transcripts since replication intermediates and sub-genomic RNAs will only be able to acquire a cap 0 structure. To improve antigen expression from saRNAs, and hence improve priming of the immune system, several researchers have explored and suggested methods to inhibit interferon signalling. Some viruses have evolved a variety of mechanisms to evade or modulate the interferon response. Vaccinia virus immune evasion proteins E3, K3 and B18 for example, inhibits PKR and interferon (reviewed in Smith et al., 2013). These immune evasion proteins were encoded in conventional mRNAs, and when delivered *in vivo* with saRNAs encoding luciferase, significantly increased expression of reporter proteins (Beissert et al., 2017). To ensure delivery of innate immune evasion proteins to saRNA transfected cells, cis-encoded innate inhibiting proteins derived from various viruses as well as targeting different points in the interferon pathway was evaluated (Blakney et al., 2021). Middle East respiratory syndrome coronavirus (MERS CoV) ORF4a and parainfluenza virus 5 (PIV-5) innate inhibiting proteins were the most efficient at increasing saRNA-encoded firefly luciferase expression *in vitro*. However, these results were not recapitulated in mice. The authors did however demonstrate increased immunogenicity in

rabbits which received saRNAs encoding rabies glycoprotein and cis-encoded MERS CoV ORF4a when compared to those that received saRNAs without innate inhibiting proteins. Using another approach, the authors also showed a modest increase in expression of firefly luciferase in mice when the JAK/STAT pathway inhibitor Ruxolitinib was administered along with saRNAs.

Interferon inhibition may seem beneficial in increasing antigen expression, however there are caveats to this approach. There is the possibility that an undesired immune response may be generated against innate inhibiting proteins. The financial benefits of using lower doses of saRNAs may be lost as additional costs would be incurred in producing mRNAs encoding innate inhibiting proteins or co-formulating saRNAs with small molecule inhibitors such as Ruxolitinib. Cis-encoded innate immune inhibitors would overcome this problem, however these were not shown to be effective *in vivo*. In addition, there are technical difficulties associated with producing longer saRNAs since they may be more prone to shearing. Others have reported promising results using saRNAs in vaccine applications without interferon inhibitors (Maruggi et al., 2022; McKay et al., 2020; Palmer et al., 2023; Vogel et al., 2018). In addition, Alphaviruses do not encode innate inhibiting proteins yet are able to successfully establish infection and viral replication. This is made possible by strategically located secondary structures and sequence motifs in the 5' CSEs of the genomic and subgenomic transcripts which allows it to evade recognition by PRRs (reviewed in Hyde et al., 2015). Thus, a balance between induction of an interferon response, which improves adaptive immune responses, and antigen translation can be achieved by saRNA vaccines.

Currently there are no mRNA-based vaccines against HBV in clinical trials. The aim of the current study was to produce and examine the immunogenicity of novel and potentially dose-sparing saRNA vaccines encoding HBV surface antigens, and to compare efficacy to currently available protein-based HBV vaccines. S-HBsAg and L-HBsAg were selected as target antigens with L-HBsAg expected to elicit a broader immune response which would improve the likelihood of conferring protection to non-responders as well. This dissertation describes the optimisation and *in vitro* characterisation of candidate saRNA vaccines. Plasmid DNA templates encoding VEEV replicon proteins with mono- and bi-cistronic antigens and/or reporter constructs were generated. These constructs were initially designed to produce bi-cistronic saRNAs capable of simultaneously expressing HBV antigen and a fluorescent reporter protein to confirm efficient *in situ* translation. This reporter protein could subsequently be replaced with another viral antigen to improve the breadth of protection elicited by the vaccine. Second generation saRNAs were designed to express a single antigen or reporter protein with

an increased poly-A tail length for improved longevity and translatability of transcripts. Optimisation of IVT reactions for longer saRNA transcripts was performed using commercially available kits and design of experiments (DOE)-based reactions, as the chemical synthesis of longer RNA requires different reactions conditions to that of conventional mRNA and is more prone to shearing. Co-transcriptional and post-transcriptional capping strategies were also compared to determine which approach produced better quality saRNAs with enhanced expression capabilities. Expression of reporter proteins and viral antigens from saRNAs was examined and confirmed *in vitro* using fluorescence microscopy and enzyme-linked immunosorbent assays respectively. The ability of saRNAs to trigger an innate immune system response *in vitro* was examined by measuring changes in mRNA transcripts encoding interferon and selected ISGs by quantitative reverse transcription polymerase chain reaction (qRT-PCR). The effect of saRNA dose and the interferon response on antigen expression was also examined *in vitro*. Finally, saRNAs encoding the reporter protein luciferase, S-HBsAg or L-HBsAg were administered intramuscularly to immunocompetent mice, using either local electroporation or cationic liposomes for delivery, to establish antigen expression kinetics, biodistribution, and immunogenicity.

2. MATERIALS AND METHODS

2.1 Design and production of bi-cistronic saRNAs

2.1.1 Sequence components of plasmids encoding bi-cistronic saRNAs

Plasmids T7-VEEV-eGFP-IRES-PuroR and T7-VEEV-Fluc-IRES-mCherry (Appendix A-Figures A1 and A2) encoding reporter proteins, and plasmids T7-VEEV-S-HBsAg-IRES-mCherry and T7-VEEV-L-HBsAg-IRES-mCherry (Appendix A-Figure A3) encoding HBV vaccine candidates were previously prepared. T7-VEEV-eGFP-IRES-PuroR was a gift from Steven Dowdy (Addgene plasmid # 58977; http://n2t.net/addgene:58977) and was designed to be used as a template for IVT of bi-cistronic saRNAs encoding codon-optimised enhanced green fluorescent protein (eGFP), and puromycin N-acetyltransferase which is under the translational control of an internal ribosome entry site (IRES) derived from the Encephalomyocarditis Virus (EMCV) (Yoshioka et al., 2013). This plasmid was used as a backbone to produce T7-VEEV-Fluc-IRES-mCherry, T7-VEEV-S-HBsAg-IRES-mCherry and T7-VEEV-L-HBsAg-IRES-mCherry.

All plasmids contained the T7 promoter sequence upstream of sequences to be included in saRNA transcripts to enable IVT using bacteriophage T7 RNA polymerase. This was followed by sequences encoding the 5' CSE of VEEV, VEEV nsP1-4 proteins required for *in situ* self-replication of saRNA transcripts, a VEEV subgenomic promoter, and the reporter protein or HBV antigen of interest. Subgenomic mRNAs were bi-cistronic and contained upstream sequences encoding Firefly luciferase (Fluc), S-HBsAg, or L-HBsAg, followed by an IRES, and downstream sequences encoding the fluorescent reporter protein mCherry which was included as a marker of efficient *in situ* translation. The 3' end of the transcript contained sequences encoding a VEEV-derived 3' CSE also required for self-replication, a stretch of 26 adenines encoding a poly-A (26) tail for efficient translation, and an *Mlu*I restriction site for linearisation of the plasmid to facilitate IVT of uniform transcripts. Plasmids also contained an origin of replication (ori) sequence to enable plasmid replication in bacteria, and an ampicillin resistance gene encoding β-lactamase.

2.1.2 Propagation of plasmids encoding saRNAs in Escherichia Coli (E. Coli)

Plasmids T7-VEEV-S-HBsAg-IRES-mCherry and T7-VEEV-L-HBsAg-IRES-mCherry were individually propagated in chemically competent NEB Turbo cells (New England Biolabs, Massachusetts, USA) (Appendix B1). Cells were thawed on ice and 20 µl aliquots were thereafter transformed with 1 µg of the respective plasmid for 15 minutes on ice. To facilitate

cellular uptake of plasmid DNA, cells were heat-shocked at 42°C for 90 seconds using a pre-heated heating block followed by cooling on ice for five minutes. The entire transformation mix was pipetted onto pre-warmed Luria Bertani (LB) agar plates supplemented with 100 µg/ml ampicillin (Appendix B2) and distributed with a sterile glass spreader. Plates were closed, placed in a loose plastic sleeve, and incubated upside down at 37°C. Following overnight incubation single colonies were picked and cultured in bacterial culture tubes containing 8 ml LB media (Appendix B2) and 100 µg/ml ampicillin. All bacterial cultures were grown overnight at 37°C in a shaking incubator at 150 revolutions per minute (rpm).

Glycerol stocks of each plasmid were prepared and stored at -80°C (Appendix B3). A small-scale plasmid DNA extraction from cultures was performed by alkaline lysis of bacterial cells followed by precipitation of plasmid DNA using isopropanol (Appendix B4). The concentration and purity of extracted plasmids was determined by spectrophotometry using the NanoPhotometer® (Implen, California, USA). Plasmid DNA samples with A260/280 ratios of 1.8-2 and A260/230 ratios of 2.0-2.2 were considered sufficiently free of protein and organic/salt contaminants respectively. A restriction digest was performed to identify plasmids based on banding patterns the resulting fragments produced following agarose gel electrophoresis. Each digestion reaction contained 1 µg of plasmid, 5 units (U) of the Fast Digest restriction enzyme *Nco*I (Thermo Fisher Scientific, Massachusetts, USA), or *Eco*RI, 2 µl of Fast Digest Green buffer (Thermo Fisher Scientific, Massachusetts, USA) and nuclease-free water to a final volume of 20 µl. The reaction was incubated at 37°C for an hour and then analysed by agarose gel electrophoresis (Appendix B5). Clones containing plasmids that produced the correct banding pattern were cultured in baffled flasks overnight using 100 ul of the respective glycerol stocks and 300 ml LB media supplemented with 100 µg/ml ampicillin.

For a large-scale extraction of plasmid DNA, 100 µl of the respective bacterial glycerol stocks were individually inoculated into 300 ml LB media supplemented with 100 µg/ml ampicillin and incubated overnight at 37°C with shaking at 150 rpm. Overnight cultures were then transferred to plastic jars and bacteria were pelleted by centrifugation at 4 000 x g for 20 minutes at 4°C. Plasmids were thereafter extracted using the QIAGEN plasmid maxi kit according to manufacturer's instructions (Qiagen, Hilden, Germany). This kit employs the method of alkaline lysis of bacterial cells to extract plasmid DNA which is thereafter purified using anion-exchange columns provided with the kit. Purified plasmid DNA was resuspended in 200 µl nuclease-free water. Concentration and purity of extracted plasmids were determined by spectrophotometry. Plasmids were stored at -20°C. A final restriction digest was performed, as

described above, to verify the identity of T7-VEEV-S-HBsAg-IRES-mCherry and T7-VEEV-L-HBsAg-IRES-mCherry.

2.1.3 Linearisation of plasmids encoding saRNAs by restriction digestion

To prevent continuous IVT of the circular plasmid DNA template by T7 RNA polymerase, all plasmids were linearised immediately after the poly-A tail by restriction digestion. This ensured that saRNA transcripts produced by IVT were the correct length and contained only the desired sequences for *in situ* replication and translation. Digestion reactions included plasmid DNA, the restriction enzyme *Mlu*I (Thermo Fisher Scientific, Massachusetts, USA) at a concentration of 1U/µg of plasmid DNA, 1x Buffer R (Thermo Fisher Scientific, Massachusetts, USA) and nuclease-free water to an appropriate final volume to ensure the glycerol content of the reaction was below 5%. The reactions were incubated at 37°C for two hours. Complete linearisation of plasmids was confirmed by agarose gel electrophoresis. Linearised plasmids were purified using either EconoSpin® silica membrane mini spin columns (Epoch Life Science Inc., Texas, USA) (Appendix B6) or sodium acetate (NaOAc) precipitation (Appendix B7).

2.1.4 Synthesis of uncapped saRNAs by IVT

Bi-cistronic saRNAs were *in vitro* transcribed from linearised plasmid templates using the commercially available Ampliscribe™ T7 Flash™ transcription kit (Epicentre Biotechnologies, Wisconsin, USA) and the RiboMAX™ Large scale RNA production system (Promega, Wisconsin, USA). IVT using the Ampliscribe™ T7 Flash™ transcription kit was initially performed according to manufacturer's protocols (Appendix B8). To improve saRNA yield and integrity the following modifications were thereafter examined: a) increasing incubation time from 30 minutes to one/two hours, b) increasing incubation temperature from 37°C to 42°C, and c) increasing plasmid DNA concentration from 1µg to 2µg.

Following IVT, DNA templates present in the reaction were degraded with DNaseI (Thermo Fisher Scientific, Massachusetts, USA) for 15 minutes at 37°C at a concentration of 1U/µg plasmid DNA in 1x DNase buffer. saRNA transcripts were precipitated with equal volumes of 5 M ammonium acetate (NH_4OAc) and incubated for 15 minutes on ice. Transcripts were pelleted by centrifugation at 10 000 x g for 15 minutes at 4°C and rinsed with 500 µl of ice-cold 70% ethanol. Transcripts were pelleted again, and ethanol was removed. Residual ethanol was evaporated by air-drying the pellet for five minutes. Transcripts (saRNA-eGFP-IRES-PuroR, saRNA-Fluc-IRES-mCherry, saRNA-S-HBsAg-IRES-mCherry, and saRNA-L-

HBsAg-IRES-mCherry) were resuspended in 100-200 µl of nuclease-free water and stored at -80°C (Figure 4).

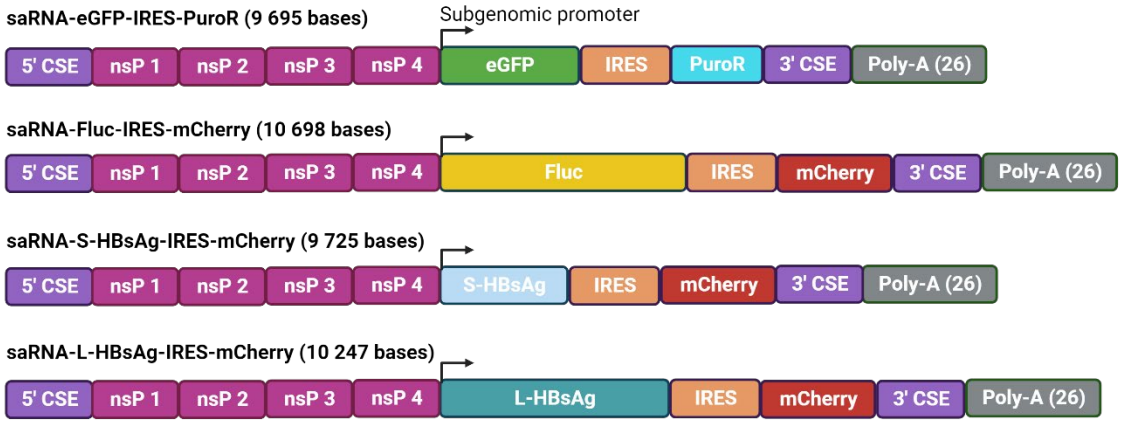

Figure 4. Schematic of bi-cistronic saRNA transcripts.

Bi-cistronic saRNA transcripts produced by IVT contained sequences encoding Venezuelan Equine Encephalitis Virus (VEEV)-derived 5'CSE, non-structural proteins 1-4 (nsPs1-4) and sub-genomic promoter. Sequences encoding the antigen of interest (eGFP, Fluc, S-HBsAg or L-HBsAg), an internal ribosome entry site (IRES), puromycin N-acetyltransferase (PuroR) or the reporter protein mCherry, VEEV-derived 3' CSE, and poly-A(26) tail are located downstream of the sub-genomic promoter and represent sub-genomic mRNAs. Created using BioRender.com.

2.1.5 Post-transcriptional capping of transcripts using the Vaccinia capping system

To evade recognition by the innate immune system and improve *in situ* translation of saRNAs, transcripts were enzymatically capped (cap 1) post-transcriptionally using the Vaccinia capping system and mRNA cap 2′-O-methyltransferase according to manufacturer's instructions. The vaccinia capping system, when used on its own incorporates a cap 0 structure at the 5' end of mRNA transcripts. The addition of mRNA cap 2′-O-methyltransferase facilitates methylation at the 2'-O site of the first nucleotide adjacent to the cap 0 structure, producing a transcript with a cap 1 structure at the 5' end. Prior to capping, 10 µg of saRNA transcripts in a final volume of 14 µl of nuclease-free water was denatured at 65 °C for five minutes. The solution was cooled on ice before adding the following components in the specified order and at the indicated final concentrations in a 20 µl reaction: 1x capping buffer, 0.5 mM GTP, 0.2 mM S-adenosylmethionine, 10 U/µl vaccinia capping enzyme, 50 U/µl mRNA cap 2'-O-methyltransferase, and 1 U/µl Murine RNase inhibitor. All reagents used in enzymatic capping

were obtained from New England Biolabs (Massachusetts, USA). The reaction was incubated at 37°C for one hour. Capped transcripts were precipitated with NH_4OAc as described in section 2.1.4 and resuspended in 10-20 µl nuclease-free water. Capped transcripts were stored at -80°C.

2.1.6 Extraction of full-length saRNA transcripts by Oligo d(T)$_{25}$ magnetic beads

Full-length saRNA transcripts, which contain a 3' poly-A tail, was separated from incomplete or degraded transcripts by complementary base pairing to oligo d(T)$_{25}$ coupled magnetic beads (New England Biolabs, Massachusetts, USA). A microcentrifuge tube containing 500 µl of beads was placed on a magnetic rack for one minute to separate beads from solution. Supernatant was removed and beads were rinsed in 250 µl binding buffer and resuspended in 500 µl binding buffer. saRNA-eGFP-IRES-PuroR (8µg) was diluted in an equal volume of binding buffer and heated at 65°C for 10 minutes to denature secondary structures which could interfere with binding to beads. Denatured saRNAs were then added to the beads in binding buffer and incubated at room temperature for 20 minutes on a rotating mixer to facilitate binding. saRNAs bound to beads were then separated from solution by placing the tube in the magnetic rack for one minute. The supernatant was removed, and beads were rinsed in 500 µl wash buffer for one minute on the rotating mixer. The tube was placed in the magnetic rack again and supernatant was removed. Beads were then rinsed with 500 µl low-salt wash buffer. All buffers used were prepared in accordance with manufacturer's instructions. To release saRNAs into solution, rinsed beads were incubated in 20 µl of nuclease-free water at 50°C for two minutes. The microcentrifuge tube was placed in the magnetic rack and supernatant containing purified full-length saRNAs were transferred to a sterile tube and stored at -80°C.

2.1.7 Size and integrity analysis of saRNAs

The concentration and purity of uncapped and capped saRNAs were determined by spectrophotometry using the NanoPhotometer®. Protein and salt contamination of samples was assessed by examining A260/A280 and A260/A230 ratios respectively. saRNAs with both ratios above 2 was considered suitable for downstream analysis. Size and integrity of transcripts were determined by denaturing formaldehyde gel electrophoresis (Appendix B9).

2.2 Design and production of single-cistron saRNAs

2.2.1 Restriction enzyme cloning of plasmids encoding single-cistron saRNAs with extended poly-A tails

To enable production of single-cistron saRNAs encoding either a reporter protein or HBV antigen of interest, the IRES and downstream PuroR or mCherry sequences were removed from plasmid IVT templates. To improve *in situ* translation of transcripts, a longer poly-A tail (poly-A ((60)) was incorporated into the design downstream of the 3' CSE. These modifications were achieved using a 2-step cloning strategy.

Step 1: Extension of poly-A tail by cloning

Subcloning plasmid pUC57-saRNA-MCS-poly-A (60) containing a multiple cloning site (MCS) and downstream VEEV-derived 3' CSE, extended poly-A (60) sequence, and *Mlu*I restriction site, was synthesised by GenScript Biotech (New Jersey, USA) (Appendix A-Figure A4). The MCS contained *Nde*I and *Not*I restriction sites which were used to insert reporter protein or HBV surface antigen sequences. To obtain the plasmid backbone into which individual antigens of interest could be inserted, the subcloning plasmid was digested with the restriction enzymes *Nde*I and *Not*I (New England Biolabs, Massachusetts, USA). Digest fragments were resolved on a 1% agarose gel and the plasmid backbone was extracted from the gel using the QiaQuick® Gel extraction kit (Qiagen, Hilden, Germany) and EconoSpin® silica membrane mini spin columns according to manufacturer's instructions. Sequences encoding antigens of interest (S-HBsAg and L-HBsAg), previously amplified by PCR and digested to produce complementary 5' *Nde*I and 3' *Not*I overhangs, were ligated to the sub-cloning plasmid backbone in a 1:3 backbone:insert molar ratio to produce plasmids pUC57-S-HBsAg-poly-A (60) and pUC57-L-HBsAg poly-A (60) (Appendix A-Figure A5). The amount of insert DNA to be ligated was calculated using the following equation:

$$Ng\ insert\ required = [\left(\frac{Kb\ of\ insert}{Kb\ of\ backbone}\right) \times ng\ backbone\ ]\ x\ ligation\ ratio$$

Each 20 µl ligation reaction contained 1x ligation buffer (New England Biolabs, Massachusetts, USA), 50 µg backbone DNA, insert DNA fragments as calculated using the above equation, 1 µl of T7 DNA ligase (New England Biolabs, Massachusetts, USA), and nuclease-free water. Ligation reactions were incubated overnight in a water bath at 16 °C. A volume of 5 µl of the ligation reaction was used to transform 50 µl of NEB Turbo competent cells. Protocols for transformation of bacteria, culturing of clones and extraction of plasmids were as described in

section 2.1.2. Positive clones were identified by restriction digestion using the Fast Digest enzymes *Alw*44I and *Apa*I (Thermo Fisher Scientific, Massachusetts, USA) and analysis of banding patterns by agarose gel electrophoresis.

Step 2: Cloning of antigen sequences with extended poly-A (60) tail into T7-VEEV plasmid backbone

T7-VEEV-eGFP-IRES-PuroR was digested with *Nde*I and *Mlu*I (New England Biolabs, Massachusetts, USA) to produce a backbone which excluded the eGFP-IRES-PuroR sequences. pUC57-S-HBsAg-poly-A (60) and pUC57-L-HBsAg poly-A (60) were also digested with *Nde*I and *Mlu*I to excise insert fragments containing antigen sequences, downstream 3'CSE and extended poly-A tail. Both digests were resolved on a 1% agarose gel and backbone and insert sequences were extracted and ligated overnight at 16℃ in a 1:3 backbone:insert molar ratio as described above to produce saRNA-encoding plasmids T7-VEEV-S-HBsAg and T7-VEEV-L-HBsAg (Appendix A-Figure A6). The cloning strategy is summarized in Figure 5. Protocols for transformation of bacteria, culturing of clones and extraction of plasmids were as described in section 2.1.2. Plasmid T7-VEEV-Luc2 which was used to produce single-cistron transcripts encoding codon-optimised synthetic luciferase 2 (Luc2) (Promega, Wisconsin, USA) was prepared using a similar cloning strategy (Appendix A-Figure A7). The final plasmid constructs contained the T7 promoter sequence, VEEV-derived 5' CSE, nsP1-4 proteins and subgenomic promoter, sequences encoding the antigen of interest (Luc2, S-HBsAg, or L-HBsAg), VEEV-derived 3' CSE, poly-A (60) tail, and *Mlu*I restriction site.

.

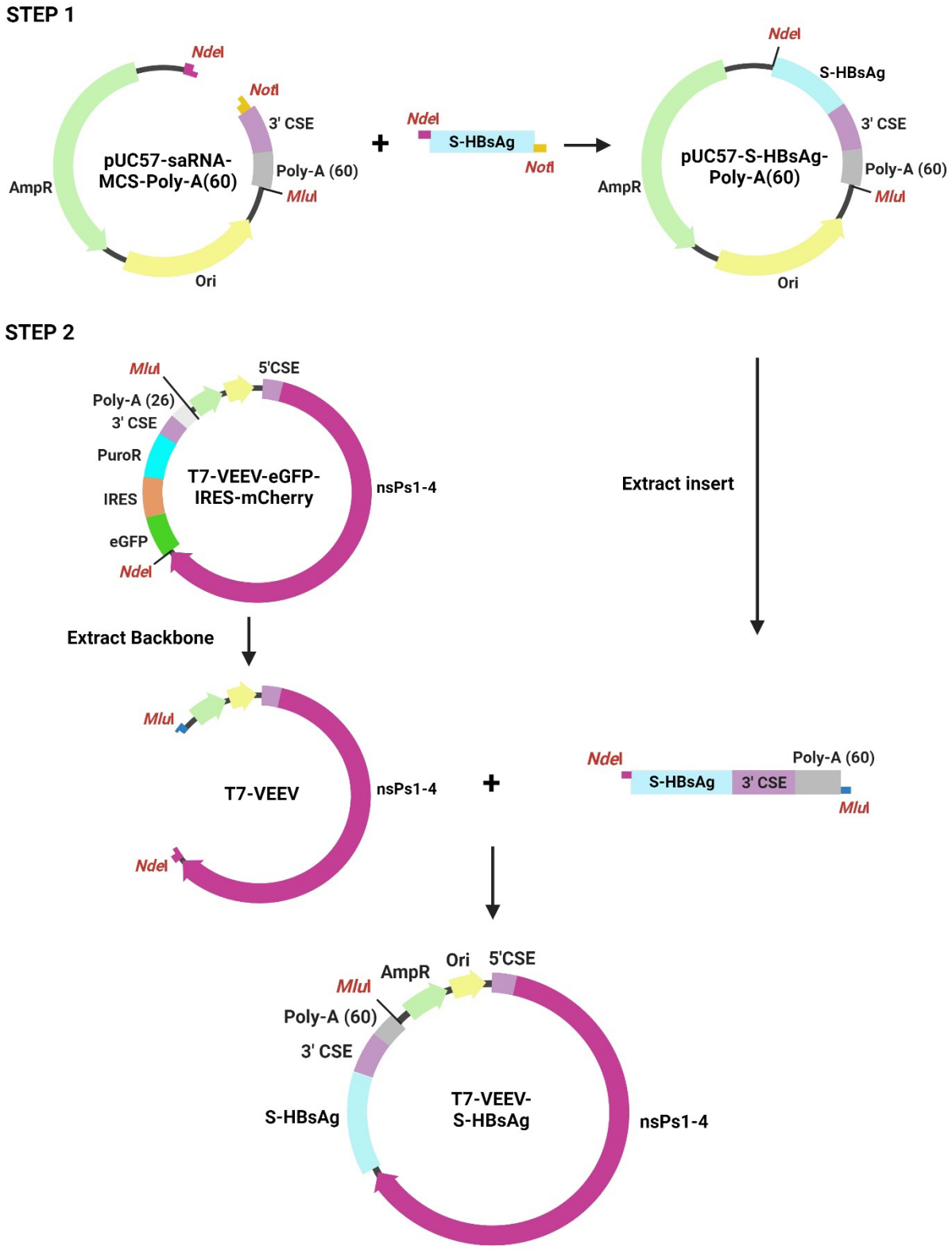

Figure 5. Representative cloning strategy to produce plasmids encoding single-cistron saRNAs.

STEP 1: Antigen sequences (S-HBsAg or L-HBsAg) were cloned into pUC57-saRNA-MCS-poly-A (60) using the *Nde*I and *Not*I restriction sites, to extend the poly-A tail for improved translation. **STEP 2:** Antigen sequences, 3'CSE and extended poly-A tail were excised from subcloning plasmids using *Nde*I and *Mlu*I, and ligated into T7-VEEV backbone from which eGFP-IRES-PuroR sequences had been excised. Created using BioRender.com.

T7-VEEV-S-HBsAg and T7-VEEV-L-HBsAg were verified by restriction digest with *Nco*I (Thermo Fisher Scientific, Massachusetts, USA) as described in section 2.1.2. In addition, antigen inserts and flanking restriction enzyme sites were sequenced by Sanger sequencing (Inqaba Biotec, Pretoria, South Africa) using the forward primers listed in Table 1. Primer binding sites are shown in Appendix A-Figures A5 and A6. Sequencing results were aligned to plasmid DNA template sequences and examined for mismatches using an online alignment tool available at https://benchling.com.

Table 1. Forward primers used for Sanger sequencing of subcloning plasmids and plasmids encoding single-cistron saRNAs

Plasmid	Primer name	Primer sequence (5'-3')
pUC57-S-HBsAg-poly-A (60)	MCS-Fw	CAGCTTGTCTGTAAGCGG
pUC57-L-HBsAg-poly-A (60)	MCS-Fw	CAGCTTGTCTGTAAGCGG
	SHBs-IF	TCCTTCTAGTTGGGCCTTCG
T7-VEEV-S-HBsAg	nsP4-Fw	AACTTCCATCATAGTTATGGCCATG
	SHBs-IF	TCCTTCTAGTTGGGCCTTCG
T7-VEEV-L-HBsAg	nsP4-Fw	AACTTCCATCATAGTTATGGCCATG
	LHBs-IF	CGCTAGTCACATCAGTTCAATTAGC
	SHBs-IF	TCCTTCTAGTTGGGCCTTCG

2.2.2 Correction of single point mutation in T7-VEEV-L-HBsAg by restriction enzyme cloning

Sequencing of pUC57-L-HBsAg poly-A (60) and T7-VEEV-L-HBsAg and alignment to reference sequences revealed a non-synonymous base substitution error (T → G; C398G) in the C-terminal domain of L-HBsAg. This base substitution error was not present in the open reading frame of S-HBsAg within the pUC57-S-HBsAg poly-A (60) plasmid. Since both HBV antigens share the same C-terminal domain, the cloning strategy used to produce a plasmid with the correct L-HBsAg sequence, was simply to incorporate the L-HBsAg encoding sequences

upstream of the mutation into the pUC57-saRNA-S-HBsAg-poly-A (60) plasmid containing the correct C-terminal domain sequence.

pUC57-L-HBsAg-poly-A (60) was digested with *Nde*I and *Apa*I (Thermo Fisher Scientific, Massuchusetts, USA) which cleaves just upstream of the Kozak sequence and the point mutation respectively. The insert extracted thus included the Kozak sequence and entire L-HBsAg sequence up to but excluding the C-terminal point mutation. pUC57-S-HBsAg-poly-A (60) was also digested with *Nde*I and *Apa*I to produce a backbone with the correct C-terminal sequence. Digests were run on an agarose gel and backbone and insert fragments were extracted and ligated as described in section 2.2.1 to produce pUC57-L-HBsAg poly-A (60) with the correct sequence (Figure 6). Protocols for transformation of bacteria, culturing of clones and extraction of plasmids were as described in section 2.1.2. Cloning of T7-VEEV-L-HBsAg was performed as described in step two of section 2.2.1.

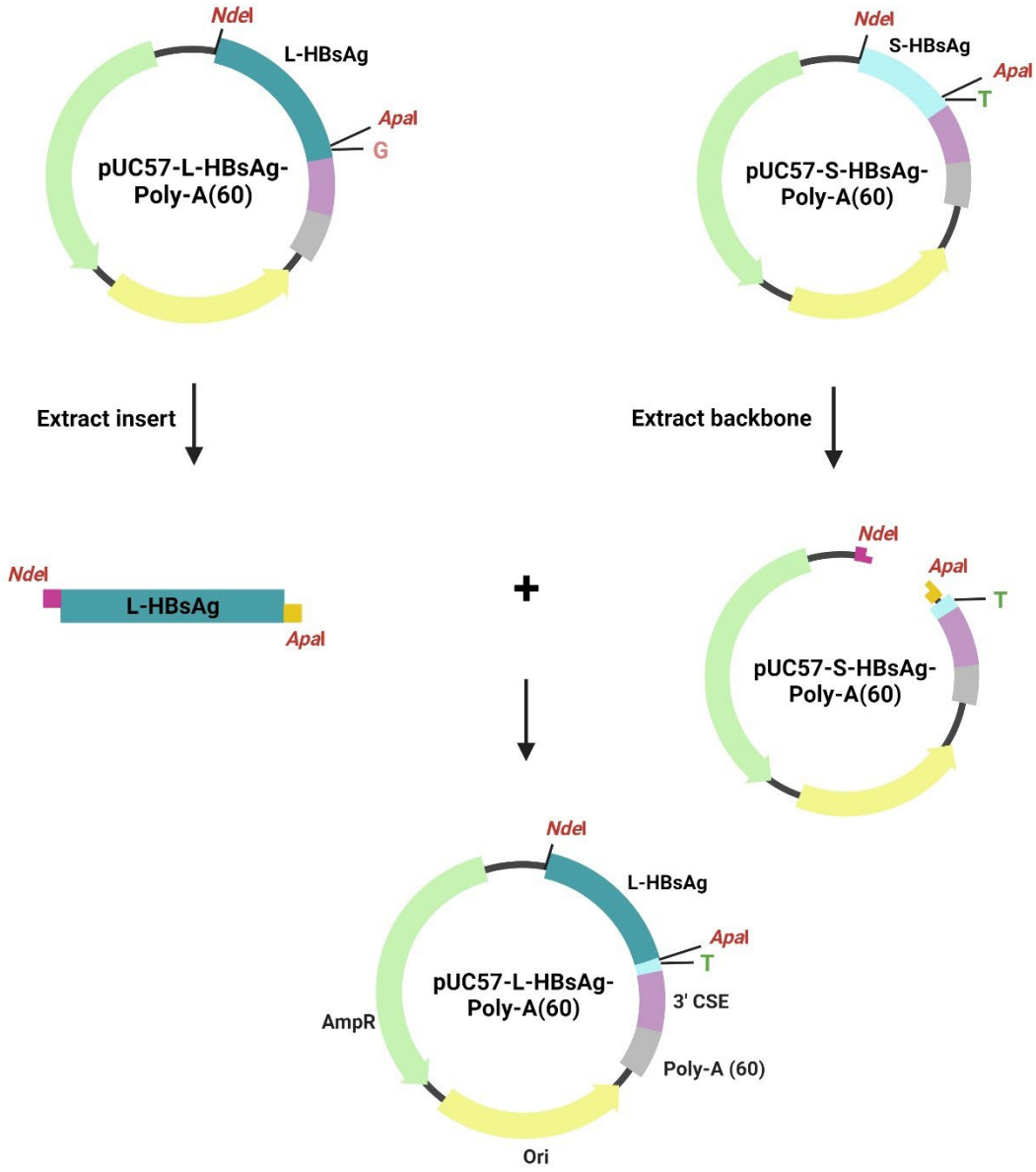

Figure 6. Cloning strategy to correct base substitution error located in C-terminus of L-HBsAg.

(Top left) Sanger sequencing identified a non-synonymous single base substitution error T to G in the C-terminus of subcloning plasmid pUC57-L-HBsAg-Poly-A (60) as well as T7-VEEV-L-HBsAg. The *Nde*I and *Apa*I restriction sites were used to excise L-HBsAg sequences upstream of the mutation. (Top right) Subcloning plasmid pUC57-S-HBsAg-Poly-A (60), which contains the correct nucleotide (T), was digested with the same enzymes to produce a

backbone into which the partial L-HBsAg insert could be ligated producing pUC57-L-HBsAg-poly-A (60) with the correct C-terminal sequence. Created using BioRender.com.

To confirm that newly cloned pUC57-L-HBsAg poly-A (60) and T7-VEEV-L-HBsAg contained the correct C-terminal sequence, the S-HBsAg domain from both plasmids were amplified by polymerase chain reaction (PCR) and amplicons were sequenced. Primer binding sites are shown in Appendix A-Figures A5 and A6. To ensure high-fidelity replication of amplicons during PCR, the Q5 high-fidelity polymerase (New England Biolabs, Massachusetts, USA) was used. Each 25 µl reaction contained 1x Q5 high-fidelity mastermix, 5 ng plasmid template, 0.5 µM of each forward and reverse primers (Table 2) and nuclease-free water. PCR was performed using the Biorad T100™ Thermal Cycler (Bio-Rad Laboratories, California, USA). Thermocycling conditions consisted of initial denaturation at 98℃ for 30 seconds, followed by 40 cycles of denaturation at 98℃ for 10 seconds, annealing at 69.0℃ for 30 seconds and extension at 72℃ for 20 seconds. A final extension was performed at 72℃ for two minutes. Specificity of amplification and amplicon size were examined by electrophoresis of 5 µl of each PCR in 1x DNA loading dye on an agarose gel. Amplicons were extracted from the gel and sequenced (Inqaba Biotec, Pretoria, South Africa) using the SHBs-IF primer (Table 1).

Table 2. Forward (F) and reverse (R) primers used in PCR amplification of S-HBsAg domain-encoding sequence from pUC57-L-HBsAg-poly-A (60) and T7-VEEV-L-HBsAg

Primer name	Primer sequence (5'-3')
SHBs_F2	GATCGGTCTCCATGGAGAATATTACTTCCGGACTG
HBsAg_R2	GATCGGTCTCGCGAGTCAAATGTAGACCCACAGACAG

2.2.3 Synthesis of single-cistron saRNAs by IVT with co-transcriptional capping

Plasmids encoding single-cistron saRNAs were linearised immediately downstream of the poly-A (60) tail using the restriction enzyme *Mlu*I and purified by NaOAc precipitation as described in section 2.1.3. Single-cistron saRNAs were transcribed using a Design of Experiments (DOE) buffer and protocol optimised for the synthesis of longer mRNAs such as saRNAs (Samnuan et al., 2022) (Appendix B8). This buffer contained magnesium acetate ($Mg(OAc)_2$) with a total nucleotide triphosphate (NTP):magnesium (Mg) molar ratio of 1:1.875, which is optimal for synthesis of saRNAs. Each IVT reaction contained 100 ng/µl linearised plasmid DNA template, 10 mM of each unmodified NTP (ATP, CTP, GTP and UTP), 0.2 U/µL Murine RNase inhibitor, 8 U/µL T7 RNA polymerase, 1× DOE buffer, and nuclease-

free water up to a final volume of 100 µl. To minimise handling and possible degradation of saRNAs, and to produce transcripts with a naturally occurring cap 1 structure, CleanCap® AU reagent (Trilink Bio Technologies, California, USA) was added to the reaction at a final concentration of 8 mM to facilitate co-transcriptional capping of saRNAs. IVT reactions were incubated in a pre-heated heating block at 37°C for 2 hours. Enzymes and NTPs used for IVT were obtained from New England Biolabs (Massachusetts, USA).

Following IVT, DNA templates present in the reaction were degraded with DNaseI (Thermo Fisher Scientific, Massachusetts, USA) for 15 minutes at 37°C at a concentration of 1U/µg plasmid DNA in 1x DNase buffer. Transcripts were precipitated with 0.5 volumes of a solution containing 7.5 M lithium chloride (LiCl) and 50 mM Ethylenediaminetetraacetic acid EDTA and incubated for 30 minutes at -20°C. Transcripts (saRNA-Luc2, saRNA-S-HBsAg and saRNA-L-HBsAg) were purified and stored as described in section 2.1.4 (Figure 7).

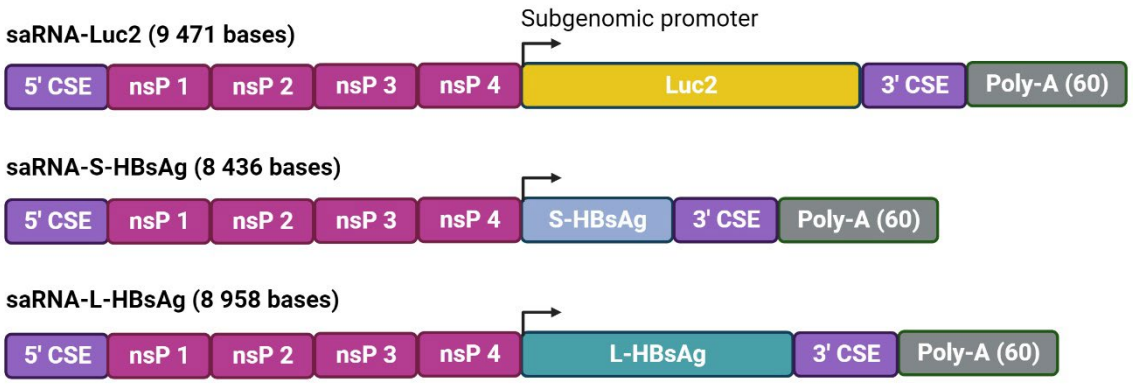

Figure 7. Schematic of single-cistron saRNA transcripts.

Single-cistron saRNA transcripts produced by IVT contained sequences encoding Venezuelan Equine Encephalitis Virus (VEEV)-derived 5'CSE, non-structural proteins 1-4 (nsPs1-4) and sub-genomic promoter. Sequences encoding the antigen of interest (Luc2, S-HBsAg or L-HBsAg), VEEV-derived 3' CSE, and extended poly-A(60) tail are located downstream of the sub-genomic promoter and represent sub-genomic mRNAs. Created using BioRender.com.

2.3 *In vitro* transfection of Human Embryonic Kidney (HEK) 293T cells with saRNAs and detection of antigen expression

HEK 293T cells, which are adherent cells, were grown and maintained in complete media [Dulbecco's Modified Eagle Medium (Life Technologies, California, USA) supplemented with 10% foetal calf serum, 100 U/mL penicillin, and 100 µg/mL streptomycin] in a humidified incubator at 37 °C and 5% CO_2. Cells were passaged when approximately 80% confluent (Appendix B10). Cells were seeded in either 48- or 6-well plates at a confluency of 40% in a volume of 250 µl or 2 mls complete media respectively and transfected when approximately 70-80% confluent.

2.3.1 Detection of eGFP by fluorescence microscopy

To determine whether eGFP was expressed from transcripts, HEK 293T cells were transfected with saRNA-eGFP-IRES-PuroR and expression of eGFP was monitored by fluorescence microscopy. Cells, seeded in a 48-well plate, were transfected with 50, 100, or 200 nanograms (ng) of saRNA-eGFP-IRES-PuroR in a volume of 25 µl per well using the liposome-based Lipofectamine™ MessengerMAX™ transfection reagent (Invitrogen, Massachusetts, USA) to facilitate uptake of saRNAs. Briefly, saRNAs and liposomes, individually diluted in reduced serum media Opti-MEM™ (Life Technologies, California, USA), were combined in an saRNA (µg) to lipid (µl) ratio of 1:1.5 and incubated at room temperature for five minutes to allow formation of lipoplexes (saRNAs complexed with liposomes). Lipoplexes were added to cells which were then incubated overnight in a humidified incubator at 37 °C and 5% CO_2. Expression of eGFP was monitored over 1-15 days using the EVOS Fluorescence Microscope (Invitrogen, Massachusetts, USA). Mock-transfected cell cultures (Lipofectamine™ MessengerMAX™ only) served as negative controls.

2.3.2 Detection of S-HBsAg by enzyme-linked immunosorbent assay (ELISA), and mCherry by fluorescence microscopy

HEK 293T cells, seeded in a 48-well plate, were transfected with 250 ng of saRNA-S-HBsAg-IRES-mCherry using Lipofectamine™ MessengerMAX™ transfection reagent as described in section 2.3.1. As a positive control, HEK 293T cells were transfected with an equal amount of pCH9-3091 using Lipofectamine™ 3 000 reagent (Invitrogen, Massachusetts, USA) according to manufacturer's protocols. pCH9-3091 is an HBV replication-competent plasmid which produces infectious HBV particles displaying all three surface antigens of which S-HBsAg is

the most abundant. Cells were examined 48 hours after transfection for the concurrent expression of S-HBsAg and mCherry by ELISA and fluorescence microscopy respectively.

Expression of S-HBsAg and secretion into cell culture media was measured by sandwich ELISA using the Monolisa™ HBs Ag Ultra ELISA kit (Biorad, California, USA) according to manufacturer's instructions. A volume of 100 µl of cell culture media (neat or diluted in phosphate buffered solution, pH 7.2) was transferred into wells of the provided microtiter plate, which was pre-coated with murine monoclonal antibodies targeting S-HBsAg. Thereafter, 50 µl of peroxidase-conjugated goat polyclonal and murine monoclonal anti-HBsAg antibody mixture was added to each well. The plate was sealed and incubated at 37°C for 90 minutes. Following incubation, unbound conjugate antibodies were removed by washing the plate five times with the provided wash buffer at a 1x dilution using an automated plate washer. A volume of 100 µl of the colorimetric enzyme substrate solution consisting of tetramethyl benzidine was added to each well and the plate was covered in foil and incubated at room temperature for 30 minutes. The reaction was thereafter halted by the addition of 100 µl 1N sulphuric acid and left at room temperature for five minutes. Absorbance of each well was measured at 490 nm (primary wavelength) and 655 nm (reference wavelength) using the iMark Microplate Absorbance Reader (Bio-Rad, California, USA) or Multiskan SkyHigh microplate spectrophotometer (Thermo Fisher Scientific, Massuchusetts, USA). Wavelength correction was performed by subtracting the absorbance at the reference wavelength from the absorbance at the primary wavelength. Final absorbance was calculated by subtracting background absorbance from mock-transfections and then adjusting for sample dilutions.

2.3.3 Detection of L-HBsAg from saRNA-L-HBsAg by ELISA

Since L-HBsAg contains the S-HBsAg domain, expression of L-HBsAg was also examined using the Monolisa™ HBs Ag Ultra ELISA kit as described in section 2.3.2. HEK 293T cells were seeded in 48-well plates and transfected with 250 ng of saRNA-L-HBsAg using Lipofectamine™ MessengerMAX™ transfection reagent as described in section 2.3.1. At 48 hours post-transfection cell culture supernatant was harvested for analysis of secreted L-HBsAg. To detect intracellularly retained L-HBsAg, cells were lysed with 200 µl 1x passive lysis buffer (Promega, Wisconsin, USA) and mixed on a platform shaker at room temperature for 15 minutes. Crude lysates and supernatants were stored at -20°C until analysis by ELISA.

2.4 Detection of innate immune responses to saRNAs by qRT-PCR and effect on antigen expression

To determine whether unmodified cap1-saRNAs and dsRNA replication intermediates triggered the innate immune response *in vitro*, gene expression analysis of IFN-β and IFN-inducible genes (OAS1, IFIT1 and PKR) was performed by qRT-PCR. HEK 293T cells were first seeded in a 6-well plate and transfected as described in section 2.3.1 with 250, 500 or 1000 ng of saRNA-Luc2, saRNA-S-HBsAg or Polyinosinic:polycytidylic acid (Poly I:C), which is a double-stranded RNA known to trigger the innate immune system. Cells transfected with the corresponding volume of Lipofectamine™ MessengerMAX™ alone served as negative controls.

At 24 hours post-transfection, cell culture supernatants were removed and stored at -20°C until S-HBsAg expression analysis by ELISA. Total RNA was extracted from cells using TRIzol™ reagent (Invitrogen, Massachusetts, USA). Cells were homogenised with 1 ml TRIzol™ reagent per well and transferred to microcentrifuge tubes. A volume of 200 µl chloroform was added to each tube and samples were thoroughly mixed before incubation at room temperature for two minutes. Samples were then centrifuged at 12 000 x g for 15 minutes at 4°C. The upper aqueous layer containing total RNA was transferred to a clean microcentrifuge tube. RNA was precipitated with 500 µl 100% isopropanol and incubated at room temperature for 10 minutes. Samples were then centrifuged at 12 000 x g for 10 minutes at 4°C. The supernatant was discarded and precipitated RNA was resuspended in 85 µl of nuclease-free water. Samples were treated with 5 units of DNaseI in 1x DNaseI buffer at 37°C for an hour to remove contaminating DNA. RNA was precipitated using 500 µl 100% ethanol and incubated at -20°C for 30 minutes. RNA was pelleted by centrifugation at 12 000 x g for 10 minutes at 4°C. Supernatant was discarded and RNA pellets were rinsed with 500 µl 70% ethanol and centrifuged again at 12 000 x g for 10 minutes at 4°C. Total RNA was resuspended in nuclease-free water. Concentration and purity of RNA was analysed using the NanoPhotometer®. Presence of DNA contaminants and integrity of RNA were assessed by agarose gel electrophoresis. Prior to electrophoresis, 500 ng of RNA was first denatured at 70°C for 10 minutes in 1x RNA gel loading dye to allow RNAs to migrate through the agarose gel according to their size. Samples were stored at –80°C until further analysis.

The LUNA® Universal One-Step RT-qPCR kit (New England Biolabs, Massachusetts, USA) was used to reverse-transcribe extracted mRNAs into cDNA, and thereafter amplify cDNA encoding IFN-β, OAS1, IFIT1, PKR and the housekeeping gene glyceraldehyde 3-phosphate

dehydrogenase (GAPDH) using gene-specific primers (Table 3). Reactions containing GAPDH primers without reverse transcriptase (no RT control) were included to identify contaminating DNA. Each 20 µl reaction contained 500 ng total RNA, 1x Luna WarmStart RT enzyme mix, 1x Luna Universal One-Step Reaction mix, forward and reverse primers at a final concentration of 0.4 µM each, and nuclease-free water. Thermocycling was performed using the Biorad C1000™ Touch thermocycler with the CFX96™ real-time PCR detection system (Bio-Rad Laboratories, California, USA). Thermocycling conditions consisted of reverse transcription at 55℃ for 10 minutes and initial denaturation at 95℃ for 60 seconds. This was followed by 40 cycles of denaturation at 95℃ for 10 seconds, annealing at 58℃ for 30 seconds and extension at 60℃ for 60 seconds. Specificity of amplification was verified by melt-curve analysis (60-95℃). Expression of genes was normalised to GAPDH expression, and relative fold change in expression between transfected and mock transfected samples was determined using the delta delta Ct method (Livak and Schmittgen, 2001).

Table 3. Forward (F) and Reverse (R) primers used for qRT-PCR of transcripts encoding innate immune response proteins

Gene	Primer Name	Primer Sequence (5'-3')	Amplicon size (bp)
OAS1	OAS1-F	CGAGGGAGCATGAAAACACATTT	84
	OAS1-R	GCAGAGTTGCTGGTAGTTTATGAC	
PKR	PKR2-F	GAAGTGGACCTCTACGCTTTGG	106
	PKR2-R	TGATGCCATCCCGTAGGTCTGT	
IFN-β	IFN-β-F	TCCAAATTGCTCTCCTGTTGTGCT	110
	IFN-β-R	CCACAGGAGCTTCTGACACTGAAAA	
IFIT	IFIT-F	CCCTGAAGCTTCAGGATGAAGG	182
	IFIT-R	AGAAGTGGGTGTTTCCTGCAAG	
GAPDH	GAPDH-F	GAAGGTGAAGGTCGGAGTC	226
	GAPDH-R	GAAGATGGTGATGGGATTTC	

2.5 Formulation of saRNA-Luc2 lipoplexes for *in vivo* delivery in mice

To enable *in vivo* delivery and uptake of saRNAs following intramuscular injection, saRNA-Luc2 was formulated with the cationic liposome-CaLiVax (OZ Biosciences, California, USA). CaLiVax is composed of the cationic lipid DOTAP (N-[1-(2,3-Dioleoyloxy) propyl]-N,N,N trimethyl-ammonium methyl-sulfate), and cholesterol in a 1:1 molar ratio. These positively

charged liposomes are capable of spontaneous binding to negatively charged saRNAs, forming lipoplexes which can be administered *in vivo*. A total of 50 µg saRNA-Luc2 was diluted in 1x HEPES buffer (20 mM HEPES, 150 mM sodium chloride (NaCl), pH 7.5) and combined with CaLiVax in a 2.5:1 N:P ratio. The N:P ratio describes the molar ratio of nitrogen atoms in DOTAP to the phosphate atoms in the saRNA. The solution was gently mixed on a platform shaker for an hour at room temperature to allow formation of lipoplexes. A 25x dilution of the formulation, using nuclease-free water, was prepared in a cuvette and the size of lipoplexes and polydispersity index of the formulation was measured using the Malvern ZetaSizer Pro Blue (Malvern Panalytical, Malvern, UK). Lipoplexes were stored at 4 °C.

2.6 Quantification of saRNA-Luc2 complexed to CaLiVax liposomes by Ribogreen™ assay

To quantify the amount of saRNA-Luc2 complexed to the exterior of CaLiVax liposomes and determine dose for *in vivo* studies, the Quant-it™ RiboGreen RNA kit (Invitrogen, Massachusetts, USA) was used. This kit quantifies unbound saRNAs using a fluorescent RNA binding dye and interpolation to a standard curve. Samples used to produce a standard curve with concentrations ranging from 0.1 to 2.5 ng/ul were prepared using the provided ribosomal RNA (rRNA) standard. The required amount of rRNA for each standard was diluted in 1X Tris EDTA (TE) buffer with 1% Triton™ X-100 (Sigma Aldrich, Missouri, USA) in a final volume of 100 µl. CaLiVax-saRNA-Luc2 was diluted 125x using 1x TE buffer in a final volume of 100 µl per well to quantify free unbound saRNAs. To quantify total saRNAs (complexed and free) CaLiVax-saRNA-Luc2 was diluted 125x using 1x TE buffer with 1% Triton™-X100 in a final volume of 100 µl per well to lyse lipoplexes and release complexed saRNAs. Blank samples using HEPES buffered saline diluted in 1x TE buffer with and without 1% Triton™-X100 were also prepared. All standards, samples, and blanks were prepared in duplicate and plated in a black 96-well plate. The plate was incubated at 37°C for 10 minutes. The Quant-iT™ RiboGreen™ RNA reagent was diluted 100x with 1x TE buffer and 100 µl was added to each well. Fluorescence was measured using the GloMax® Explorer (Promega, Wisconsin, USA) using an excitation wavelength of 475 nm and emission wavelength of 500-550 nm. A standard curve was prepared and the concentration of saRNAs present in all samples were interpolated from the curve and adjusted for background fluorescence and dilution factor. The percentage of complexed RNA was calculated using the following equation:

$$\left(1 - \frac{Fluorescence\ Value\ of\ Lipoplexes\ Lysed\ with\ Triton™ - X100}{Fluorescence\ Value\ of\ Lipoplexes\ in\ TE\ buffer}\right) \times 100$$

2.7 *In vitro* transfection of HEK 293T cells with CaLiVax-saRNA-Luc2 lipoplexes and detection of Luc2 expression

To examine whether lipoplexes were successfully taken up by cells *in vitro*, HEK 293T cells were seeded in a 48 well-plate and transfected with 250 ng saRNA-Luc2 formulated with CaLiVax in a volume of 25 µl Opti-MEM™. Negative controls consisted of cells transfected with CaLiVax alone. Following a 72-hour incubation, cell culture media was removed, and cells were lysed with 65 µl of 1x passive lysis buffer (Promega, Wisconsin, USA) for 15 minutes on a shaking platform. Following incubation, 20 µl of each lysate was transferred to a white 96-well plate and 100 µl of Luciferase assay substrate reconstituted in Luciferase assay buffer II (Promega, Wisconsin, USA) was added to each well. Luciferase activity in the form of relative light units was measured using the GloMax® Explorer (Promega, Wisconsin, USA).

2.8 Animal studies

All *in vivo* experiments were performed on female Naval Medical Research Institute (NMRI) mice, aged approximately 8 weeks. Mice were obtained from the National Institute for Communicable Diseases and housed at the Wits Research Animal Facility. A minimal acclimation period of one week was allowed prior to commencement of interventions. Mice were weighed weekly, and wellness checks were performed daily. Additional wellness monitoring was performed twice on the day of an intervention and the day after. All experiments were approved by the Animal Research Ethics Committee (AREC clearance certificate number:2021/08/06/C).

A prime-boost vaccination regimen was adopted, with mice receiving the first and second doses on days 0 and 28 respectively. saRNA-Luc2, saRNA-S-HBsAg, and saRNA-L-HBsAg were diluted to a concentration of 0.1 µg/µl using RNase-free saline. Groups of mice received either saline (n=3), 5 µg of unformulated saRNA-Luc2 (n=3), saRNA-S-HBsAg (n=2) or saRNA-L-HBsAg (n=2) delivered by electroporation, or 5 µg saRNA-Luc2 formulated with CaLiVax. Injections were delivered to the left hind limb in a maximum volume of 50 µl. *In vivo* electroporation was performed using the Teresa DNA delivery device (Shanghai Teresa Healthcare Sci-Tech, Shanghai, China). Six 60 V pulses, each lasting 50 milliseconds with a

one-second interval between pulses, was applied around the injection site to facilitate uptake of unformulated saRNAs.

To examine *in vivo* expression of luciferase, mice that received saRNA-Luc2 by electroporation or formulated with CaLiVax, underwent bioluminescence imaging on days 3 and 7 following the initial priming dose, and 7 days post-booster using the IVIS Kinetic imaging system (Caliper Life Sciences, Massachusetts, USA). Mice were first injected intraperitoneally with 150 mg/kg D-luciferin and placed in a chamber containing 5% Isofor. Once sedated, mice were transferred to the imaging chamber where the Isofor concentration was reduced to 1%. Images were taken at 1-, 5-, 10- and 30-seconds post exposure.

Blood samples were collected from mice (retro-orbital sampling) prior to prime and booster injections, and a terminal bleed was performed two weeks post-booster injections. Blood was allowed to clot at room temperature for 30 minutes before centrifugation at 2 000 x g for 20 minutes. Serum was harvested for analysis of immune responses and stored at -80°C. Mice were sedated using Isofor and euthanised by carbon dioxide asphyxiation.

2.9 Software and statistical analysis

Figures were produced using BioRender (https://www.biorender.com) and Microsoft Word. SnapGene version 7.0.1 was used to generate plasmid maps and design primers for sequencing and PCR. Sequencing data were analysed and aligned using Benchling (https://benchling.com).

Data generated from qRT-PCR, ELISAs, luciferase assays and RiboGreen™ assays were plotted and analysed using Microsoft Excel. Statistical differences were determined using a Student's t-test with $p < 0.05$ indicating significance.

3. RESULTS

3.1. Preparation of plasmid DNA templates for IVT of bi-cistronic saRNAs

3.1.1 Verification of plasmids by diagnostic restriction digest

Plasmids T7-VEEV-S-HBsAg-IRES-mCherry and T7-VEEV-L-HBsAg-IRES-mCherry were used as IVT templates to produce saRNA HBV vaccine constructs. These plasmids were propagated in competent *E. coli* cells, extracted by alkaline lysis, and purified using anion-exchange columns. To verify the identity of plasmids, restriction digests followed by analysis of fragment banding patterns by agarose gel electrophoresis were performed. To verify size, T7-VEEV-S-HBsAg-IRES-mCherry and T7-VEEV-L-HBsAg-IRES-mCherry were linearised with *Eco*RI, which was expected to produce single bands of 11 550 and 12 072 base pairs (bp), respectively (Table 4) (Appendix A-Figure A3). The DNA molecular weight marker used to estimate the size of fragments had a maximum size standard of 10 kb, therefore it was not possible to confirm the correct size of linearised plasmids. However, prominent bands migrating just above the 10 kb molecular weight standard were observed indicating linearised plasmids (Figure 8). Plasmids were also digested with *Nco*I, which cuts at six specific sites within each plasmid to produce six fragments (Table 4) (Appendix A-Figure A3). Five fragments were common to both plasmids. The sixth fragment, generated by digestion at sites flanking the antigen sequence, was larger in T7-VEEV-L-HBsAg-IRES-mCherry allowing a distinction to be made between the two HBV antigen encoding plasmids. Digestion of both plasmids with *Nco*I produced the correct banding pattern confirming their identity (Figure 8). Similarly sized fragments (4 081 and 3 910 bp) were not fully resolved and were observed as a more prominent band around 4 000 bp.

Table 4. Expected size of fragments generated by restriction enzyme digestion of T7-VEEV-S-HBsAg-IRES-mCherry and T7-VEEV-L-HBsAg-IRES-mCherry

Plasmid	Fragment sizes (bp)	
	***Eco*RI**	***Nco*I**
T7-VEEV-S-HBsAg-IRES-mCherry	11 550	4 081
		3 910
		1 301
		1 090
		733
		435
T7-VEEV-L-HBsAg-IRES-mCherry	12 072	4 081
		3 910
		1 823
		1 090
		733
		435

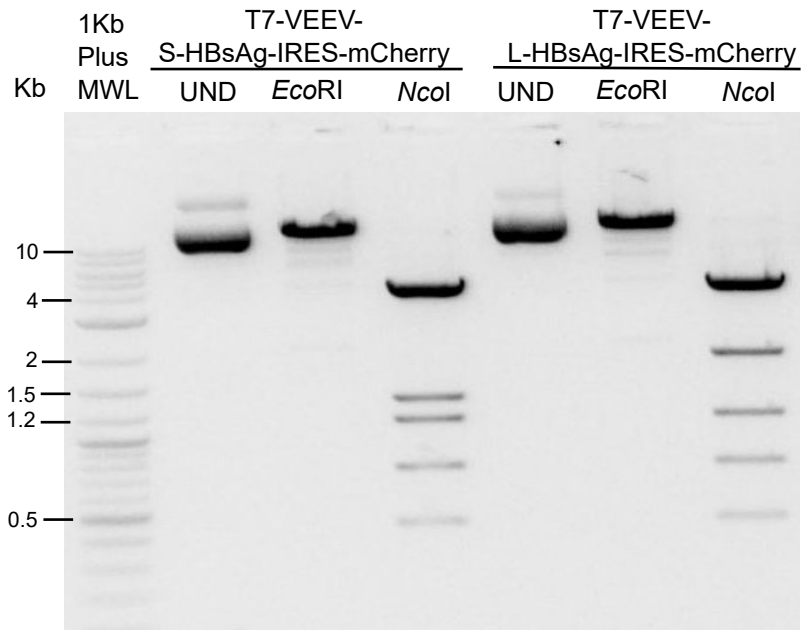

Figure 8. Restriction digest of plasmids encoding bi-cistronic saRNA vaccine constructs.

T7-VEEV-S-HBsAg-IRES-mCherry and T7-VEEV-L-HBsAg-IRES-mCherry were digested with restriction enzymes *Eco*RI and *Nco*I. Resulting fragments (1µg) were analysed by agarose

gel electrophoresis to confirm identity of plasmids based on expected banding patterns. MWL = molecular weight ladder; UND = undigested controls.

3.1.2 Confirmation of linearisation and purification of IVT templates

Prior to IVT, plasmids were linearised by restriction digestion with *Mlu*I, which cleaves just after the poly-A tail sequence. Linearisation ensures that T7 RNA polymerase, which initiates transcription of saRNAs at the upstream T7 promoter site, runs off the 3' end of the DNA template, ceasing transcription immediately after the poly-A tail sequence to produce uniformly sized synthetic saRNA transcripts. Cleavage with *Mlu*I generates a 5' overhang at the end of the transcript, however this does not promote the formation of aberrant transcripts as observed with templates containing 3' overhangs (Schenborn and Mierendorf, 1985).

Complete linearisation of all plasmids was achieved (Figure 9). Expected band sizes for linearised T7-VEEV-eGFP-IRES-PuroR, T7-VEEV-Fluc-IRES-mCherry, T7-VEEV-S-HBsAg-IRES-mCherry and T7-VEEV-L-HBsAg-IRES-mCherry were 11 521, 12 523, 11 550, and 12 072 bp respectively (larger than the 10 kb molecular weight standard). In comparison, the undigested plasmid controls produced two bands: a faint higher molecular weight band indicative of nicked plasmid DNA, and a more prominent lower molecular weight band representing supercoiled plasmid DNA. Both these conformations are not conducive to IVT. Linearised plasmids were purified using silica-packed spin columns with an average recovery of template of 77%, indicating that a small amount of template was retained in the column. Subsequent purifications of linearised plasmid templates were performed using sodium acetate and ethanol precipitation which had a higher average yield of 90.5%.

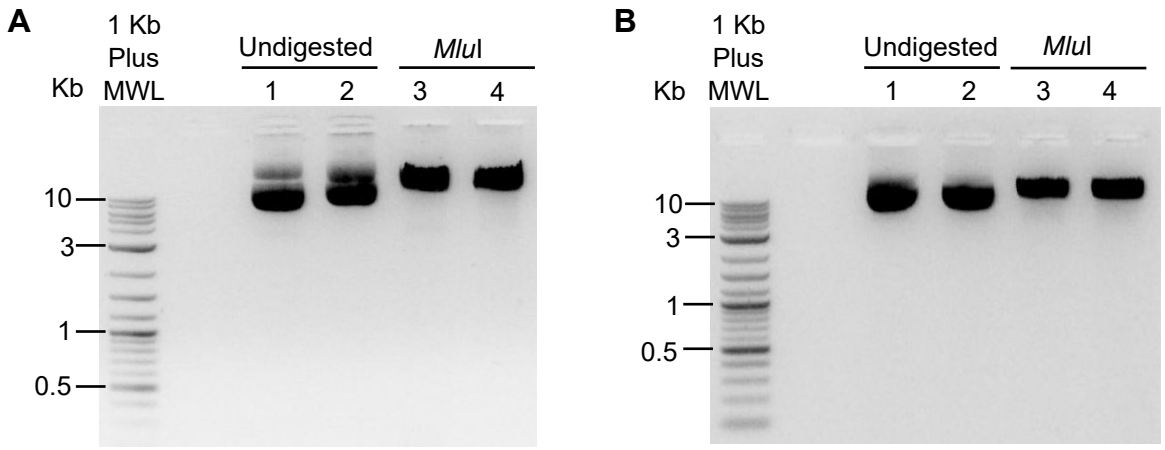

Figure 9. Linearisation of plasmid templates in preparation for IVT.

(A) T7-VEEV-eGFP-IRES-PuroR (1) and T7-VEEV-Fluc-IRES-mCherry (2), were linearised using *Mlu*I to produce single bands of 11 521 (3) and 12 523 (4) base pairs respectively. **(B)** Similarly, HBV vaccine-encoding plasmids T7-VEEV-S-HBsAg-IRES-mCherry (1) and T7-VEEV-L-HBsAg-IRES-mCherry (2) were linearised using *Mlu*I to produce single bands of 11 550 (3) and 12 072 (4) base pairs respectively. Approximately 1µg of each digest was analysed by agarose gel electrophoresis to confirm complete linearisation.

3.2 Synthesis of bi-cistronic saRNAs by IVT and analysis of protein expression

3.2.1 IVT using the Ampliscribe™ T7 Flash™ kit

The commercially available Ampliscribe™ T7 Flash™ kit was used to synthesise saRNA-Fluc-IRES-mCherry (10 698 bases) from linearised T7-VEEV-Fluc-IRES-mCherry. One microgram of plasmid template was used to transcribe saRNAs in a 20 µl IVT reaction, which was incubated at 37 °C for 30 minutes. A linearised positive control DNA template provided in the kit was also transcribed under the same conditions. Transcripts were subsequently purified by ammonium acetate and ethanol precipitation. A yield of 159 µg saRNAs was achieved which was similar to the yield obtained for the kit control (155 µg). However, size and integrity analysis by formaldehyde gel electrophoresis revealed smearing along the sides of the wells below the expected band (Figure 10). This indicated the presence of incomplete or degraded transcripts. The smearing along the sides of the wells could be an artefact of the gel as the molecular weight standards were also concentrated along the sides of the wells. The positive control was successfully transcribed with minimal smearing. Although the same amount of

control mRNA and saRNA was loaded onto the gel, the smaller control mRNA stained more intensely, forming a more prominent band.

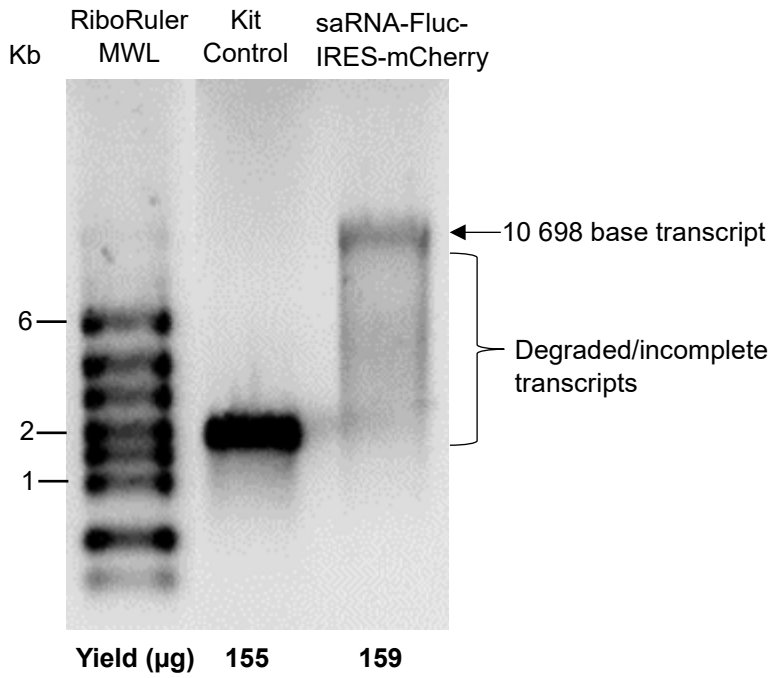

Figure 10. Integrity of saRNA-Fluc-IRES-mCherry produced with the Ampliscribe™ T7 Flash™ kit.

saRNA-Fluc-IRES-mCherry (10 698 bases) was synthesised using the Ampliscribe™ T7 Flash™ kit and purified using ammonium acetate and ethanol precipitation. mRNA/saRNA yield obtained for each reaction is depicted below the gel. Each lane was loaded with 0.5 µg of the respective sample.

To improve the quality and yield of saRNAs, the following modifications to the standard protocol were investigated: a) IVT reaction time was increased to one hour to allow more time for synthesis of longer saRNAs; b) reaction temperature was increased to 42 °C to increase the processivity of T7 RNA polymerase; and c) linearised plasmid DNA was increased from 1 µg to 2 µg to provide more template DNA for IVT. Increasing incubation time to one hour increased saRNA yield by 244%. Increasing incubation temperature to 42 °C together with a one hour incubation time resulted in a 335% increase in transcript yield. Doubling the DNA template together with a one hour incubation time did not improve yield, which was less than the yield obtained under recommended conditions. Under all conditions tested, incomplete or degraded transcripts were still observed (Figure 11).

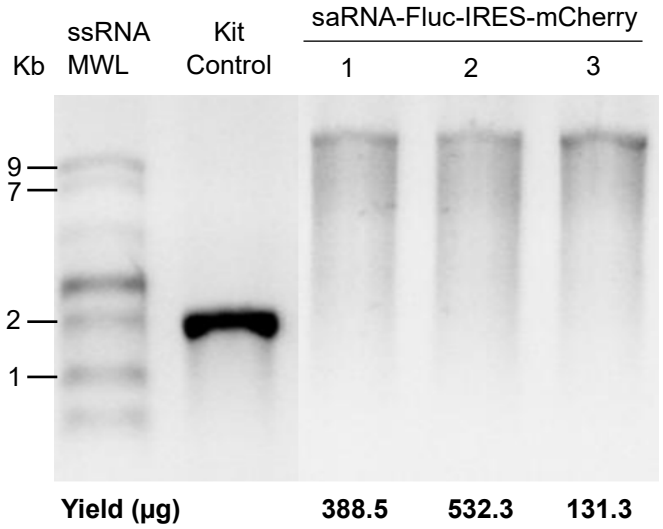

Figure 11. Effect of modifications to recommended IVT reaction conditions on RNA integrity and yield using the Ampliscribe™ T7 Flash™ kit.

IVT reaction time for the synthesis of saRNA-Fluc-IRES-mCherry was increased to one hour (1), temperature was increased to 42 ℃ with incubation time of one hour (2), and plasmid DNA template was doubled to 2 µg with incubation time of one hour (3). saRNA yield obtained for each reaction is depicted below the gel. Each lane was loaded with 0.5 µg of the respective sample.

saRNA-eGFP-IRES-PuroR, which encodes the eGFP fluorescent reporter and used to visually confirm transfection and translation of saRNAs, was transcribed in a standard IVT reaction but with an increased incubation period of two hours, to determine whether further improvement to saRNA yield could be achieved. A yield of 182 µg was achieved, which was less than the yield achieved with a one-hour incubation period. Further research into the activity of the T7 RNA polymerase used in the kit revealed that unlike T7 RNA polymerases used in other commercial kits, maximum RNA yield was achieved around one hour with no further increases in yield even with longer incubation periods (Appendix C-Figure C1). Analysis of transcripts by formaldehyde gel electrophoresis revealed a distinct band depicting full-length transcripts (9 695 bases), however, the degree of degradation/incomplete transcripts was greater than before (Figure 10A). saRNA-eGFP-IRES-PuroR (10 µg) was enzymatically capped with a cap 1 structure, using the Vaccinia capping system, to mimic endogenous mRNAs. Capped transcripts were purified using ammonium acetate and ethanol precipitation, however this resulted in further degradation of saRNA transcripts and a 15% loss in transcript recovery

(Figure 12A). Nevertheless, remarkable expression of eGFP was observed in HEK 293T cells transfected with 100 ng of cap 1-saRNA-eGFP-IRES-PuroR at 24 hours post-transfection (Figure 12B). Expression of eGFP was observed for as long as 15 days after transfection. Good expression was also observed in cells transfected with as little as 50 ng, highlighting the advantage of using saRNAs for prolonged antigen expression.

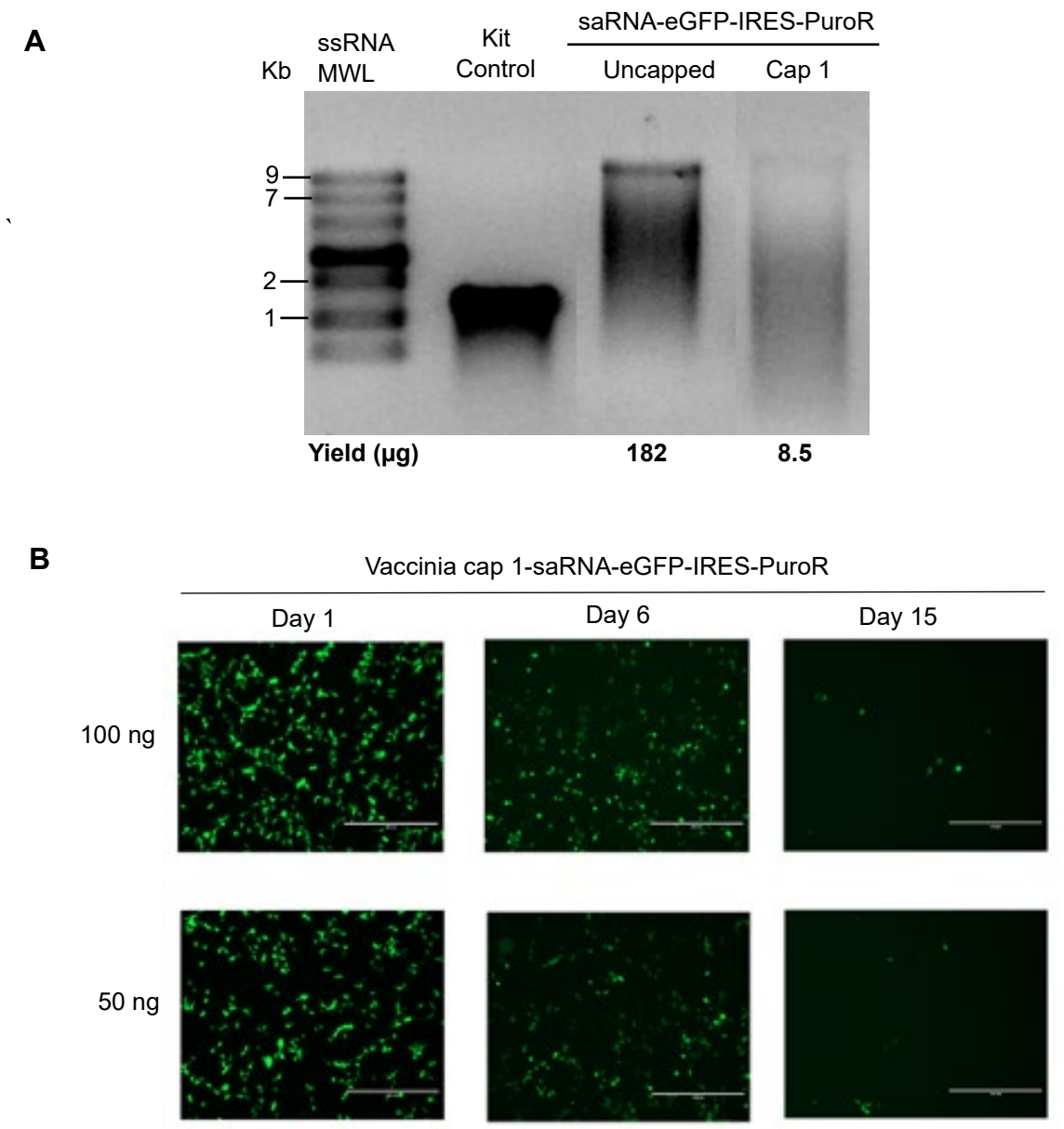

Figure 12. IVT, enzymatic capping, and *in vitro* expression of saRNA-eGFP-IRES-PuroR.

(A) Integrity and size analysis of saRNA-eGFP-IRES-PuroR (9 695 bases) following standard IVT with 2-hour incubation period before and after capping with the Vaccinia capping system. Gels were loaded with 1 µg of each sample for better visualisation of the expected band. **(B)** Expression of eGFP in HEK 293T cells transfected with cap 1-saRNA-eGFP-IRES-PuroR detected by fluorescence microscopy. Scale bar: 400 µm.

3.2.2 IVT using the RiboMAX™ Large scale RNA production system

To determine whether improved saRNA yields and transcript integrity could be achieved using another commercially available kit, the RiboMAX™ Large scale RNA production system was used to transcribe saRNA-eGFP-IRES-PuroR. To increase the yield, a 100 µl reaction was performed according to kit instructions. This protocol differed from the Ampliscribe™ T7 Flash™ kit by using a higher concentration of plasmid DNA (100 ng/µl), lower NTP concentration (5 mM), and incubation for two hours (Appendix B8). Ampliscribe™ T7 Flash™ kit buffer constituents were proprietary and thus unavailable for further comparison. A yield of 674 µg was achieved, but importantly, a greater proportion of transcripts appeared to be full-length (9 696 bases) (Figure 13A).

Natural *in situ* replication of cap 1 saRNAs will result in the production of transcripts with a cap 0 structure. To determine whether there was a difference in expression between cap 0 and cap 1 transcripts, saRNA-eGFP-IRES-PuroR was capped with cap 0 or cap 1 using the Vaccinia capping system. Full-length transcripts were observed post-capping with low molecular weight smearing still present (Figure 13B). Post-transcriptional capping also resulted in a loss of saRNA yield, with an average of 66.5% of capped transcripts recovered following purification. Expression of eGFP from both cap 0 and cap 1 transcripts was observed in HEK 293T cells 24 hours post-transfection, with slightly greater expression from cap 1 transcripts (Figure 13C).

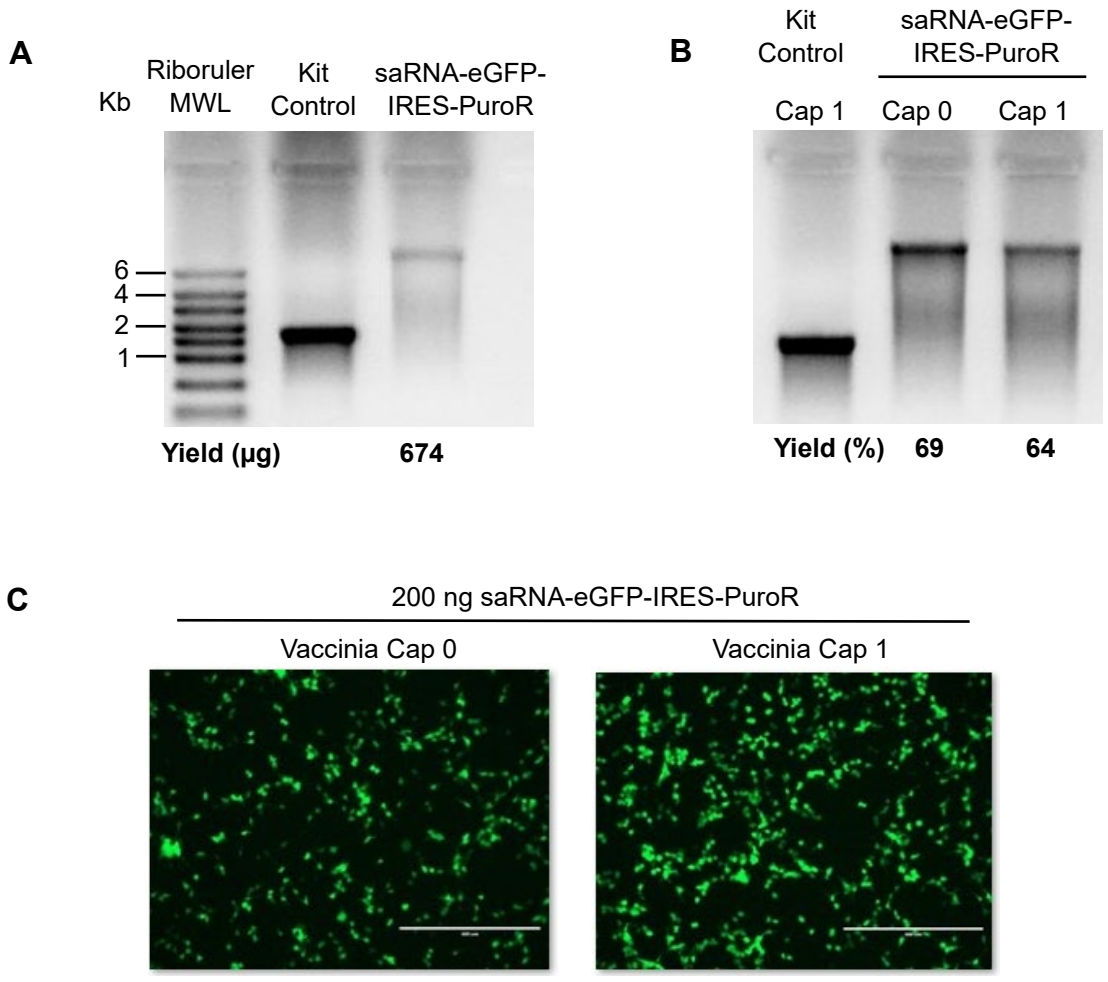

Figure 13. Integrity and expression of saRNA-eGFP-IRES-PuroR synthesised using the RiboMAX™ Large scale RNA production system.

(A) Integrity and size analysis of uncapped saRNA-eGFP-IRES-PuroR (9 695 bases) transcribed in a 100 µl reaction using the RiboMAX™ Large scale RNA production system. The yield obtained is indicated at the bottom of the gel. **(B)** Integrity analysis of transcripts post-transcriptionally capped with a cap 0 or cap 1 structure using the Vaccinia capping system. Percentage recovery is indicated at the bottom of the gel. Gels were loaded with 1 µg of each sample. **(C)** Expression of eGFP in HEK 293T cells 24 hours post-transfection with 200 ng of cap 0 or cap 1 saRNA-eGFP-IRES-PuroR. Scale bar: 400 µm.

saRNA-S-HBsAg-IRES-mCherry was transcribed and capped with a cap 1 structure using the same protocols. Degradation of capped transcripts was more evident, however, a faint band of the expected size (9 725 bases) was present (Figure 14A). Since eGFP expression was previously observed from seemingly degraded transcripts, cap 1 saRNA-S-HBsAg-IRES-mCherry was used to transfect HEK 293T cells to determine whether S-HBsAg and mCherry

could be simultaneously expressed from the bi-cistronic transcript. Expression of mCherry was examined by fluorescence microscopy, and cell culture supernatant was analysed by ELISA for expression of secreted S-HBsAg. Following a 24-hour incubation, neither mCherry nor S-HBsAg was detected (Figure 14B). It is likely that saRNAs encoding S-HBsAg and mCherry were taken up by cells, but translation of the proteins may have been inhibited.

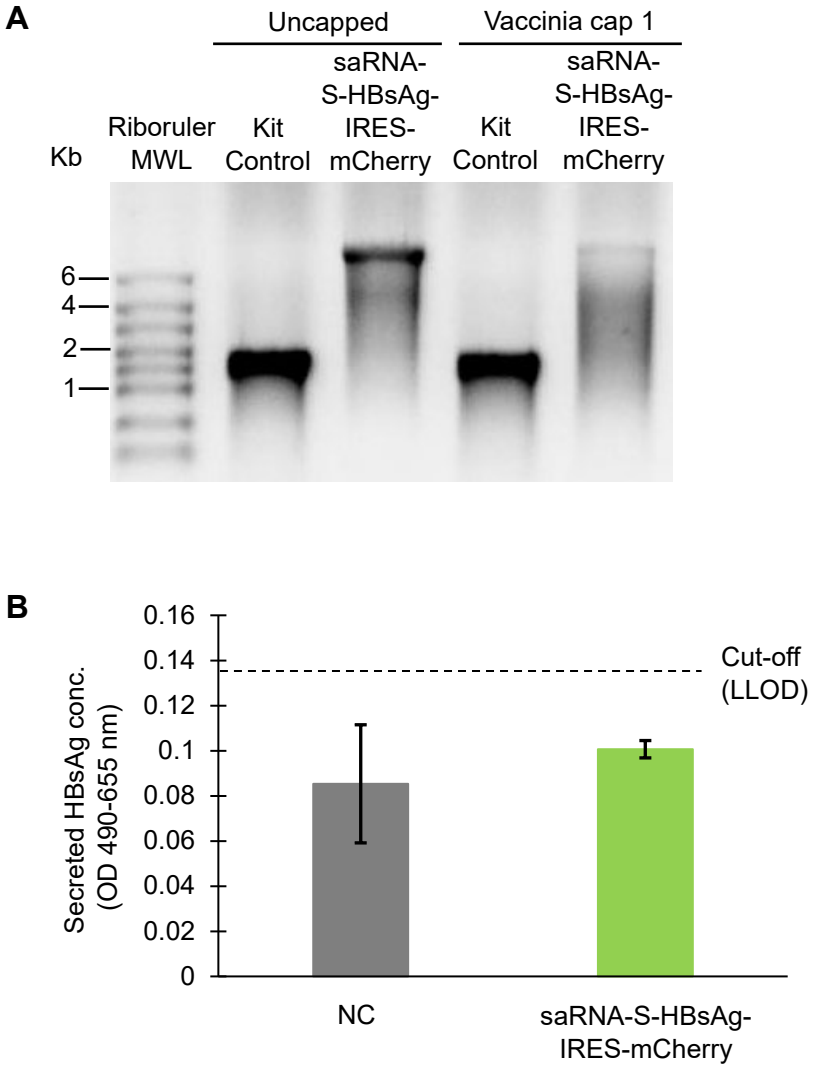

Figure 14. Integrity and expression of saRNA-S-HBsAg-IRES-mCherry synthesised using the RiboMAX™ Large scale RNA production system.

(A) Integrity and size analysis of uncapped and vaccinia cap 1 saRNA-S-HBsAg-IRES-mCherry (9 725 bases) **(B)** Expression of secreted S-HBsAg determined by the Monolisa™ HBs Ag Ultra ELISA kit. Cut-off = Average OD of Negative Control (NC) + 0.05. LLOD = Lower limit of detection

3.3. Isolation of full-length saRNAs using Oligo d(T)25 magnetic beads

To purify full-length transcripts oligo $d(T)_{25}$ conjugated magnetic beads were used to bind to poly-A tails of saRNA-eGFP-IRES-mCherry allowing separation from degraded or incomplete transcripts. A recovery of 28% saRNAs was achieved. This was lower than expected since integrity analysis of transcripts prior to oligo $d(T)_{25}$ purification suggested that a higher proportion of transcripts were full-length. It should be noted that oligo $d(T)_{25}$ magnetic beads are successfully used for purification of smaller mRNAs. Thus, is likely that the longer length of saRNAs and the relatively fewer number of poly-A tails in a corresponding amount starting material hinders efficient binding. Size and integrity analysis by gel electrophoresis demonstrated that full-length transcripts were successfully isolated as indicated by the absence of low molecular weight smears observed in previous gels (Figure 15).

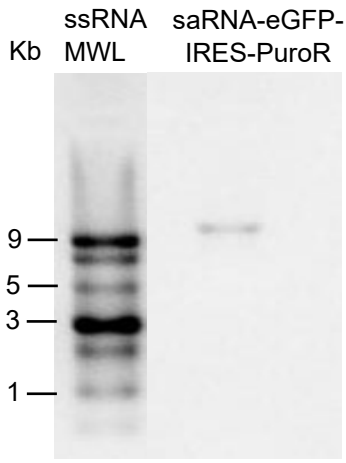

Figure 15. Integrity of saRNAs purified using Oligo $d(T)_{25}$ magnetic beads.

Full-length saRNA-eGFP-IRES-mCherry (9 695 bases) was isolated using oligo $d(T)_{25}$ magnetic beads. As a result of low concentration following purification, approximately 355 ng of purified transcripts was assessed for presence of degraded or incomplete transcripts.

3.4 Cloning of plasmids encoding single-cistron saRNAs

saRNA vaccine constructs were designed to express two proteins (viral antigens/reporter proteins) from the sub-genomic mRNA by inclusion of an IRES between the sequences encoding the proteins. However it has been previously demonstrated that an IRES within a bi-cistronic construct can alter expression kinetics or even inhibit expression of some proteins (Hennecke et al., 2001). This provides a plausible explanation for the lack of expression of

mCherry and S-HBsAg using the current bicistronic designs. Thus, saRNA vaccine constructs were re-designed to enable expression of the single antigen of interest. Using a two-step cloning strategy (Figure 5), all plasmids encoding saRNAs were re-constructed to encode a single reporter or antigen of interest by excluding the IRES and downstream mCherry/PuroR sequences. In addition, an extended poly-A (60) tail was also incorporated into plasmids to increase the *in situ* longevity and translatability of transcripts.

Sequences encoding S-HBsAg (681 bp) or L-HBsAg (1203 bp) were ligated into the MCS of subcloning plasmid pUC57-saRNA-MCS-poly-A (60), upstream of sequences encoding a VEEV-derived 3' CSE, poly-A (60) tail, and *Mlu*I restriction site (Figure 5). The resulting plasmids were propagated in competent cells and purified. Positive clones for pUC57-S-HBsAg-poly-A (60) and pUC57-L-HBsAg-poly-A (60) were identified by restriction digestion using the enzymes *Alw*44I and *Apa*I. This digestion was expected to produce four fragments and positive clones were identified by examining banding patterns produced following agarose gel electrophoresis (Table 5; Figure 16A). Positive clones for each plasmid were thereafter digested with *Not*I and *Mlu*I restriction enzymes to excise sequences encoding S-HBsAg or L-HBsAg, 3' CSE and extended poly-A tail. These insert fragments were then individually ligated into the T7-VEEV backbone, which was generated by digestion with *Not*I and *Mlu*I to remove sequences encoding eGFP-IRES-PuroR (Figure 5). Successful ligation resulted in plasmids T7-VEEV-SHBsAg and T7-VEEV-L-HBsAg, which were used as templates to produce single-cistron saRNA-S-HBsAg and saRNA-L-HBsAg, respectively. Positive clones were identified by restriction digest with *Nco*I which cuts at four sites within each plasmid to produce four fragments (Table 5; Figure 16B).

Table 5. Expected size of fragments following restriction enzyme digestion of subcloning plasmids and plasmids encoding single-cistron saRNAs

Subcloning plasmids	**Fragment sizes (bp)** (*Alw*44I and *Apa*I)	**Single-cistron saRNA-encoding plasmids**	**Fragment sizes (bp)** (*Nco*I)
pUC57-S-HBsAg-Poly-A (60) (3 354 bp)	1 246	T7-VEEV-S-HBsAg (10 261 bp)	4 528
	987		3 910
	624		1 090
	497		733
pUC57-L-HBsAg-Poly-A (60) (3 876 bp)	1 246	T7-VEEV-L-HBsAg (10 783 bp)	5 050
	1 146		3 910
	987		1 090
	497		733

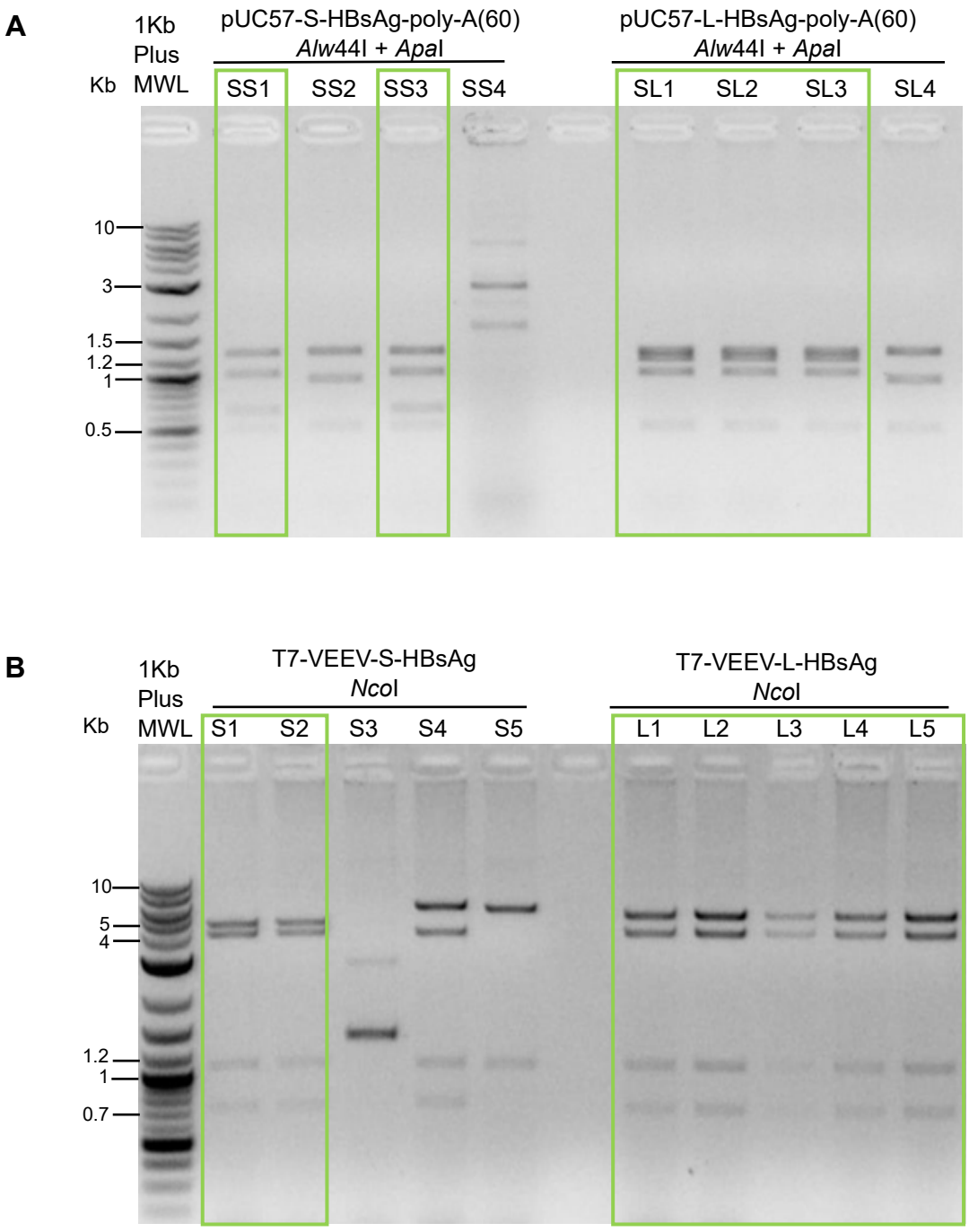

Figure 16. Identification of positive clones by restriction digestion.

(A) Clones SS1-SS4 and SL1-SL4 were screened by restriction digestion with *Alw*44I and *Apa*I to identify subcloning plasmids pUC57-S-HBsAg-Poly-A (60) and pUC57-L-HBsAg-Poly-A (60). **(B)** Clones S1-S5 and L1-L5 were screened by restriction digestion with *Nco*I to identify saRNA-encoding plasmids T7-VEEV-S-HBsAg and T7-VEEV-L-HBsAg. Positive clones which produced the expected banding pattern are outlined in green. Each lane was loaded with 1 µg of the respective samples.

3.5 Correction of base substitution error in L-HBsAg open reading frame

To confirm successful cloning and verify key sequences encoding antigens of interest and immediate flanking regions, subcloning plasmids and single-cistron saRNA encoding plasmids were sequenced by Sanger sequencing. Alignment of sequencing chromatograms with reference sequences revealed a base substitution error (T→G) at the C-terminus of the L-HBsAg ORF in both pUC57-L-HBsAg-Poly-A (60) and T7-VEEV-L-HBsAg (Appendix C; Figure C2 and C3). This incorrect base was most likely present in the L-HBsAg amplicon used to produce pUC57-L-HBsAg-Poly-A (60) and may have been introduced during PCR. The T→G substitution resulted in a non-synonymous mutation, altering the codon encoding cysteine (TGT) at amino acid position 395 of L-HBsAg, to glycine (GGT). Since pUC57-S-HBsAg-Poly-A (60) contained the correct C-terminal sequence, this plasmid was used to produce pUC57-L-HBsAg-Poly-A (60) with the correct sequence using a simple cloning strategy (Figures 6 and 17A). To confirm that pUC57-L-HBsAg-poly-A (60) and T7-VEEV-L-HBsAg contained the correct C-terminal sequence, the S-HBsAg domain from both plasmids were amplified by PCR using a high-fidelity polymerase (Appendix C; Figure C4), and amplicons were sequenced. Sanger sequencing confirmed the correct sequence in both plasmids (Figures 17 B and C).

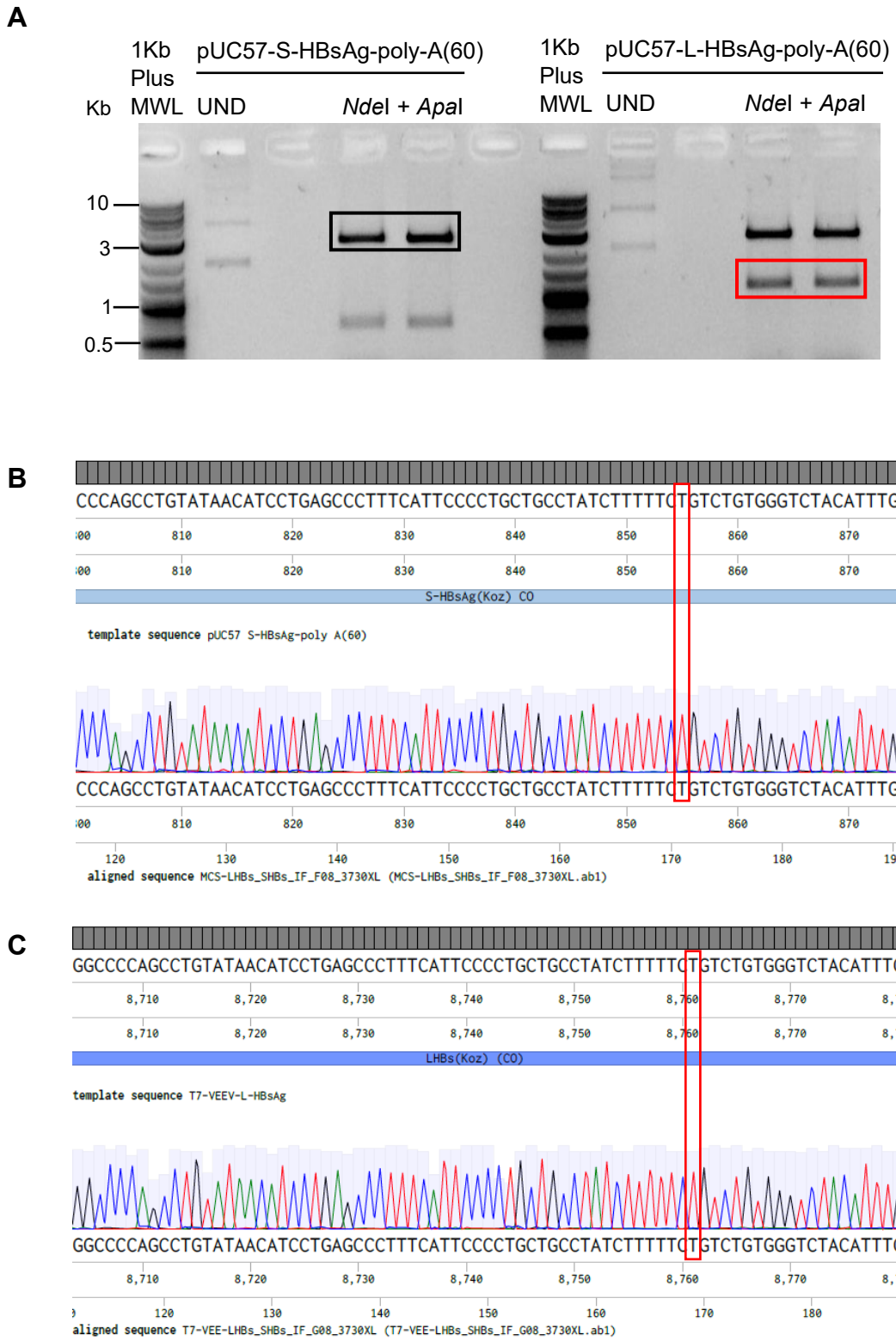

Figure 17. Correction of base substitution error in C-terminus of L-HBsAg open reading frame.

(A) pUC57-S-HBsAg-Poly-A (60) was digested with *Nde*I and *Apa*I to produce a 2 737 bp backbone (black box) with the correct HBsAg C-terminal sequence. Sequences encoding L-HBsAg upstream of the mutation (1 139 bp) was excised from pUC57-L-HBsAg-Poly-A (60)

(red box) using the same enzymes and ligated to the pUC57-S-HBsAg-Poly-A (60) backbone to produce pUC57-L-HBsAg-Poly-A (60) with the correct sequence. Sequence alignment of S-HBsAg domain amplified from corrected pUC57-L-HBsAg-poly-A(60) **(B)**, and T7-VEEV-L-HBsAg **(C),** with reference sequences. Red boxes indicate the location of base substitution errors identified previously.

3.6 *In vitro* transcription of single-cistron saRNAs

Plasmids T7-VEEV-Luc2 (11 296 bp), T7-VEEV-S-HBsAg (10 261 bp) and T7-VEEV-L-HBsAg (10 783 bp) were linearised after the poly-A (60) tail with the *Mlu*I restriction enzyme and purified using sodium acetate and ethanol precipitation in preparation for IVT. Complete linearisation was confirmed by agarose gel electrophoresis with both plasmids producing single bands greater than 10 kb (Figure 18A). An IVT buffer, optimised for the synthesis of saRNAs by inclusion of a high concentration of magnesium acetate, was prepared in-house and used for IVT of saRNA-Luc2 (9 471 bases), saRNA-S-HBsAg (8 436 bases) and saRNA-L-HBsAg (8 958 bases). This buffer solution, with an NTP:magnesium ion ratio of 1:1.875, has been reported to improve IVT yield of saRNAs (Samnuan et al., 2022). To reduce handling and loss of saRNAs, co-transcriptional capping using CleanCap® AU reagent (cap 1), was performed. These modifications resulted in a higher proportion of full-length saRNA transcripts compared to vaccinia capped transcripts (Figure 18 B). The average yield of capped saRNAs in a 100 µl reaction was 421 µg.

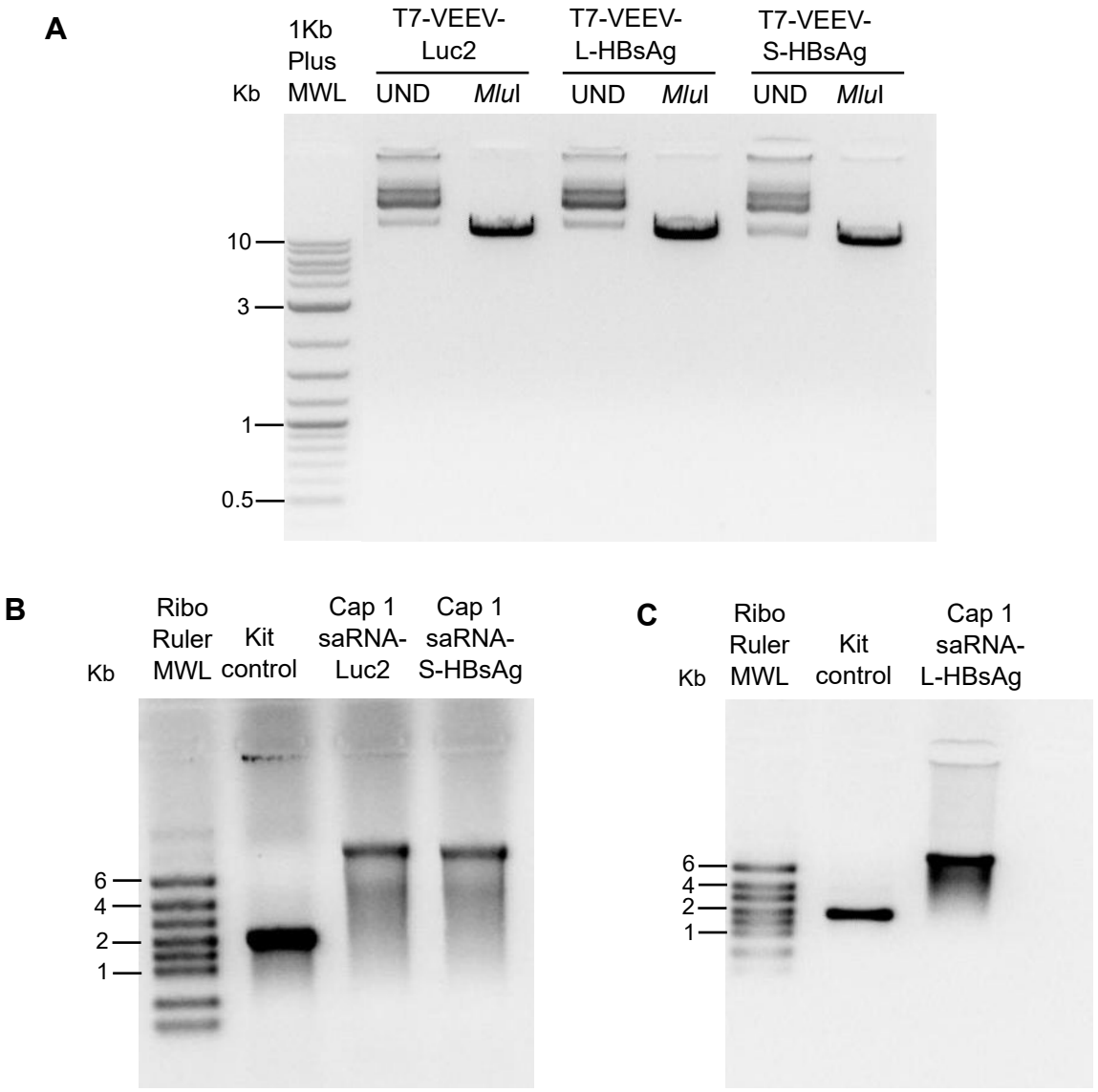

Figure 18. Linearisation of IVT templates and integrity analysis of single-cistron saRNA transcripts.

(A) Confirmation of complete linearisation of plasmids T7-VEEV-Luc2, T7-VEEV-S-HBsAg and T7-VEEV-L-HBsAg with the restriction enzyme *Mlu*I. **(B and C)** Size and integrity analysis of cap 1 saRNA-Luc2 (9 471bases), saRNA-S-HBsAg (8 436 bases) and saRNA-L-HBsAg (8 958 bases) transcripts produced using an optimised IVT protocol involving co-transcriptional capping with CleanCap® AU reagent (1µg/well). UND = undigested controls

3.7 Expression of S-HBsAg and L-HBsAg from single cistron transcripts

To determine whether S-HBsAg and L-HBsAg was expressed from single-cistron transcripts, HEK 293T cells were transfected with saRNA-S-HBsAg and saRNA-L-HBsAg and examined for expression of antigens using the Monolisa™ HBs Ag Ultra ELISA kit. This sandwich ELISA detects epitopes located in the S-HBsAg domain which is also present in L-HBsAg. S-HBsAg was detected in the supernatant of transfected cells, at quantities higher than that of cells transfected with an equal concentration of the positive control HBV replication-competent plasmid pCH9-3091 (Figure 19A). In contrast, L-HBsAg was only detected in lysates of cells transfected with saRNA-L-HBsAg indicating that the antigen was not secreted (Figure 19B).

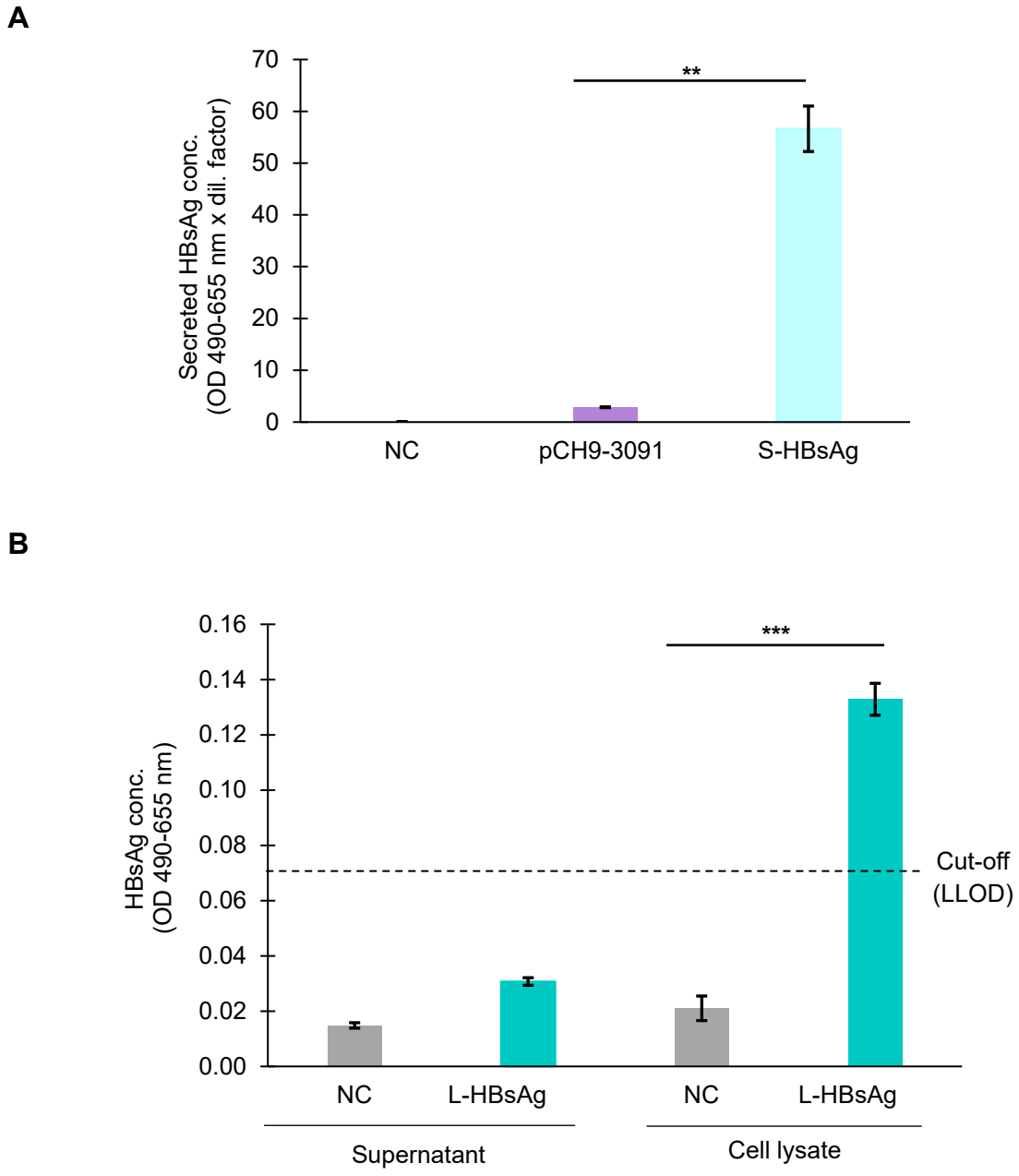

Figure 19. Detection of *in vitro* antigen expression from single-cistron saRNAs by ELISA.

(A) Comparison of S-HBsAg expression 48 hours after transfection of HEK 293T cells with 250 ng saRNA-S-HBsAg or an equivalent amount of the HBV replication-competent plasmid positive control pCH9-3091 in a 48-well plate (n=3). Supernatant dilution factors: pCH9-3091 = 4; S-HBsAg = 80. **(B)** Detection of L-HBsAg expression in supernatant and cell lysate of HEK 293T cells 48 hours after transfection with 250 ng saRNA-L-HBsAg in a 48 well plate (n=3). Results are depicted as the mean with standard error of the mean. Significant differences were calculated using a student's T test. **p < 0.01, ***p < 0.001. Cut-off = Negative control + 0.05. LLOD = Lower limit of detection.

3.8 *In vitro* innate immune response to saRNA and effect on antigen expression

3.8.1 Detection of innate immune system response to saRNAs by qRT-PCR

To determine the extent to which cap 1 saRNAs induce a type 1 interferon response *in vitro*, HEK 293T cells, transfected with increasing concentrations of saRNA-S-HBsAg or saRNA-Luc2, were examined for changes in the number of transcripts encoding IFN-β and interferon-inducible genes (OAS1, IFIT1, and PKR). Cells transfected with Lipofectamine alone served as negative controls whereas cells transfected with poly I:C served as positive controls. Total RNA was extracted 24 hours post-transfection and mRNA quality was inferred from integrity analysis of rRNA subunits by agarose gel electrophoresis. Two distinct bands representing the 28S and 18S rRNA subunits were observed, indicating intact rRNA subunits (Figure 20). Higher molecular weight bands representative of genomic DNA contaminants, which can also be amplified by qRT-PCR, were not observed in any of the samples. mRNA was thus deemed suitable for use in qRT-PCR.

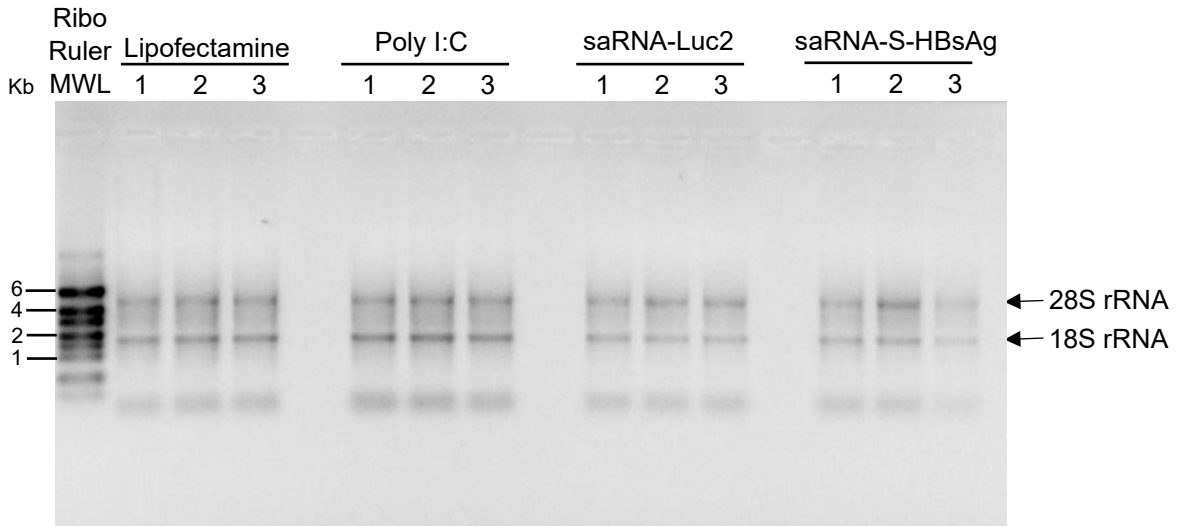

Figure 20. Integrity analysis of total RNA extracted from transfected HEK 293T cells.

Representative gel showing integrity of ribosomal RNA (rRNA) subunits (500 ng/well) that were extracted from HEK 293T cells transfected with Lipofectamine, Poly I:C, saRNA-Luc2 or saRNA-S-HBsAg (n=3).

Following RNA isolation, mRNA was reverse transcribed into cDNA. Gene-specific primer pairs were then used to amplify regions of cDNA encoding IFN-β, OAS1, IFIT1, PKR, and GAPDH (housekeeping gene) by real-time PCR. The absence of contaminating genomic DNA was confirmed by examining the Ct values for no reverse transcriptase control reactions with GAPDH-specific primers (Appendix C-Table C1). Ideally, no amplification should be observed in these samples, indicating the absence of genomic DNA. However, no RT controls with Ct values greater than 35, or at least five cycles greater than experimental samples, were considered acceptable.

Relative fold change in expression of IFN-β and IFN-inducible genes between transfected and mock transfected samples was determined using the delta delta Ct method (Figure 21). At the highest dose of 1000 ng, an increase in the expression of IFN-β (33.9-fold), IFIT1 (17.5-fold) and OAS1 (270-fold) was detected in cells transfected with saRNA-S-HBsAg. At the same concentration, saRNA-Luc2 induced a smaller increase in expression of IFN-β (5.5-fold), IFIT1 (2.5-fold) and OAS1 (13.8-fold). A lower 500 ng dose elicited weaker interferon-related responses. In cells transfected with saRNA-Luc2, an increase in only OAS1 was detected (5.8-fold), whereas cells transfected with saRNA-S-HBsAg had increased OAS1 (44.9-fold) and

IFIT1 (1.9-fold) expression. Since these genes are IFN-β inducible, it suggests that IFN-β was expressed, but may have already reached baseline by the 24-hour timepoint. The 250 ng dose elicited an increase of OAS1 expression alone (2.2-fold increase for saRNA-S-HBsAg and 1.9-fold increase for saRNA-luc2). The positive control, Poly I:C, induced a much stronger interferon response. This is expected since saRNAs are much longer compared to Poly I:C and therefore an equivalent concentration of saRNAs would contain fewer molecules to activate pattern recognition receptors. At the highest dose, Poly I:C induced significant increases in transcripts encoding OAS1 (647.6-fold), IFN-β (51.4-fold), and IFIT1 (31.5-fold). The 500 ng dose elicited significant increases in transcripts encoding OAS1 (208.6-fold) and IFIT1 (3.4-fold). mRNAs encoding PKR were not upregulated at any of the doses tested for all constructs including the poly I:C positive control. Average delta Ct values, fold change in expression, and statistical analysis of results can be found in Appendix C-Table C2. Thus, saRNAs can stimulate the innate immune system in a dose-dependent manner which may have an impact on antigen expression.

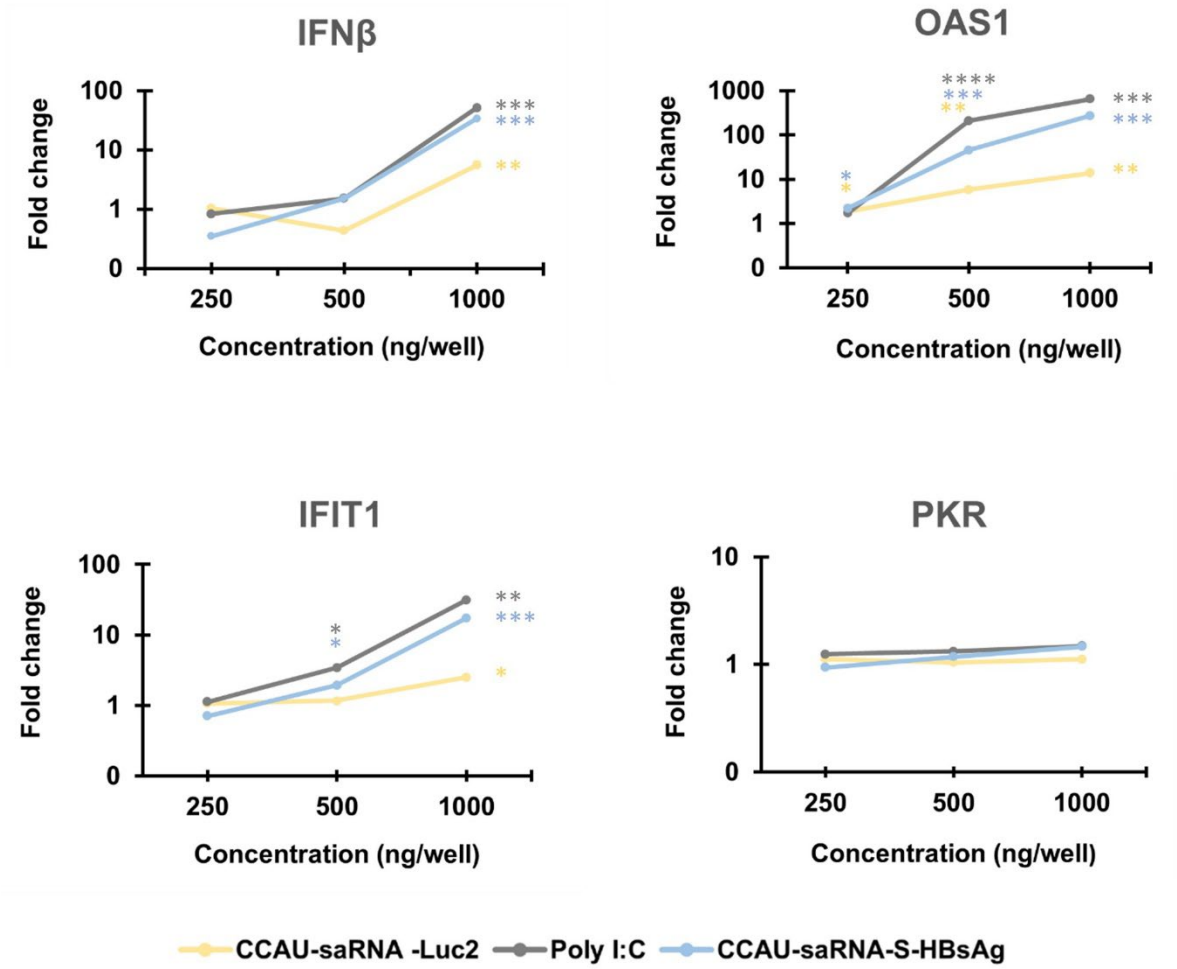

Figure 21. Induction of innate immune response by saRNAs.

Fold changes in mRNA transcripts encoding interferon-β and interferon-inducible genes in HEK 293T cells transfected with cap 1 saRNA-Luc2, cap 1 saRNA-S-HBsAg or Poly I:C determined by qRT-PCR. Expression of genes was normalised to glyceraldehyde 3-phosphate dehydrogenase (GAPDH) expression, and relative fold change in expression between transfected and mock transfected samples (n=3) was determined using the delta delta Ct method. Significant differences were calculated using a student's T test. *$p < 0.05$, **$p < 0.01$, ***$p < 0.001$, ****$p < 0.0001$. Poly I:C = positive control, IFN-β = Interferon beta, OAS1 = 2'-5'-oligoadenylate synthetase 1, IFIT1 = interferon-induced proteins with tetratricopeptide repeats 1, PKR = Protein Kinase R, CCAU = Cleancap® AU reagent.

3.8.2 Effect of innate immune response on antigen expression

To determine the extent to which the induction of an innate immune response against saRNAs impacts antigen expression, cell culture supernatants from transfected cells were harvested at 24 and 48 hours after transfection and assessed by ELISA to determine S-HBsAg expression. Despite the induction of a strong innate immune response by saRNA-S-HBsAg there was a dose-dependent increase in antigen expression with impressive amounts of antigen expressed at the highest dose (Figure 22). Expression at 48 hours was higher than expression at 24 hours for all doses, however the percentage increase in expression from 24 to 48 hours was lower for the 1000 nanogram dose. This could be a result of saturation of cellular translational machinery at high saRNA concentrations. Nevertheless, the ability of saRNAs to elicit an innate response does not appear to impact antigen expression *in vitro*, most likely by its ability to rapidly self-replicate and its natural ability to evade recognition by innate immune system proteins, thus inhibition of antigen translation does not appear to be a concern.

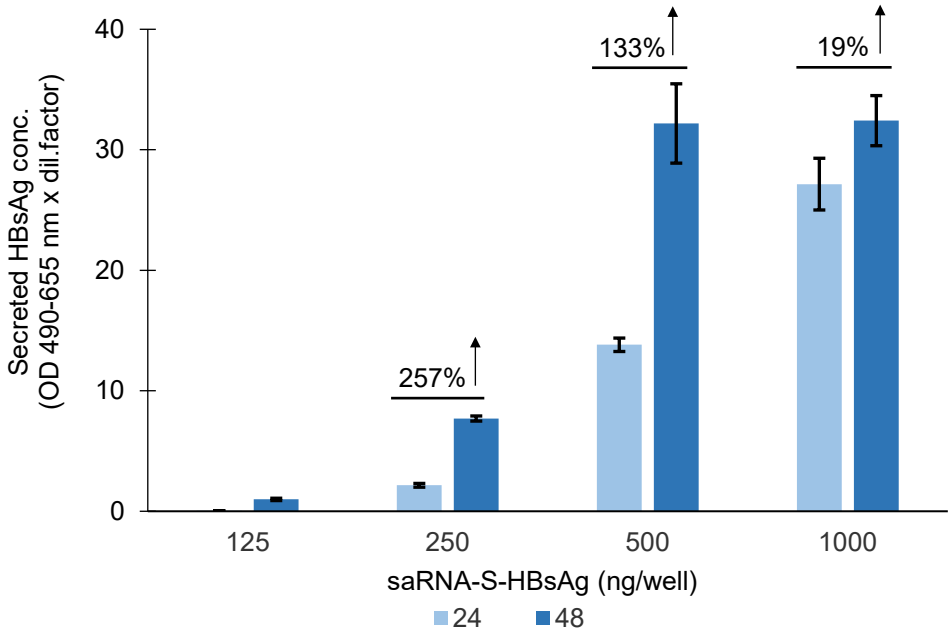

Figure 22. Dose-response pattern of S-HBsAg expression *in vitro*.

S-HBsAg secretion from HEK 293T cells transfected with the indicated amounts of cap 1 saRNA-S-HBsAg was measured by ELISA at 24- and 48-hours post-transfection. Percent increases in S-HBsAg expression from 24-48 hours is indicated above the respective bar graphs. Supernatant dilution factors: 500 ng and 1000 ng at both time points = 50; 250 ng at 24 hours

= 5; 250 ng at 48 hours = 10; 125 ng at 24 hours = undiluted; 125 ng at 48 hours = 5. Results are depicted as the mean with standard error of the mean (n=3).

3.9 Characterisation of CaLiVax formulated saRNA-Luc2

saRNA-Luc2, encoding the bioluminescent reporter protein luciferase, was used to examine *in vivo* expression from saRNAs. To protect saRNAs from degradation by RNases and facilitate cellular uptake *in vivo*, saRNA-Luc2 transcripts were adsorbed to permanently cationic DOTAP liposomes (CaLiVax) to form lipoplexes. The size of lipoplexes formed can influence the half-life and efficacy of vaccine formulations, therefore, the physical characteristics of lipoplexes were examined by dynamic light scattering (Hassett et al., 2021). Empty CaLiVax liposomes had an average diameter size of 111.7 nanometres (nm) (Figure 23A). In contrast, CaLiVax-saRNA-Luc2 lipoplexes were much larger than empty liposomes, with an average size of 305.5 nm. This increase in size is expected following RNA adsorption. Multiple particle size measurements of the formulation (n=4) indicated variability in lipoplex size (Figure 23B). This was confirmed by measuring the polydispersity index (PDI) of the formulation. The PDI reflects particle size distribution and ranges from a value of 0, for solutions containing particles of the same size, to 1, indicating great variation in particle size. Particles had a PDI of 0.3245 indicating slight variability in size. In addition, a small number of larger particles, indicated by the smaller peak on the far right of the x-axis, were also present in the formulation (Figure 23B).

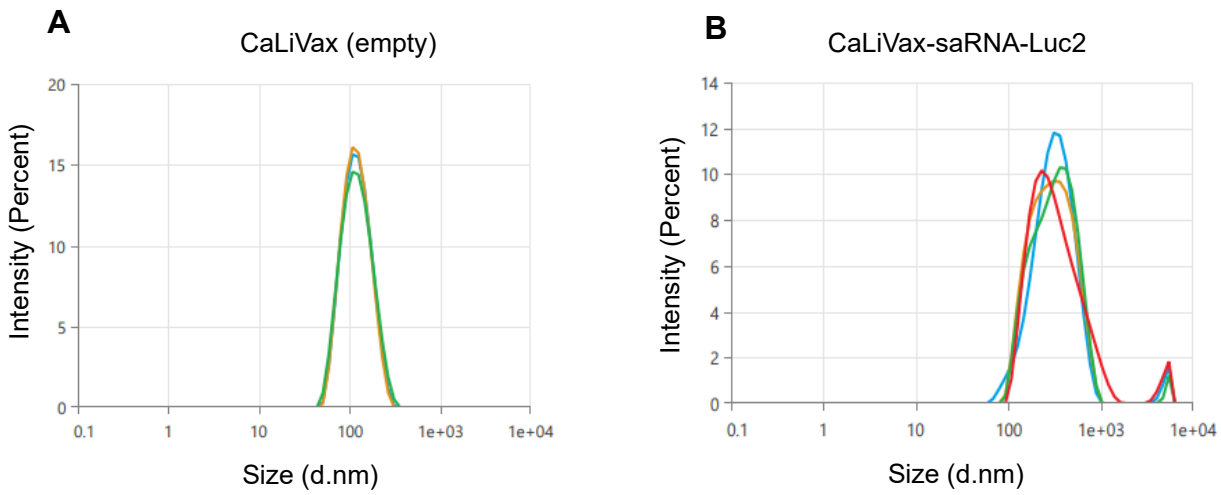

Figure 23. Characterisation of CaLiVax-saRNA-Luc2 lipoplexes.

Diameter size (d.nm) of **(A)** empty cationic liposomes, and **(B)** lipoplexes consisting of CaLiVax and adsorbed saRNA-Luc2 measured by dynamic light scattering.

To determine the percentage of saRNAs complexed to liposomes and establish dose, a RiboGreen assay was performed (Appendix C-Table C3; Figure C5). Complexation efficiency of 98.9% was achieved and the average effective saRNA concentration of the formulation was 172.9 ng/µl (Appendix C: Table C4). To determine whether CaLiVax-saRNA-Luc2 could be delivered into cells *in vitro*, HEK 293T cells were transfected with lipoplexes and examined for expression of Luc2 by luciferase assay. Luminescence from lipoplex-transfected cells was significantly greater than mock-transfected cells, demonstrating successful expression of luciferase (Figure 24).

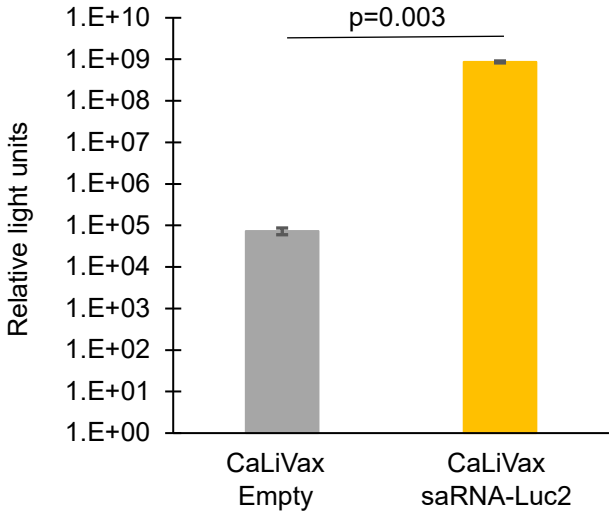

Figure 24. *In vitro* expression of luciferase from CaLiVax-saRNA-Luc2.

Expression of luminescence in HEK 293T cells 72 hours after transfection with CaLiVax only (mock transfection) or 250 ng CaLiVax-saRNA-Luc2. Data is represented as the mean with standard error of the mean (n=3). Significant differences were calculated using a student's T test with $p < 0.05$ indicating significance.

3.10 *In vivo* characterisation of saRNA expression and biodistribution

To determine whether saRNAs could be delivered into cells and expressed *in vivo*, NMRI mice were injected intramuscularly with 5 ug of unformulated saRNA-Luc2 accompanied by electroporation, or 5 ug of CaLiVax-saRNA-Luc2 (n=3). The expression of luciferase was examined by bioluminescence imaging following intraperitoneal injection of the enzyme substrate D-luciferin. Similar to *in vitro* luciferase assays, delivery of enzyme substrate will result in bioluminescence in cells that are expressing luciferase. This allows the expression of protein to be monitored over time while also enabling visualisation of vaccine biodistribution. No bioluminescence was observed on days three and seven post-injection in both groups of mice even at an exposure time of 30 seconds (Figure 25). Considering the lack of expression at these time points at which maximum expression is expected, mice were not imaged on day ten. To determine whether a higher dose was required for luciferase expression, mice from the group that received unformulated saRNA-Luc2 by electroporation were boosted four weeks later with 10 µg saRNA-Luc2 followed by electroporation, and imaged seven days thereafter (day 35 after prime injection). Even at a higher dose, no expression of luciferase was detected indicating that

neither electroporation nor CaLiVax was able to facilitate cellular uptake of saRNA-Luc2. Since delivery and expression of reporter proteins could not be confirmed, it was assumed that viral antigens were also not efficiently delivered and expressed in mice that received saRNA-S-HBsAg or saRNA-L-HBsAg. Therefore, immunogenicity studies using serum from mice injected with candidate vaccines were not performed.

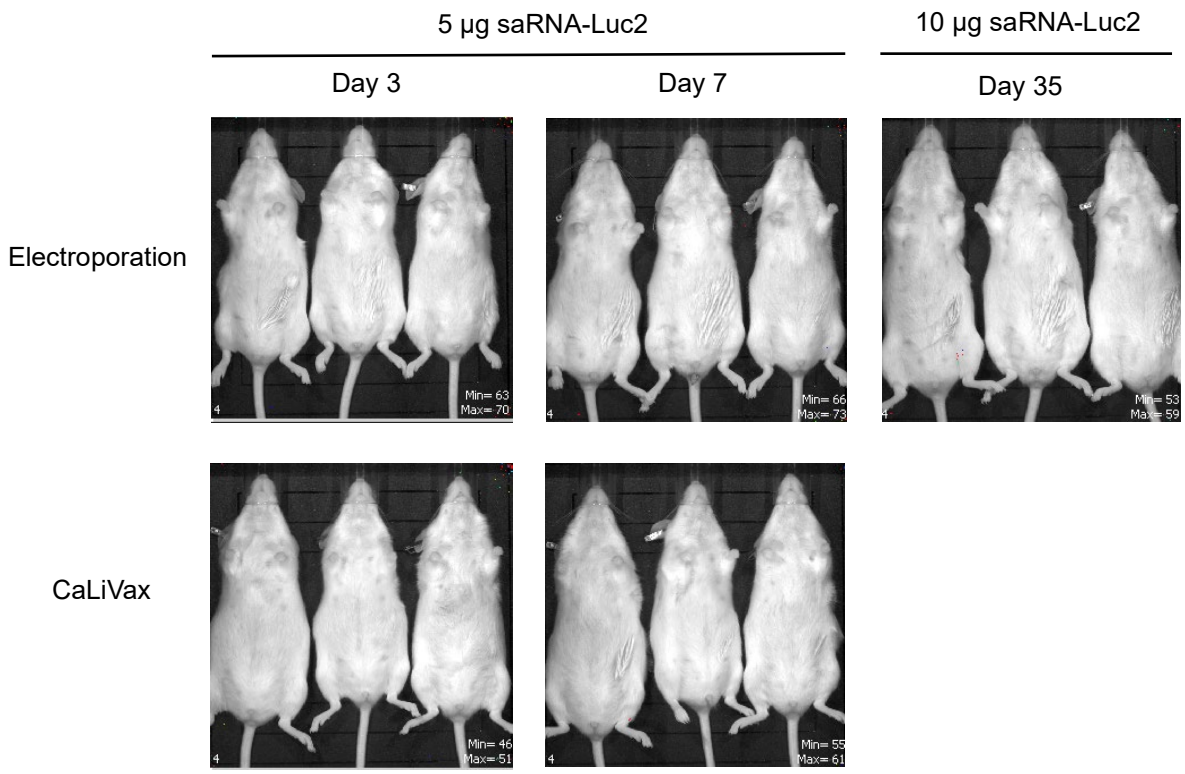

Figure 25. Bioluminescence imaging of NMRI mice.

NMRI mice received a priming dose of 5 µg saRNA-Luc2 by intramuscular injection to the left hind limb, either by electroporation or formulated with the cationic liposome CaLiVax (n=3). Mice that received unformulated saRNA-Luc2 by electroporation received a booster dose of 10 µg on day 28. Expression of luciferase was examined by bioluminescence imaging following intraperitoneal injection of D-luciferin at the indicated timepoints.

4. DISCUSSION

Non-responsiveness to currently available protein-based vaccines by a modest proportion of vaccinees has necessitated the development of more potent vaccines designed to target the more immunogenic L-HBsAg. In addition, protein-based vaccines are only capable of eliciting a humoral immune response, which is not effective against intracellular pathogens. Thus, an improved HBV vaccine should also be able to elicit a cell-mediated immune response which also has therapeutic potential. The aim of this study was to develop and assess the immunogenicity of saRNA vaccines encoding S-HBsAg, or L-HBsAg which would provide greater protection against HBV infection. Moreover, optimisation and characterisation of the vaccine platform would assist in paving the way for local development of other life- saRNA saving vaccines and therapeutics.

Like conventional mRNA, saRNAs are produced by IVT. There are several commercially available kits used for IVT, all of which produce excellent results when transcribing conventional mRNAs. saRNA vaccine constructs are significantly larger than conventional mRNAs, therefore IVT of saRNAs using commercially available kits under the same conditions may not yield the same quantity of full-length transcripts. Indeed, a low proportion of full-length saRNA transcripts was produced using the Ampliscribe™ T7 Flash™ kit. To increase the yield of full-length transcripts, several modifications to the IVT process were implemented. These included increasing incubation time, incubation temperature, and plasmid DNA template concentration.

As observed with the Ampliscribe™ T7 Flash™ kit, increasing incubation time to one hour increased the yield substantially, however, doubling the incubation period to two hours resulted in a smaller than expected increase. As described by the manufacturers of the kit, the rate of mRNA synthesis decreases after 30 minutes and plateaus after an hour. This is most likely a result of loss in enzyme activity rather than substrate depletion since NTPs are provided at higher than required concentrations and are not limiting. Increasing plasmid DNA concentration from 50 ng/µl to 100 ng/µl together with an increased incubation time of one hour surprisingly showed no improvement in yield. Increasing the temperature of an enzymatic reaction can increase the rate of reaction. The processivity of the T7 RNA polymerase used in the Ampliscribe™ T7 Flash™ kit was thus improved by increasing the reaction temperature by 5°C, resulting in a 37% increase in saRNA yield. As with increasing the incubation time, the characteristics of the T7 RNA polymerase employed must be taken into consideration when increasing the reaction temperature. Too high an increase may alter the active site of some T7

RNA polymerases which would result in decreased yield. Engineered thermostable RNA polymerases are available and can be utilised at temperatures up to 50°C which could improve yield (Wu et al., 2020). However, the integrity of saRNAs produced at such high temperatures in combination with prolonged incubation times would need to be examined.

The RiboMAX™ Large scale RNA production system was used to upscale the IVT reaction in an attempt to increase saRNA yield. A two hour incubation period with 100 ng/µl plasmid DNA template yielded more full-length saRNA transcripts when compared to the Ampliscribe™ T7 Flash™ kit. It is possible that the processivity of the T7 RNA polymerase used in the RiboMAX™ Large scale RNA production system is maintained throughout the prolonged incubation period. However, other factors, such as differences in buffer components, concentrations of plasmid DNA template and T7 RNA polymerases, may have also contributed to the improved yield of full-length transcripts.

An in-house prepared buffer that was optimised for the synthesis of saRNAs using a Design of Experiments (DoE) approach was also examined. This approach involved a systematic analysis of reagents used in various IVT protocols with the goal of identifying key reaction components that affected saRNA yield and integrity (Samnuan et al., 2022). The final optimised buffer contained HEPES, DTT, spermidine, sodium acetate, and ($Mg(OAc)_2$). The most influential buffer component was ($Mg(OAc)_2$), which produced an approximate 3-fold increase in yield by increasing ($Mg(OAc)_2$) concentration from 40 mM to 60 mM in combination with an NTP concentration of 10 mM each. Magnesium ions are divalent cations required for catalytic activity of T7 RNA polymerase and are also associated with negatively charged triphosphate groups on free NTPs (reviewed in Svetlov and Nudler, 2013). Thus, there exists a stoichiometric relationship between NTPs and magnesium ions which was optimal for saRNA synthesis when used at a ratio of 1:1.875.

Regardless of the IVT protocol adopted, varying degrees of smearing below the expected saRNA band was observed. This smearing was unlikely to be caused by enzymatic degradation by ubiquitous RNases since RNase inhibitor was included in all reactions and degradation was not observed in control mRNAs. This smearing is more likely an indication of incomplete transcripts. This was confirmed when full length transcripts, which contain a poly-A tail, were captured using oligo $d(T)_{25}$ magnetic beads which bind to poly-A sequences. A single band of the expected size was observed following purification. This suggests that the lower molecular weight saRNA transcripts do not contain a poly-A tail and are incomplete transcripts. Considering the large size of saRNA transcripts, it is expected for some incomplete transcripts to be present at the end of the IVT incubation period. While full length transcripts can be

purified using oligo d(T) magnetic beads, this method of purification resulted in substantial loss of product and may require optimisation to achieve higher recovery. Alternatively, full-length saRNAs can be purified using oligo d(T) affinity chromatography columns which is also easily scalable (Mencin et al., 2023). This purification method will be investigated in future studies.

Post-transcriptional enzymatic capping of saRNA transcripts using the Vaccinia capping system is another stage of production at which loss of transcripts is observed, with approximately 66.5% of transcripts recovered. Varying degrees of degradation was also observed following capping. This degradation could be related to shearing of the transcripts during the additional processing and purification steps. To maximize recovery of full-length saRNAs while reducing saRNA handling and production time, co-transcriptional capping is a more suitable approach. In this study co-transcriptional capping was achieved by including CleanCap® AU reagent in the IVT reaction to produce naturally occurring cap 1 transcripts for enhanced translation. Considering the high cost of CleanCap® AU reagent, it is vital to ensure saRNA yield and integrity is maximized for this approach to be feasible. The average yield obtained was 421 µg in a 100 µl reaction with a high proportion of transcripts appearing to be full-length. For the purposes of this proof-of-concept study, the quality and yield of co-transcriptionally capped saRNAs produced using the DoE buffer were deemed suitable for use in *in vivo* immunogenicity studies.

The saRNA vaccine constructs examined in this study were initially bi-cistronic, containing an IRES flanked by an upstream ORF encoding reporter proteins or HBV surface antigen, and a downstream ORF encoding a reporter protein. Apart from the expression of upstream eGFP, no expression of HBV antigens or the downstream reporter protein mCherry was detected in HEK 293T cells. Previous studies have shown that the presence of a highly structured IRES, such as the EMCV IRES used in this study, can hinder the expression of certain sequences, and sometimes result in preferential expression of one antigen over the other depending on its sequence and position relative to the IRES (Hennecke et al., 2001; Mizuguchi et al., 2000). Removal of the IRES and downstream ORF resulted in successful expression of all antigens from single-cistron saRNA transcripts. It is thus possible that the IRES was responsible for hindering expression of HBV antigens and mCherry and thus, this strategy of producing bi-cistronic saRNAs using an IRES may not be compatible with the design of our saRNA vaccine constructs. Alternative strategies to produce multivalent constructs will be explored in future studies.

The dose sparing properties of saRNA vaccines was confirmed when expression of fluorescent reporter protein eGFP was observed for as long as 15 days *in vitro* from doses as low as 50 ng.

Interestingly, this expression was observed from seemingly degraded transcripts and may have been facilitated by self-replication of the few full-length transcripts that were transfected. Expression of eGFP was also observed from transcripts with a cap 0 and cap 1 structure, indicating that cap 1 is not necessary for translation of saRNAs. However, a cap 1 structure would increase the longevity of primary transcripts by avoiding recognition by innate immune system pattern recognition receptors thus allowing for lower concentrations per dose to be administered to achieve the same level of antigen expression.

S-HBsAg was successfully expressed from single-cistron saRNAs and secreted into cell culture supernatant at concentrations approximately 20-fold greater compared to cells transfected with the positive control pCH9-3091. Detecting expression of saRNA encoding L-HBsAg proved to be more challenging, as the protein is not readily secreted. L-HBsAg, when expressed on its own, is capable of particle formation. However, unlike S-HBsAg particles, L-HBsAg particles are retained intracellularly in association with membrane structures (Xu et al., 1997). As such, L-HBsAg was not detected in cell culture supernatant when expressed in HEK293T cells, but rather in the cell lysate fraction. This confirmed that that L-HBsAg encoded by the current saRNA vaccine construct is translated, but not secreted. The lower amount of L-HBsAg detected, relative to S-HBsAg, could be a result of insufficient release of L-HBsAg particles from membrane structures following cell lysis. It is also important to note that although L-HBsAg and S-HBsAg share the same C-terminal domains, the Monolisa™ HBsAg Ultra kit used to detect antigen expression is not optimised to detect L-HBsAg. It is possible that the external conformation of the Pres1 and PreS2 domains present in L-HBsAg may hinder access of detection antibodies to the S-HBsAg domain resulting in decreased detection. Therefore, an ELISA designed to detect PreS1 and PreS2 domain epitopes would be better suited to gauge the expression of L-HBsAg. Future work that involves re-design of L-HBsAg by inclusion of a signal peptide would facilitate secretion of L-HBsAg and potentially improve the immune response.

One of the most important hurdles to overcome in the development of mRNA vaccines is to prevent recognition of exogenous mRNAs and double-stranded transcription by-products by the innate immune system. Triggering of the innate immune system hampers antigen production and contributes to vaccine reactogenicity. To limit recognition by the immune system, methods such as uridine depletion, sequence optimisation, use of modified nucleotides, and removal of dsRNA are applied (reviewed in Kairuz et al., 2022). Unfortunately, these modifications cannot be applied to the saRNA vaccine platform. saRNAs rely on Alphaviral sequences to form a 5' stem-loop secondary structure that is required for *in situ* replication. Alterations to the

thermodynamic stability of this secondary structure by uridine depletion or using modified nucleotides during IVT could have a negative impact on self-replication. These characteristics make saRNAs inherently immunogenic, raising concerns regarding whether enough antigen can be produced to stimulate the immune system, and if reactogenicity will be high to these vaccines. saRNAs encoding S-HBsAg and Luc2 was found to trigger the innate immune system in a dose dependent manner, resulting in transcription of IFN-β, IFIT1, and OAS1 in transfected cells. At 24-hours post-transfection, the most upregulated gene was OAS1. OAS1 activates RNase L which degrades cellular RNAs to prevent viral replication during infection. Despite this, large amounts of antigen were secreted *in vitro*, possibly due to the rapid self-replication and translation rates of the antigen in relation to host immune responses. Inhibition of translation of saRNAs by IFIT 1 is not a concern since saRNAs possess a 5' stem-loop structure which effectively blocks recognition and binding by IFIT 1 (reviewed in Hyde et al., 2015). It is more likely that after 24 hours, saRNAs are degraded by RNase L diminishing the number of transcripts available for translation. This is counteracted to an extent by the self-replication of saRNAs. This effect was observed *in vitro* where the expression of eGFP was observed for up to 15 days. saRNAs encoding the reporter protein Luc2 also induced an innate immune response but to a lesser extent, suggesting decreased immunogenicity of sequences encoding Luc2.

The immune response to an antigen is directed by the interactions between multiple immune cell types, cytokines, and lymphoid tissues and thus a fully functioning immune system is required to assess immunogenicity of candidate vaccines. In this study, immunocompetent NMRI mice were used for pre-clinical assessment of vaccine candidates. Electroporation and cationic lipid nanoparticle formulation was used to facilitate *in vivo* delivery of saRNAs. Electroporation has been successfully used by us and others to facilitate *in vivo* cellular uptake of mRNAs and saRNAs (Cu et al., 2013) . Electroporation involves the application of an electric current to the site of injection causing transient destabilisation of the cellular membrane and formation of pores (Luft and Ketteler, 2015). Electroporation-mediated delivery of saRNA-Luc2 was unsuccessful as no expression of luciferase was observed in mice, even at the high dose of 10 µg. Electroporator malfunction could have been a cause of lack of luciferase expression as saRNAs in circulation would have been rapidly degraded by endogenous RNases in blood plasma (Probst et al., 2006).

As an alternative method of delivery, saRNA-Luc2 was formulated with commercially available liposomes to produce saRNA-Luc2 lipoplexes. These cationic lipoplexes are first adsorbed to the negatively charged cell membrane and then taken up by endocytosis (Tenchov

et al., 2021). Once in the cell, lipoplexes are disrupted and saRNAs are released into the cytoplasm where they are translated into protein. This method of delivery was successful *in vitro* as confirmed by the expression of luciferase. However, expression of luciferase was not observed *in vivo*. Lack of expression could be attributed to large particle size which may not be conducive to *in vivo* delivery as larger cationic lipoplexes are rapidly cleared by the reticular endothelial system (reviewed in Sercombe et al., 2015). Since expression of luciferase was not achieved, *in vivo* antigen expression kinetics and biodistribution could not be evaluated and optimal vaccine dose could not be ascertained. It must be noted that *in vivo* studies were conducted on a small number of mice (n = 3) as a pilot study recommended by the Animal Research Ethics Committee. There is a possibility that the effects of an intervention may not be observed when using such small sample sizes. However, luciferase was expressed *in vitro*, thus it is likely that the mode of delivery needs to be optimised for i*n vivo* applications. Immunogenicity of candidate HBV vaccines will be investigated in future related studies using larger sample sizes (n = 7), as determined by the resource equation method, once delivery of saRNAs has been optimised (Charan and Kantharia, 2013).

5. CONCLUSION

In summary, transcription of long saRNA vaccine constructs has been optimised and *in vitro* expression of antigen was confirmed, even at low concentrations of saRNAs. This demonstrates the dose-sparing properties of saRNAs and its potential to be employed as a platform for the development of cost-effective next-generation vaccines against HBV and other pathogens. As with any new technology, initial costs of vaccine production will be high. The mRNA vaccine platform is currently being established in Africa, however, improvements to the technology and optimisation of large-scale production will eventually result in lower manufacturing costs for any vaccine produced using this versatile platform. Since saRNAs are effective at lower doses compared to conventional mRNAs and do not require the use of expensive modified nucleotides, the cost of saRNA vaccines is expected to be even lower. When compared to currently available HBV vaccines, which require three doses to elicit protective immunity, a two-dose saRNA vaccine strategy could potentially be more cost-effective while providing enhanced protection. Although HBV vaccine candidates could not be assessed *in vivo*, the preliminary *in vitro* results from this study are promising. Successful formulation of the saRNA will be key for efficient *in vivo* delivery of the HBV vaccine candidates and remains a priority for future studies. These constructs in conjunction with an efficient delivery system constitute novel therapeutics which possess great potential to replacing current subunit vaccines, especially as enhanced T-cell responses could lead to therapeutic vaccination strategies. SaRNA vaccine candidates against other infectious diseases have demonstrated enhanced humoral and cell-mediated immune responses at lower doses when compared to their mRNA vaccine counterparts. If the same can be achieved for HBV, this would enable the implementation of an accelerated HBV vaccine schedule, improving adherence and ensuring that a larger proportion of vaccinees achieve broader seroprotection in a shorter period with the added benefits of cell-mediated immunity.

APPENDICES

Appendix A-Plasmid maps

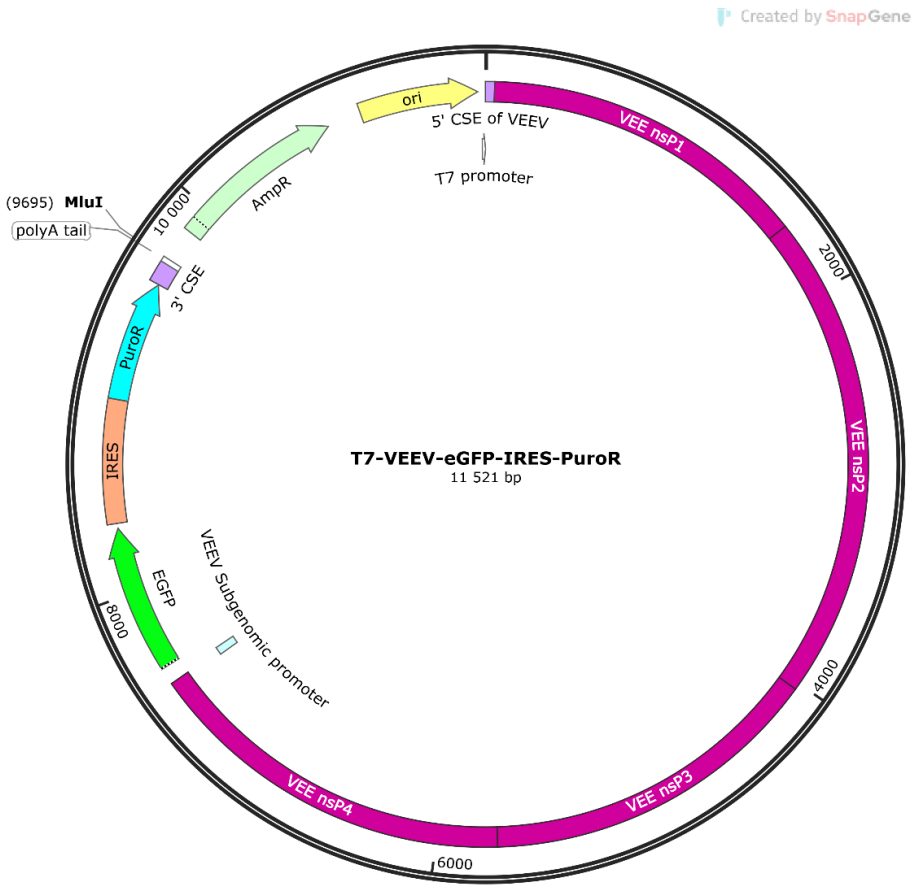

Figure A1. Plasmid map of T7-VEEV-eGFP-IRES-PuroR.

Commercially available T7-VEEV-eGFP-IRES-PuroR was used as the backbone for production of plasmids encoding saRNA vaccine candidates. This plasmid contains a T7 promoter sequence to enable *in vitro* transcription by T7 RNA polymerase. Downstream sequences encoding Venezuelan equine encephalitis virus (VEEV)-derived 5' conserved sequence elements (CSEs), non-structural proteins (nsPs 1-4), and 3' CSEs ensure *in situ* self-replication of saRNAs. At the 3' end of nsP4 is a subgenomic promoter required to produce subgenomic transcripts encoding the proteins of interest. This is followed by sequences encoding enhanced green fluorescent protein (eGFP), an internal ribosome entry site (IRES),

nd puromycin N-acetyltransferase. A poly-A (26) tail is included after the 3' CSE followed by an *Mlu*I restriction site for linearisation of the plasmid prior to *in vitro* transcription.

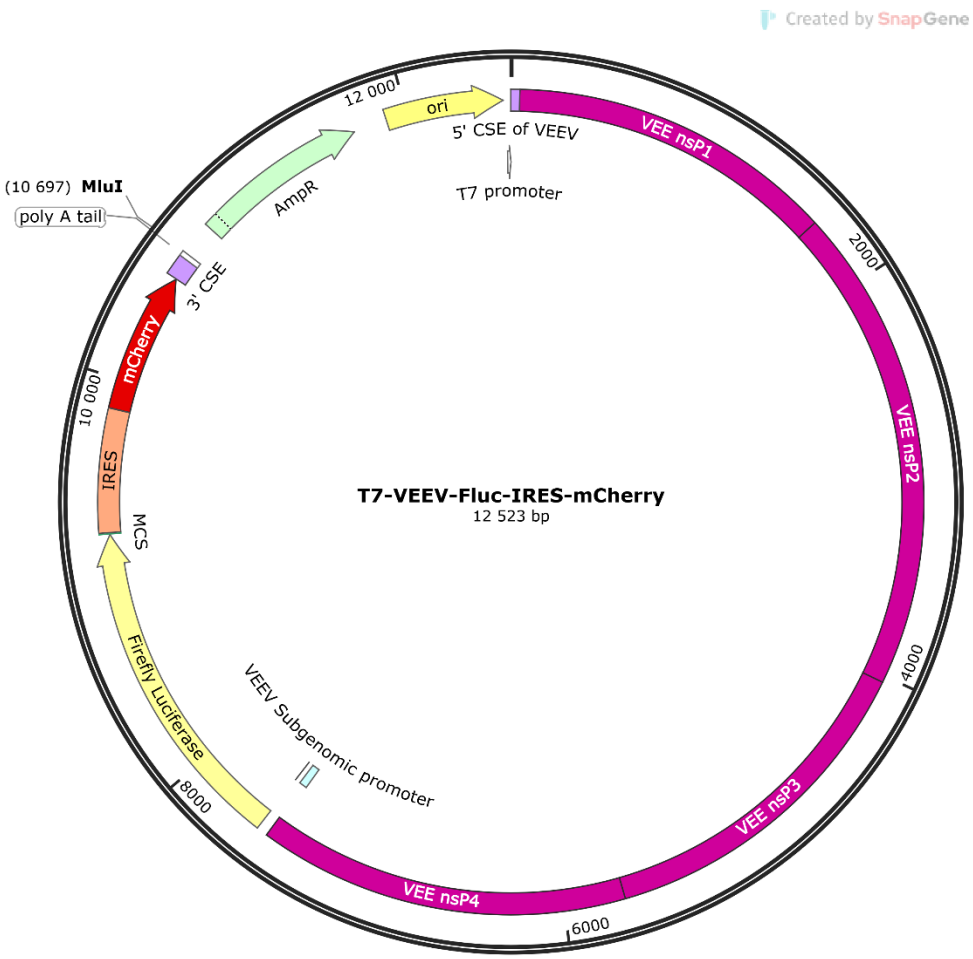

Figure A2. Plasmid used to produce bi-cistronic saRNAs encoding reporter proteins Firefly luciferase and mCherry.

T7-VEEV-Fluc-IRES-mCherry was produced using T7-VEEV-eGFP-IRES-PuroR as the backbone. Sequences encoding eGFP and downstream PuroR were replaced with sequences encoding Firefly luciferase (Fluc) and mCherry respectively.

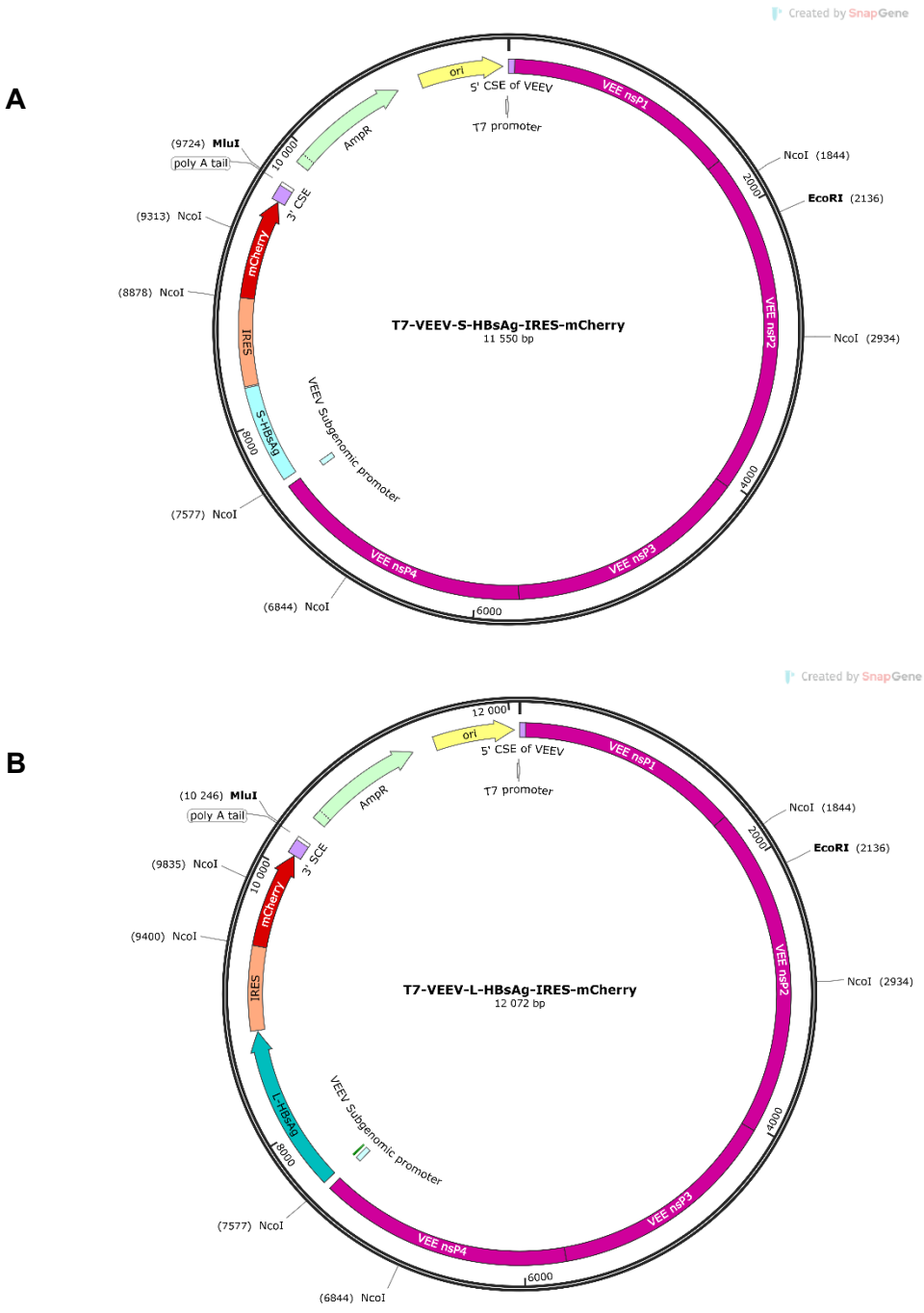

Figure A3. Plasmids used to produce bi-cistronic saRNA vaccine candidates.

(A) T7-VEEV-S-HBsAg-IRES-mCherry and (B) T7-VEEV-L-HBsAg-IRES-mCherry were produced using T7-VEEV-eGFP-IRES-PuroR as a backbone and encode either small surface

antigen (S-HBsAg) or large surface antigen (L-HBsAg) respectively, and downstream mCherry. Restriction sites for *Mlu*I, *Nco*I and *Eco*RI are also indicated.

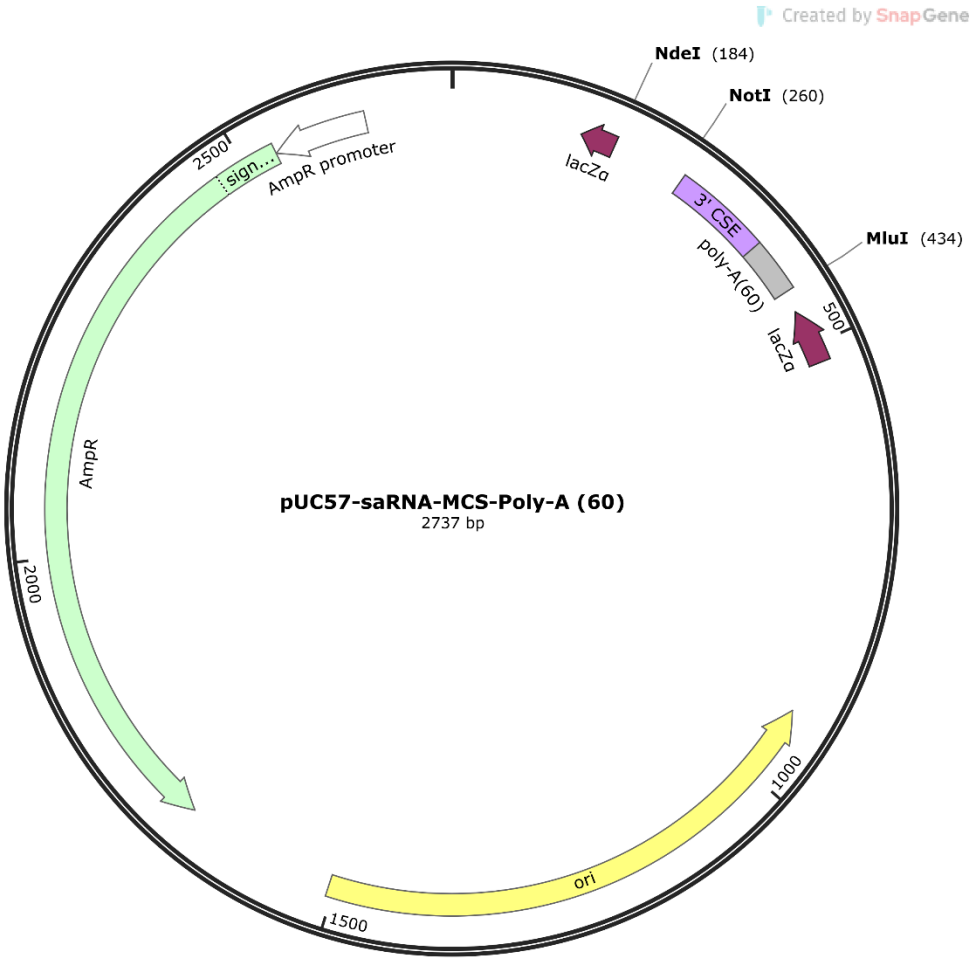

Figure A4. Plasmid map of pUC57-saRNA-MCS-Poly-A (60).

pUC57-saRNA-MCS-Poly-A (60) was used as a subcloning plasmid to extend poly-A tails of saRNA transcripts. The *Nde*I and *Not*I restriction sites located in the multiple cloning site were used to insert antigens of interest. This cloning strategy placed the antigens of interest upstream of a VEEV-derived 3' CSE, and extended poly-A (60) tail.

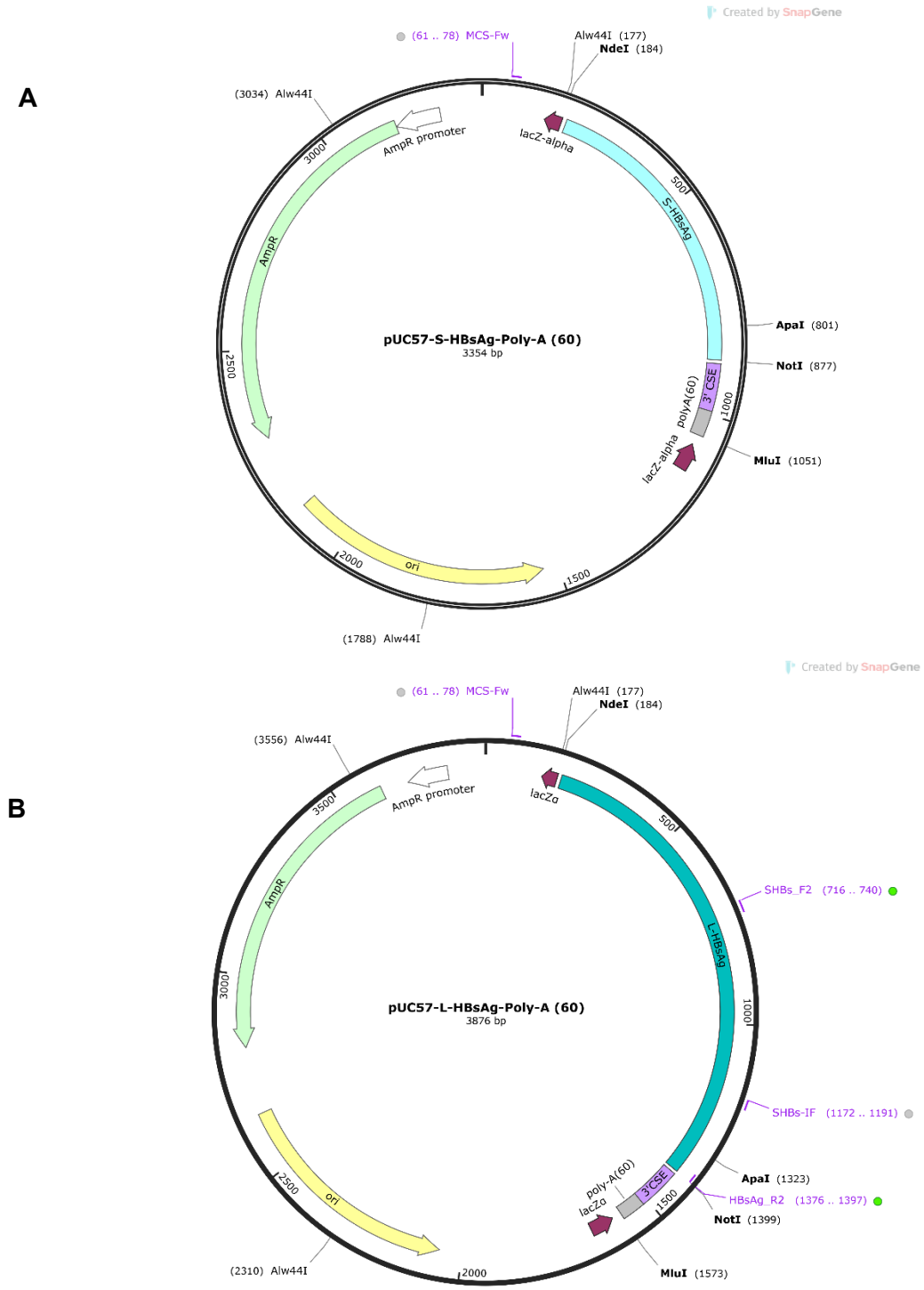

Figure A5. Subcloning plasmids encoding HBV antigens with extended poly-A (60) tails.

Subcloning plasmids (A) pUC57-S-HBsAg-poly-A (60) and (B) pUC57-L-HBsAg-poly-A (60) produced using pUC57-saRNA-MCS-poly-A (60*). Nde*I and *Mlu*I restriction sites were used to excise sequences encoding antigen, 3' CSE and extended poly-A tail. *Alw*44I and *Apa*I

restriction sites used for plasmid verification are indicated. Annealing sites for forward sequencing primers (grey circles) and PCR amplification primers (green circles) are indicated.

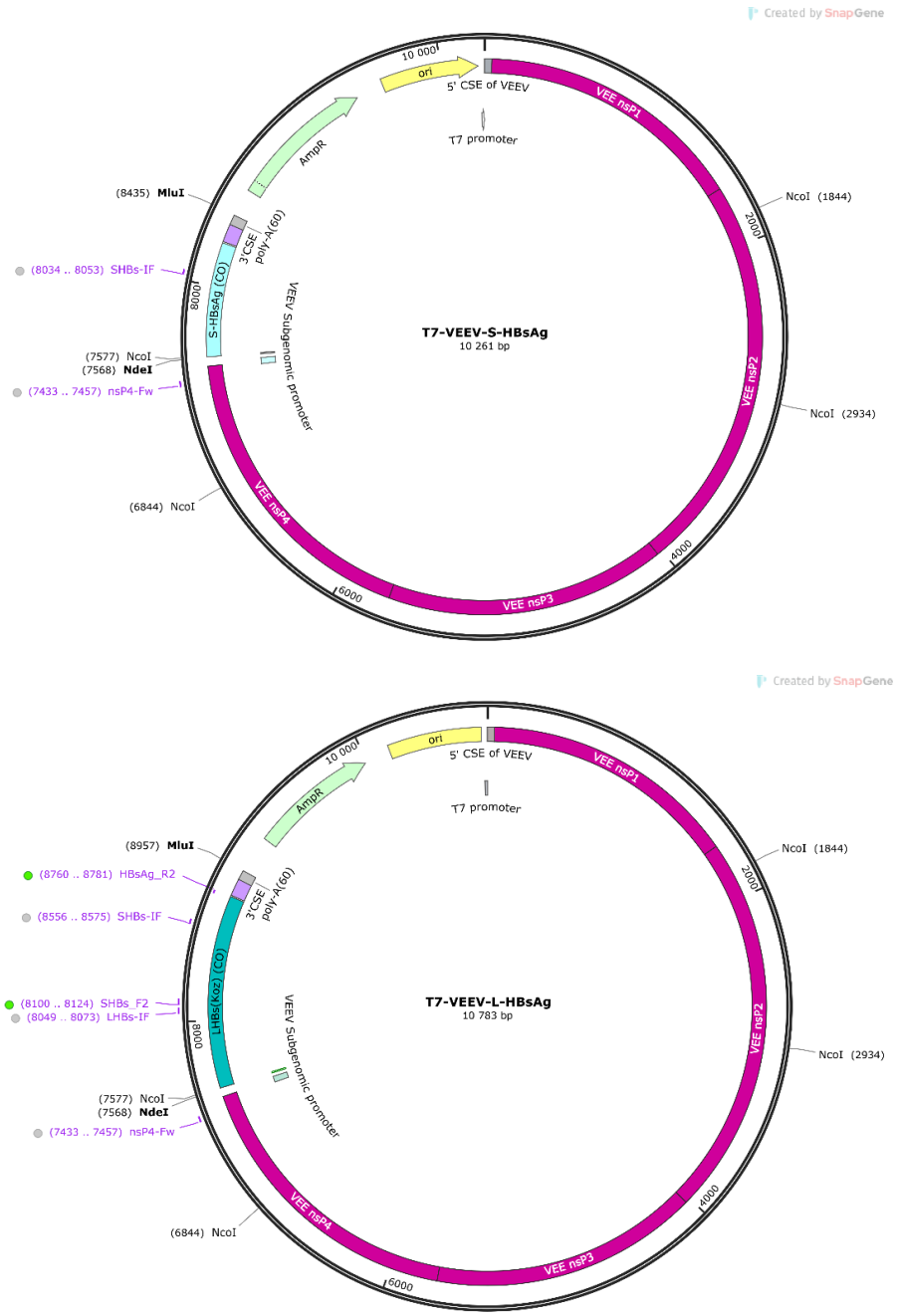

Figure A6. Plasmids encoding single-cistronic saRNA vaccine candidates.

(A) T7-VEEV-S-HBsAg and (B) T7-VEEV-L-HBsAg were used as templates to produce single-cistron saRNAs encoding either S-HBsAg or L-HBsAg respectively. An *Mlu*I restriction site located immediately after the poly-A (60) tail facilitated linearisation of the plasmid in preparation for IVT. *Nco*I restriction sites used for plasmid verification are indicated. Annealing

sites for forward sequencing primers (grey circles) and PCR amplification primers (green circles) are indicated.

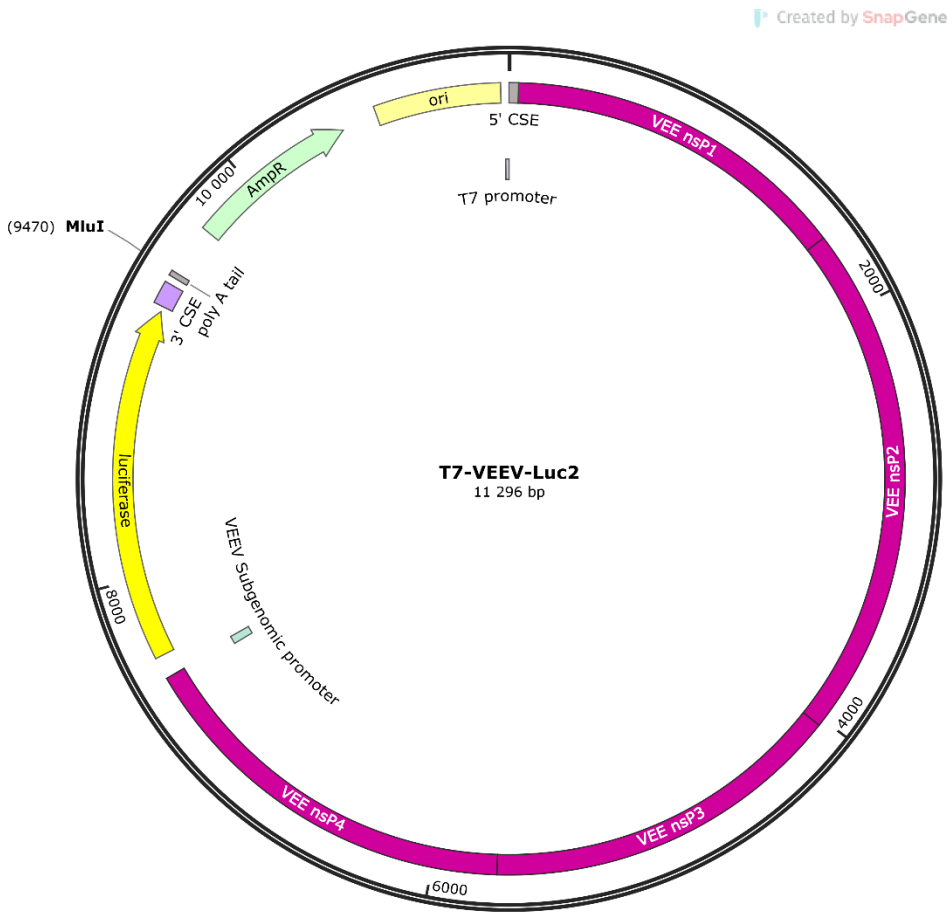

Figure A7. Plasmid encoding single-cistron saRNA encoding Luc2.

T7-VEEV-Luc2 was used as a template to produce single-cistron saRNAs encoding fluorescent reporter protein luciferase. An *Mlu*I restriction site located immediately after the poly-A (60) tail facilitated linearisation of the plasmid in preparation for IVT.

Appendix B-General laboratory protocols

B1-Preparation of chemically competent cells

A volume of 5 ml LB broth (Appendix B2) was inoculated with 5 µl of NEB Turbo cells (excluding antibiotics) and incubated overnight at 37℃ with shaking at 150 rpm. Following overnight incubation, two small flasks containing 100 ml LB broth each (excluding antibiotics) were inoculated with 1 ml of the overnight culture. Flasks were then incubated in a shaking incubator at 150 rpm and at 37℃ for two and a half hours or until cell cultures had reached log phase growth (OD 600 = 0.4-0.6) as determined by spectrophotometry using the NanoPhotometer®. Cultures were transferred to 50 ml centrifuge tubes and cells were pelleted by centrifugation at 500 x g for five minutes at 4℃. The supernatant was discarded and 5 ml of Rubidium Chloride ($RbCl_2$) transformation buffer 1 (Table B1) was added to each tube which was gently swirled to resuspend the pellet. Cells were incubated on ice for 15 min before centrifugation at 500 x g for five minutes at 4℃. The supernatant was discarded and 1 ml of $RbCl_2$ transformation buffer 2 (Table B1) was added to each pellet which was resuspended by gentle swirling. Cells were incubated on ice for 15 minutes, aliquoted into microcentrifuge tubes at a volume of 100 µl and stored immediately at -80℃.

Table B1. Buffers used to prepare chemically competent *E. Coli*

Buffer	Components
$RbCl_2$ transformation buffer 1	10 µM 3-N-Morpholino propanesulfonic acid (MOPS) (pH 5.8) 100 µM $RbCl_2$ 10 µM Calcium chloride ($CaCl_2$) 50 mM NaCl
$RbCl_2$ transformation buffer 2	10 mM Piperazine-N,N'-bis(2-ethanesulfonic acid) (PIPES), pH 6.8 75 mM $CaCl_2$ 10 mM $RbCl_2$ 15% Glycerol

B2-Preparation of LB media and LB ampicillin plates

LB media was prepared by dissolving tryptone, yeast and NaCl in double-distilled water at final concentrations of 10g/L, 5g/L and 7.5g/L respectively. The solution was autoclaved for 30

minutes at 121°C and stored at room temperature. For the preparation of LB agar plates supplemented with ampicillin, agar was added to LB media at a final concentration of 10g/L and was autoclaved for 30 minutes at 121°C. Once the autoclaved media had cooled enough to be handled, ampicillin was added to a final concentration of 100 µg/ml and the solution was mixed. Approximately 25 ml of LB agar was poured into 10 cm bacterial culture plates and allowed to polymerize at room temperature with the lid slightly ajar. Plates were sealed in a plastic bag and stored upside down at 4°C.

B3-Preparation of plasmid glycerol stocks

A 50% glycerol solution was prepared by mixing 25 ml of 100% glycerol with 25 ml deionized water (dH_2O). The solution was autoclaved for 30 minutes at 121°C, allowed to cool, and stored at room temperature. To prepare a bacterial glycerol stock, 700 µl of a bacterial culture was gently mixed with 300 µl of 50% glycerol in a microcentrifuge tube and stored at -80°C.

B4-Small-scale plasmid extraction (miniprep)

Single bacterial colonies containing plasmids of interest were inoculated into 8 ml LB media (Appendix B2) supplemented with 100 µg/ml ampicillin and incubated overnight at 37°C with shaking at 150 rpm. Following overnight incubation, bacterial cultures were centrifuged for 20 minutes at 4 000 x g at 4°C. The supernatant was discarded, and the bacterial pellet was resuspended in 250 µl of Resuspension buffer P1 (Table B2) and transferred to a 1.5 ml microcentrifuge tube. Cells were lysed with 250 µl of Lysis buffer P2 (Table B2) for five minutes at room temperature. A volume of 350 µl of Neutralisation buffer P3 (Table B2) was added, and the tube was gently inverted six times or until a white flocculant precipitate formed. The reaction was incubated on ice for five minutes before centrifugation at 10 000 x g for 20 minutes at 4°C. The supernatant, which contained plasmid DNA, was transferred to a clean microcentrifuge tube and an equal volume of 100% isopropanol was added. The tube was inverted six times to mix and incubated for an hour at -20°C to allow precipitation of plasmid DNA. Plasmid DNA was thereafter pelleted by centrifugation at 10 000 x g for 15 minutes at 4°C. The supernatant was discarded, and the pellet was rinsed with 500 µl 70% ethanol before centrifugation at 10 000 x g for five minutes at 4°C. The supernatant was discarded, and the pellet was allowed to air dry for five minutes before being resuspended in 100 µl nuclease-free water. Concentration and purity of extracted plasmids were determined by spectrophotometry. Plasmids were stored at -20°C.

Table B2. Buffers used in small-scale plasmid DNA extraction

Buffer	Component
Resuspension Buffer P1	50mM Tris base 10 mM (EDTA) 100 µg/ml RNaseA pH 8.0 with Hydrochloric acid (HCl)
Lysis Buffer P2	200 mM sodium hydroxide (NaOH) 1% sodium dodecyl sulphate (w/v)
Neutralisation buffer P3	3 M potassium acetate pH 5.3 with glacial acetic acid

B5-Agarose gel electrophoresis

Agarose gels used for resolving plasmid DNA digests were prepared at a concentration of 1% agarose in 1x Tris-acetate-EDTA (TAE) buffer (40 mM Tris base, 20 mM acetate, 1 mM EDTA). The solution was heated in a glass flask until the agarose dissolved. To enable visualization of DNA under ultraviolet light, ethidium bromide was added to a final concentration of 0.5 µg/ml and the mixture was poured into a casting tray with combs and allowed to set at room temperature. Combs were removed and 0.5-1 µg of DNA samples in 1x purple gel loading dye (New England Biolabs, Massachusetts, USA) were loaded into the wells. The Quick-Load® purple 1Kb plus DNA ladder (New England Biolabs, Massachusetts, USA) (Figure B1) was run alongside samples to estimate the size of the bands. Samples were electrophoresed for 30-45 minutes at 120 volts and gels were imaged using the Omega Fluor Gel Documentation System (Aplegen, California, USA).

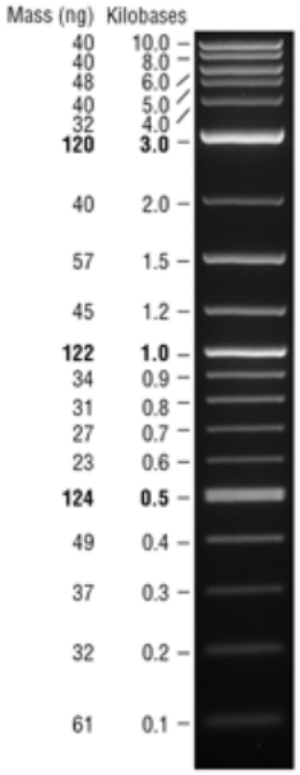

Figure B1. Quick-Load® purple 1Kb Plus DNA ladder

B6-Purification of linearised plasmids using EconoSpin® silica membrane mini spin columns

Linearised plasmids were purified using a modified protocol for the QiaQuick® Gel extraction kit and EconoSpin® silica membrane mini spin columns which has a maximum binding capacity of 40 µg. Following restriction digestion of plasmids with *Mlu*I, 900 µl of QG buffer (provided in kit) and 300 µl isopropanol was added to the reaction. The entire volume (containing less than 40 µg plasmid DNA) was then transferred to a silica membrane spin column and DNA was purified using the QiaQuick® Gel extraction kit according to manufacturer's instructions. Linearised plasmid DNA was eluted in 30 µl of nuclease-free water and concentration and purity of plasmids were determined by spectrophotometry. Linearised plasmids were stored at -20°C.

B7-Purification of linearised plasmids using NaOAc precipitation

Following restriction digestion, linearised plasmids were precipitated by addition of NaOAc to a concentration of 0.3 M, followed by 2.5 times the original volume of 100% ethanol. The solution was incubated at -20°C for 30 minutes before centrifugation at 10 000 x g at 4°C for

15 minutes. The supernatant was discarded, and pellet rinsed with 500 µl ice cold 70% ethanol before centrifugation at 10 000 x g at 4℃ for 15 minutes. Residual ethanol was aspirated, and the pellet was air-dried for five minutes. Linearised plasmid DNA was resuspended in 20 µl of nuclease-free water. Concentration and purity of linearised plasmids were determined by spectrophotometry. Linearised plasmids were stored at -20℃.

B8-IVT reaction components and conditions

Table B3. Comparison of buffer components and reaction conditions for IVT protocols

Component	Design of Experiments buffer	Ampliscribe™ T7 Flash™ transcription kit	Ribomax™ Large scale RNA production system
Buffer:			
HEPES	40 mM	unknown	80 mM
DTT	40 mM		40 mM
NaOAc	10 mM		-
$Mg(OAc)_2$	75 mM		-
$MgCl_2$	-		24 mM
Spermidine	0.2 mM		2mM
Unmodified ATP, UTP, GTP, CTP	10 mM each	9 mM each	5 mM each
Cleancap® AU	8 mM	-	-
Plasmid DNA	100 ng/µl	50 ng/µl	100 ng/µl
T7 polymerase	8 U/µl	unknown	unknown
DTT	(in buffer)	10 mM	(in buffer)
RNase inhibitor	0.2 U/µl	1 U/µl	unknown
Yeast Inorganic pyrophosphatase	-	-	unknown
Recommended incubation conditions	2 hours at 37°C	30 minutes at 37°C	2-4 hours at 37°C
NTP:Mg (mM)	1:1.875	unknown	1:1.2

B9-Formaldehyde gel electrophoresis

A 10x MOPS Buffer containing 0.2 M MOPS, 20 mM NaOAc and 10 mM EDTA was prepared using DEPC-treated or SABAX water. Prior to preparing the formaldehyde gel, the RNA electrophoresis tank, casting apparatus, flask, spatula, plastic weigh boat, and 50 ml measuring cylinder were thoroughly washed, sprayed with 70% ethanol, rinsed with SABAX water, and left to dry before UV sterilization for 15 minutes. A 1% gel was prepared by dissolving 0.5 g agarose in 36 ml DEPC-treated or SABAX water. The mixture was cooled to 60°C before adding 5 ml 10x MOPS and 9 ml 37% formaldehyde. The molten agar mixture was then poured into a casting tray and set at room temperature. saRNA samples were prepared for electrophoresis by mixing 0.5-2 µg saRNA with an equal volume of 2x RNA loading dye. Samples were denatured in a thermocycler at 70°C for 10 minutes. After cooling for one minute on ice, samples were electrophoresed at 80 V for 1 hour alongside the RiboRuler High Range RNA ladder (Thermo Fisher Scientific, Massachusetts, USA) or the NEB ssRNA ladder (New England Biolabs, Massachusetts, USA) (Figure B2).

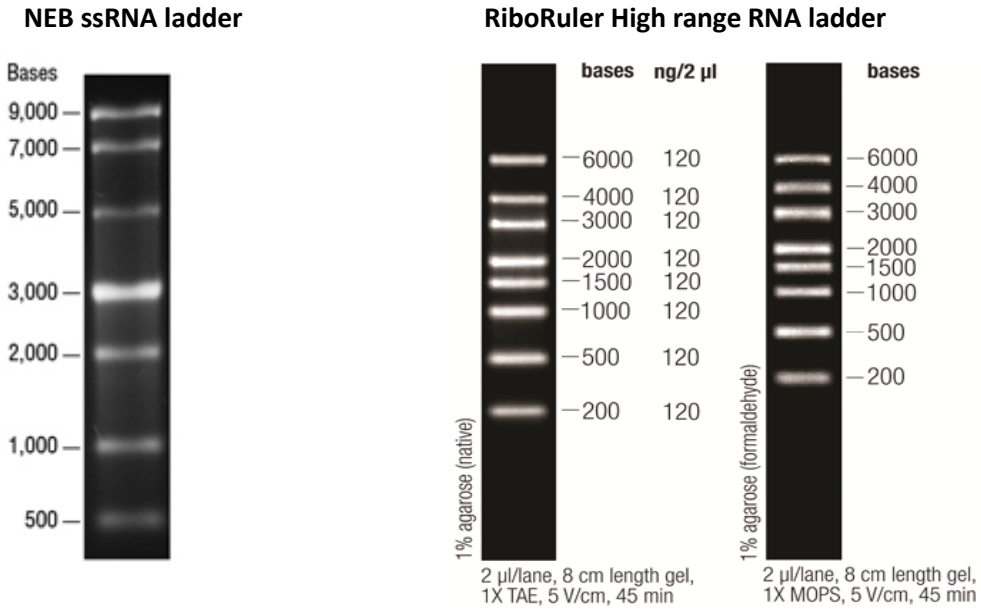

Figure B2. ssRNA molecular weight ladders used in formaldehyde gel electrophoresis to estimate size of IVT transcripts.

B10-Passaging of HEK 293T cells

HEK 293T cells grown in T175 flasks were rinsed with 10 ml saline (Ca^{2+} and Mg^{2+} free). Cells were incubated at 37°C in a humidified incubator with 3 ml TrypLE™ Express (Thermo Fisher Scientific, Massachusetts, USA) for three minutes to dissociate cells from the flask. TrypLE™ Express was deactivated by addition of 7 ml complete media and a single cell suspension was achieved by pipetting against the bottom of the flask. The desired volume of cells was re-plated and complete media was added to a final volume of 35 ml. Cells were incubated at 37°C in a humidified incubator with 5% CO_2.

Appendix C-Supplementary information

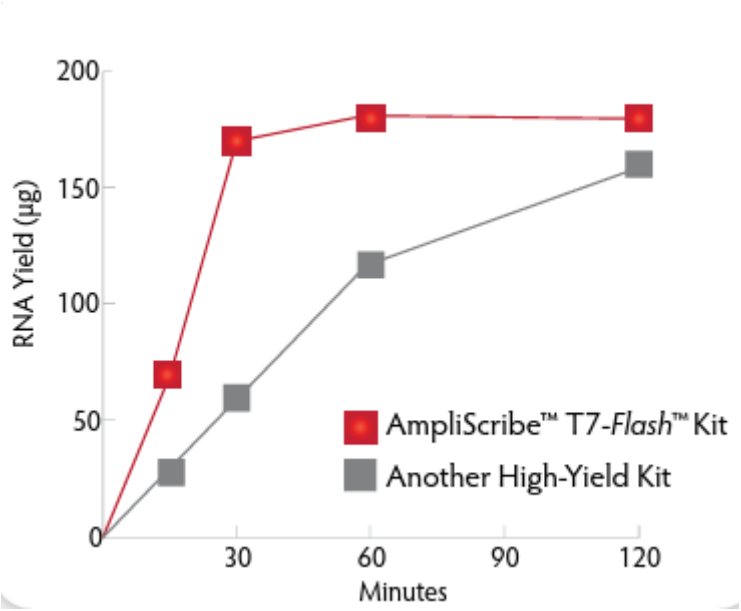

Figure C1. Comparison of RNA yield achieved using AmpliScribe™ T7-Flash™ kit and other high yield kits (AmpliScribe™ T7-Flash™ kit Product information sheet).

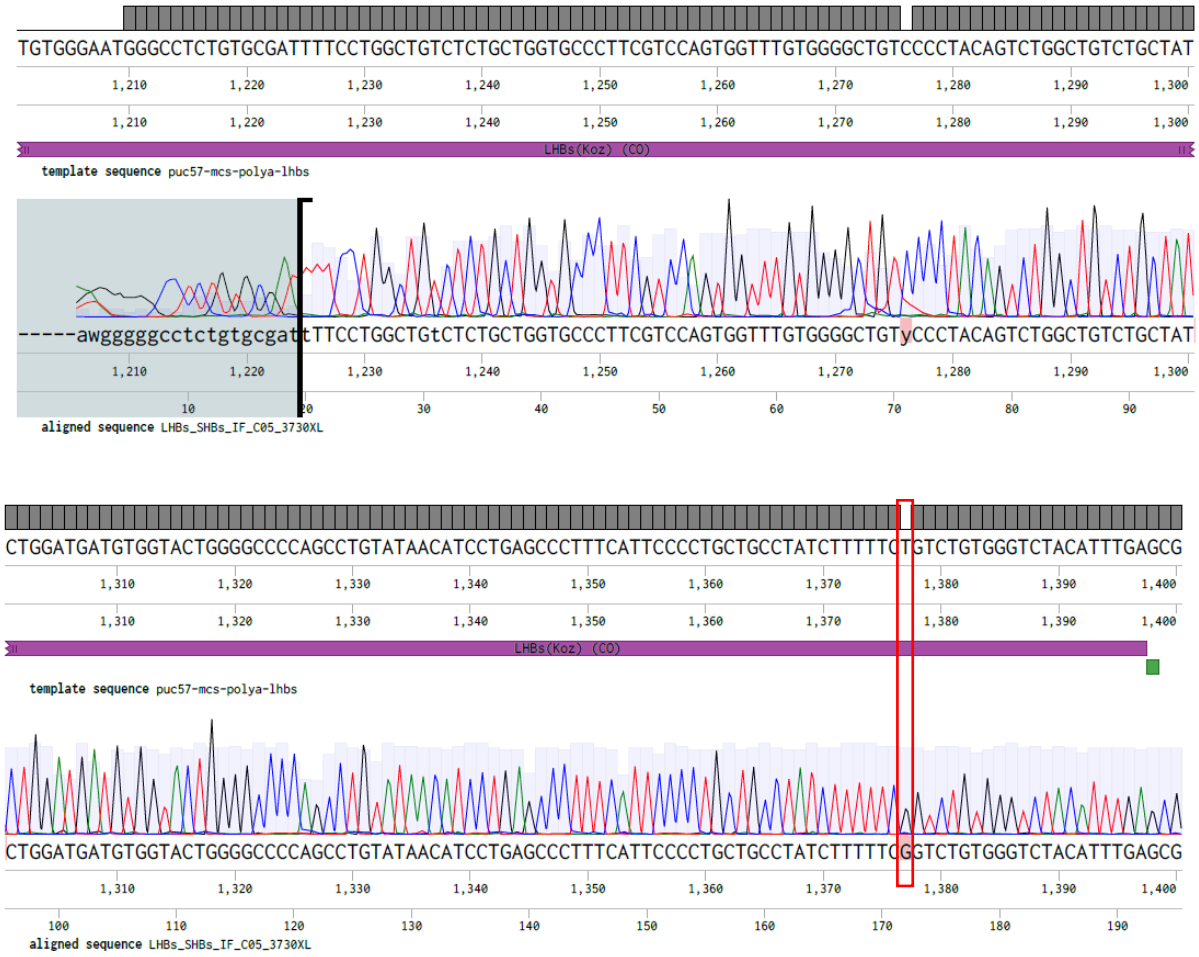

Figure C2. Sequence alignment of pUC57-L-HBsAg-poly-A(60).

Single point mutation T→G (red box) observed at 3' end of L-HBsAg open reading frame.

Figure C3. Sequence alignment of T7-VEEV-L-HBsAg.

Single point mutation T→G (red box) observed at 3' end of L-HBsAg open reading frame.

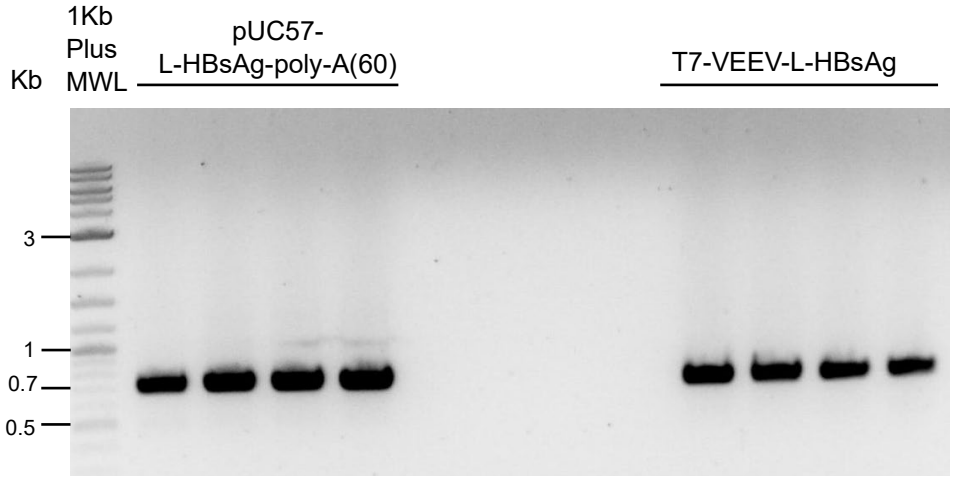

Figure C4. PCR amplicons for Sanger sequencing.

Sequences encoding the S-HBsAg domain from both pUC57-L-HBsAg-poly-A (60) and T7-VEEV-L-HBsAg were amplified by PCR to produce amplicons (682 bp) for Sanger sequencing. Each lane contains 5 µl of amplified S-HBsAg fragments from the indicated plasmids.

Table C1. Ct Values for No reverse transcriptase controls

	Mock			CCAU-saRNA-S-HBsAg			CCAU-saRNA-Luc2			Poly I:C		
	1	**2**	**3**	**1**	**2**	**3**	**1**	**2**	**3**	**1**	**2**	**3**
250 µg	ND	36.39	36.09	35.04	35.12	37.21	36.74	ND	37.58	34.92	37.54	ND
500 µg	36.29	37.90	35.45	ND	36.82	ND	ND	ND	35.09	36.35	ND	ND
1000 µg	ND	ND	ND	ND	35.75	ND	37.04	ND	37.13	ND	ND	ND

ND = Not Detected

CCAU = Cleancap® AU reagent

Table C2. Delta Ct, fold change and statistics for qRT-PCR analysis of mRNAs encoding interferon and interferon-stimulated genes in HEK 293T cells transfected with saRNAs or Poly I:C

Mock Transfections	250 µg		500 µg		1000 µg	
	ΔCt (Mean)	SEM	ΔCt (Mean)	SEM	ΔCt (Mean)	SEM
IFNβ	16.20	0.22	16.00	0.11	18.34	0.33
IFIT	9.22	0.10	9.43	0.03	9.57	0.16
OAS	22.43	0.22	23.42	0.27	22.04	0.28
PKR	7.37	0.11	7.24	0.07	7.23	0.29

CCAU-saRNA-Luc2	250 µg				500 µg				1000 µg			
	ΔCt (Mean)	SEM	Fold change	P-value	ΔCt (Mean)	SEM	Fold change	P-value	ΔCt (Mean)	SEM	Fold change	P-value
IFNβ	16.14	0.08	1.03	0.8072	17.26	0.27	0.43	0.0297	15.84	0.23	5.52	0.0048
IFIT	9.12	0.10	1.06	0.5692	9.24	0.21	1.17	0.4634	8.28	0.29	2.50	0.0296
OAS	21.50	0.14	1.88	0.0323	20.89	0.32	5.83	0.0040	18.35	0.51	13.81	0.0069
PKR	7.20	0.11	1.12	0.3507	7.20	0.19	1.04	0.8639	7.05	0.24	1.12	0.6601

CCAU-saRNA-S-HBsAg	250 µg				500 µg				1000 µg			
	ΔCt (Mean)	SEM	Fold change	P-value	ΔCt (Mean)	SEM	Fold change	P-value	ΔCt (Mean)	SEM	Fold change	P-value
IFNβ	17.70	0.09	0.35	0.0117	15.41	0.17	1.51	0.0501	13.21	0.17	33.88	0.0008
IFIT	9.71	0.07	0.71	0.0204	8.50	0.14	1.93	0.0194	5.45	0.18	17.45	0.00007
OAS	21.26	0.06	2.20	0.0277	17.93	0.28	44.90	0.00014	13.92	0.13	269.96	0.0002
PKR	7.46	0.05	0.93	0.5128	7.00	0.06	1.18	0.0669	6.64	0.11	1.46	0.1694

Poly I:C	250 µg				500 µg				1000 µg			
	ΔCt (Mean)	SEM	Fold change	P-value	ΔCt (Mean)	SEM	Fold change	P-value	ΔCt (Mean)	SEM	Fold change	P-value
IFNβ	16.44	0.08	0.83	0.3946	15.42	0.18	1.50	0.0655	12.69	0.39	51.44	0.0004
IFIT	9.05	0.08	1.12	0.2748	7.69	0.21	3.41	0.0128	4.66	0.35	31.46	0.0015
OAS	21.71	0.37	1.72	0.1907	15.75	0.35	208.63	0.00009	12.81	0.49	647.60	0.0004
PKR	7.05	0.06	1.24	0.0865	6.84	0.18	1.33	0.1468	6.63	0.18	1.48	0.1702

Note: Significant increases in mRNA expression (Fold change relative to mock transfections >1 with P-value < 0.05) are highlighted in yellow.

SEM = Standard error of the mean (n=3)

Table C3. Fluorescence values of RNA standards used to produce standard curve.

Concentration (ng/ul)	Amount (ng)	Replicate 1	Replicate 2	Average	Average - Background
2.5	500	1.42E+04	1.35E+04	1.39E+04	**13716.50**
1	200	6.98E+03	7.08E+03	7.03E+03	**6896.50**
0.5	100	3.39E+03	3.33E+03	3.36E+03	**3226.50**
0.25	50	1.61E+03	1.59E+03	1.60E+03	**1466.50**
0.1	20	6.10E+02	7.58E+02	6.84E+02	**550.50**
0	0	1.35E+02	1.32E+02	1.34E+02	**0.00**

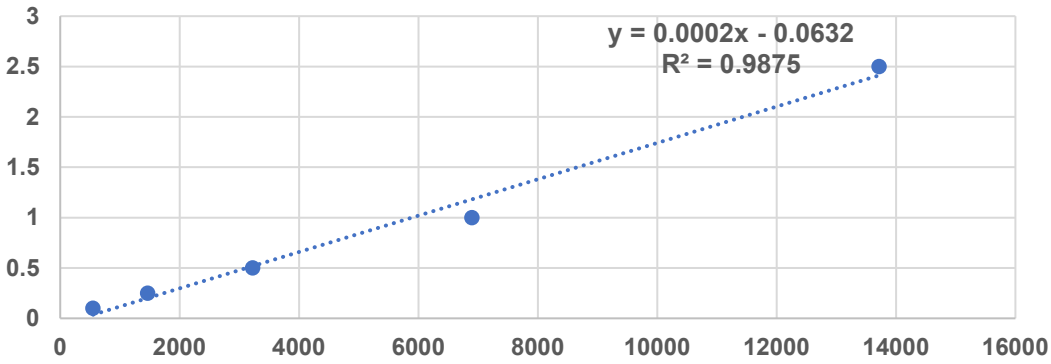

Figure C5. Standard curve used to determine concentration of unbound saRNAs in untreated and 1% Triton X-100 treated lipoplex formulations.

Table C4. Calculation of saRNA-Luc2-CaLiVax complexation efficiency and effective saRNA concentration

	-Triton				+ 1% Triton								
Sample	**Rep 1**	**Rep 2**	**Mean**	**Mean-BG**	**Rep 1**	**Rep 2**	**Mean**	**Mean-BG**	**Sample Added (ul)**	**Dilution Factor**	**Total saRNA Conc (ng/ul)**	**saRNA-liposome Complexation efficiency (%)**	**Effective saRNA conc. (ug/ml)**
CaliVax A	1.44E+02	1.61E+02	1.53E+02	92.50	7.98E+03	7.99E+03	7.99E+03	7797.50	8	125	167.99	98.81	166.00
CaliVax B	1.48E+02	1.47E+02	1.48E+02	87.50	8.30E+03	8.73E+03	8.52E+03	8327.50	8	125	179.95	98.95	178.06
HBS (Background)	5.98E+01	6.02E+01	6.00E+01	0.00	1.73E+02	2.02E+02	1.88E+02	0.00					

Appendix D-Animal ethics certificate

ANIMALS RESEARCH ETHICS COMMITTEE (AREC)

UNIVERSITY OF THE WITWATERSRAND JOHANNESBURG

STRICTLY CONFIDENTIAL

CLEARANCE CERTIFICATE NUMBER: 2021/08/06/C

APPLICANT: Ms N Samudh
School: School of Pathology; Department: N/A; Location: WRAF

PROJECT TITLE: Characterization of the type and breadth of immune responses elicited in Naval Medical Research Institute (NMRI) mice immunized with conventional and self-amplifying mRNA sequences encoding Hepatitis B virus (HBV) antigens
Category: C; Species and Numbers involved: *134X, 3-5 weeks (approximately 20 g), NMRI Female Mouse*

Approval is hereby given for the use of animals for the research project named above and described in the application reviewed by a quorate meeting of the AREC held on 31 Aug 2021. This approval remains valid until 14 Oct 2023 and is conditional to the following (if blank there are no special conditions):

Condition 1	Condition 2	Condition 3	Condition 4

All material changes to the approved research must be reported to the AREC before they are implemented. Failure to do so will invalidate this clearance certificate.

An annual progress report must be provided to the AREC.

The use of these animals is subject to AREC guidelines on the use and care of laboratory animals, is limited to the procedures described in the application and is subject to additional conditions listed below:

I, the Chair of the AREC (or my designated representative) am satisfied that the proposed research is ethical as judged by local law, international standards and University policy.

Signed: _____ _____ Date: __15/10/2021____

(Chairperson of the AREC)

I am satisfied that the persons listed in this application are competent to perform the procedures described in the application, in the context of Section 23 (1) (c) of the veterinary and Para-veterinary Professions Act (19 of 1982).

CC: Student supervisor: «Title1» «Initials1» «Supervisor_surname»
Director Wits Research Animal Facility (WRAF): Dr Kim Jardine

REFERENCES

Babiuk, S., Tsang, C., van Drunen Littel-van den Hurk, S., Babiuk, L.A., Griebel, P.J., 2007. A single HBsAg DNA vaccination in combination with electroporation elicits long-term antibody responses in sheep. Bioelectrochemistry Amst. Neth. 70, 269–274. https://doi.org/10.1016/j.bioelechem.2006.10.003

Beissert, T., Koste, L., Perkovic, M., Walzer, K.C., Erbar, S., Selmi, A., Diken, M., Kreiter, S., Türeci, Ö., Sahin, U., 2017. Improvement of *In Vivo* Expression of Genes Delivered by Self-Amplifying RNA Using Vaccinia Virus Immune Evasion Proteins. Hum. Gene Ther. 28, 1138–1146. https://doi.org/10.1089/hum.2017.121

Blakney, A.K., McKay, P.F., Bouton, C.R., Hu, K., Samnuan, K., Shattock, R.J., 2021. Innate Inhibiting Proteins Enhance Expression and Immunogenicity of Self-Amplifying RNA. Mol. Ther. J. Am. Soc. Gene Ther. 29, 1174–1185. https://doi.org/10.1016/j.ymthe.2020.11.011

Bruss, V., Lu, X., Thomssen, R., Gerlich, W.H., 1994. Post-translational alterations in transmembrane topology of the hepatitis B virus large envelope protein. EMBO J. 13, 2273–2279. https://doi.org/10.1002/j.1460-2075.1994.tb06509.x

Bruss, V., Vieluf, K., 1995. Functions of the internal pre-S domain of the large surface protein in hepatitis B virus particle morphogenesis. J. Virol. 69, 6652–6657. https://doi.org/10.1128/JVI.69.11.6652-6657.1995

Charan, J., Kantharia, N.D., 2013. How to calculate sample size in animal studies? J. Pharmacol. Pharmacother. 4, 303–306. https://doi.org/10.4103/0976-500X.119726

Cheng, K.C., Moss, B., 1987. Selective synthesis and secretion of particles composed of the hepatitis B virus middle surface protein directed by a recombinant vaccinia virus: induction of antibodies to pre-S and S epitopes. J. Virol. 61, 1286–1290. https://doi.org/10.1128/jvi.61.4.1286-1290.1987

Cu, Y., Broderick, K.E., Banerjee, K., Hickman, J., Otten, G., Barnett, S., Kichaev, G., Sardesai, N.Y., Ulmer, J.B., Geall, A., 2013. Enhanced Delivery and Potency of Self-Amplifying mRNA Vaccines by Electroporation in Situ. Vaccines 1, 367–383. https://doi.org/10.3390/vaccines1030367

Dane, D.S., Cameron, C.H., Briggs, M., 1970. VIRUS-LIKE PARTICLES IN SERUM OF PATIENTS WITH AUSTRALIA-ANTIGEN-ASSOCIATED HEPATITIS. The Lancet 295, 695–698. https://doi.org/10.1016/S0140-6736(70)90926-8

Datta, S., Chatterjee, S., Veer, V., Chakravarty, R., 2012. Molecular biology of the hepatitis B virus for clinicians. J. Clin. Exp. Hepatol. 2, 353–365. https://doi.org/10.1016/j.jceh.2012.10.003

De Pooter, D., Van Gulck, E., Chen, A., Evans, C.F., Neefs, J.-M., Horton, H., Boden, D., 2021. A Therapeutic Hepatitis B Virus DNA Vaccine Induces Specific Immune Responses in Mice and Non-Human Primates. Vaccines 9, 969. https://doi.org/10.3390/vaccines9090969

Dobrica, M.-O., Lazar, C., Branza-Nichita, N., 2020. N-Glycosylation and N-Glycan Processing in HBV Biology and Pathogenesis. Cells 9, 1404. https://doi.org/10.3390/cells9061404

Edmunds, W.J., Medley, G.F., Nokes, D.J., Hall, A.J., Whittle, H.C., 1993. The influence of age on the development of the hepatitis B carrier state. Proc. Biol. Sci. 253, 197–201. https://doi.org/10.1098/rspb.1993.0102

Fensterl, V., Sen, G.C., 2015. Interferon-Induced Ifit Proteins: Their Role in Viral Pathogenesis. J. Virol. 89, 2462–2468. https://doi.org/10.1128/JVI.02744-14

Ferrari, C., Cavalli, A., Penna, A., Valli, A., Bertoletti, A., Pedretti, G., Pilli, M., Vitali, P., Neri, T.M., Giuberti, T., Fiaccadori, F., 1992. Fine specificity of the human T-cell response to the hepatitis B virus preS1 antigen. Gastroenterology 103, 255–263. https://doi.org/10.1016/0016-5085(92)91121-J

Ferrari, C., Penna, A., Bertoletti, A., Cavalli, A., Valli, A., Schianchi, C., Fiaccadori, F., 1989. The preS1 antigen of hepatitis B virus is highly immunogenic at the T cell level in man. J. Clin. Invest. 84, 1314–1319. https://doi.org/10.1172/JCI114299

Ferraro, B., Morrow, M.P., Hutnick, N.A., Shin, T.H., Lucke, C.E., Weiner, D.B., 2011. Clinical applications of DNA vaccines: current progress. Clin. Infect. Dis. Off. Publ. Infect. Dis. Soc. Am. 53, 296–302. https://doi.org/10.1093/cid/cir334

Fleeton, M.N., Chen, M., Berglund, P., Rhodes, G., Parker, S.E., Murphy, M., Atkins, G.J., Liljeström, P., 2001. Self-replicative RNA vaccines elicit protection against influenza A virus, respiratory syncytial virus, and a tickborne encephalitis virus. J. Infect. Dis. 183, 1395–1398. https://doi.org/10.1086/319857

Franco, E., Bagnato, B., Marino, M.G., Meleleo, C., Serino, L., Zaratti, L., 2012. Hepatitis B: Epidemiology and prevention in developing countries. World J. Hepatol. 4, 74–80. https://doi.org/10.4254/wjh.v4.i3.74

Gripon, P., Le Seyec, J., Rumin, S., Guguen-Guillouzo, C., 1995. Myristylation of the Hepatitis B Virus Large Surface Protein Is Essential for Viral Infectivity. Virology 213, 292–299. https://doi.org/10.1006/viro.1995.0002

Halperin, S.A., Ward, B., Cooper, C., Predy, G., Diaz-Mitoma, F., Dionne, M., Embree, J., McGeer, A., Zickler, P., Moltz, K.-H., Martz, R., Meyer, I., McNeil, S., Langley, J.M., Martins, E., Heyward, W.L., Martin, J.T., 2012. Comparison of safety and immunogenicity of two doses of investigational hepatitis B virus surface antigen co-administered with an immunostimulatory phosphorothioate oligodeoxyribonucleotide and three doses of a licensed hepatitis B vaccine in healthy adults 18-55 years of age. Vaccine 30, 2556–2563. https://doi.org/10.1016/j.vaccine.2012.01.087

Hassett, K.J., Higgins, J., Woods, A., Levy, B., Xia, Y., Hsiao, C.J., Acosta, E., Almarsson, Ö., Moore, M.J., Brito, L.A., 2021. Impact of lipid nanoparticle size on mRNA vaccine immunogenicity. J. Controlled Release 335, 237–246. https://doi.org/10.1016/j.jconrel.2021.05.021

Heermann, K.H., Goldmann, U., Schwartz, W., Seyffarth, T., Baumgarten, H., Gerlich, W.H., 1984. Large surface proteins of hepatitis B virus containing the pre-s sequence. J. Virol. 52, 396–402. https://doi.org/10.1128/JVI.52.2.396-402.1984

Hennecke, M., Kwissa, M., Metzger, K., Oumard, A., Kröger, A., Schirmbeck, R., Reimann, J., Hauser, H., 2001. Composition and arrangement of genes define the strength of IRES-driven translation in bicistronic mRNAs. Nucleic Acids Res. 29, 3327–3334. https://doi.org/10.1093/nar/29.16.3327

Ho, J.K.-T., Jeevan-Raj, B., Netter, H.-J., 2020. Hepatitis B Virus (HBV) Subviral Particles as Protective Vaccines and Vaccine Platforms. Viruses 12, E126. https://doi.org/10.3390/v12020126

Hyakumura, M., Walsh, R., Thaysen-Andersen, M., Kingston, N.J., La, M., Lu, L., Lovrecz, G., Packer, N.H., Locarnini, S., Netter, H.J., 2015. Modification of Asparagine-Linked Glycan Density for the Design of Hepatitis B Virus Virus-Like Particles with Enhanced Immunogenicity. J. Virol. 89, 11312–11322. https://doi.org/10.1128/JVI.01123-15

Hyde, J.L., Chen, R., Trobaugh, D.W., Diamond, M.S., Weaver, S.C., Klimstra, W.B., Wilusz, J., 2015. The 5′ and 3′ ends of alphavirus RNAs – Non-coding is not non-functional. Virus Res. 206, 99–107. https://doi.org/10.1016/j.virusres.2015.01.016

Jensen, S., Thomsen, A.R., 2012. Sensing of RNA Viruses: a Review of Innate Immune Receptors Involved in Recognizing RNA Virus Invasion. J. Virol. 86, 2900–2910. https://doi.org/10.1128/JVI.05738-11

Kairuz, D., Samudh, N., Ely, A., Arbuthnot, P., Bloom, K., 2022. Advancing mRNA technologies for therapies and vaccines: An African context. Front. Immunol. 13, 1018961. https://doi.org/10.3389/fimmu.2022.1018961

Leitner, W.W., Ying, H., Restifo, N.P., 1999. DNA and RNA-based vaccines: principles, progress and prospects. Vaccine 18, 765–777. https://doi.org/10.1016/s0264-410x(99)00271-6

Leung, J.Y.-S., Ng, M.M.-L., Chu, J.J.H., 2011. Replication of alphaviruses: a review on the entry process of alphaviruses into cells. Adv. Virol. 2011, 249640. https://doi.org/10.1155/2011/249640

Livak, K.J., Schmittgen, T.D., 2001. Analysis of Relative Gene Expression Data Using Real-Time Quantitative PCR and the 2−ΔΔCT Method. Methods 25, 402–408. https://doi.org/10.1006/meth.2001.1262

Lu, X., Mehta, A., Dwek, R., Butters, T., Block, T., 1995. Evidence that N-linked glycosylation is necessary for hepatitis B virus secretion. Virology 213, 660–665. https://doi.org/10.1006/viro.1995.0038

Luft, C., Ketteler, R., 2015. Electroporation Knows No Boundaries: The Use of Electrostimulation for siRNA Delivery in Cells and Tissues. J. Biomol. Screen. 20, 932–942. https://doi.org/10.1177/1087057115579638

Lünsdorf, H., Gurramkonda, C., Adnan, A., Khanna, N., Rinas, U., 2011. Virus-like particle production with yeast: ultrastructural and immunocytochemical insights into Pichia pastoris producing high levels of the hepatitis B surface antigen. Microb. Cell Factories 10, 48. https://doi.org/10.1186/1475-2859-10-48

Luxembourg, A., Hannaman, D., Ellefsen, B., Nakamura, G., Bernard, R., 2006. Enhancement of immune responses to an HBV DNA vaccine by electroporation. Vaccine 24, 4490–4493. https://doi.org/10.1016/j.vaccine.2005.08.014

Maeng, C.-Y., Ryu, C.J., Gripon, P., Guguen-Guillouzo, C., Hong, H.J., 2000. Fine Mapping of Virus-Neutralizing Epitopes on Hepatitis B Virus PreS1. Virology 270, 9–16. https://doi.org/10.1006/viro.2000.0250

Maruggi, G., Mallett, C.P., Westerbeck, J.W., Chen, T., Lofano, G., Friedrich, K., Qu, L., Sun, J.T., McAuliffe, J., Kanitkar, A., Arrildt, K.T., Wang, K.-F., McBee, I., McCoy, D., Terry, R., Rowles, A., Abrahim, M.A., Ringenberg, M.A., Gains, M.J., Spickler, C., Xie, X., Zou, J., Shi, P.-Y., Dutt, T., Henao-Tamayo, M., Ragan, I., Bowen, R.A., Johnson, R., Nuti, S., Luisi, K., Ulmer, J.B., Steff, A.-M., Jalah, R., Bertholet, S., Stokes, A.H., Yu, D., 2022. A self-amplifying mRNA SARS-CoV-2 vaccine candidate induces safe

and robust protective immunity in preclinical models. Mol. Ther. J. Am. Soc. Gene Ther. 30, 1897–1912. https://doi.org/10.1016/j.ymthe.2022.01.001

McAleer, W.J., Buynak, E.B., Maigetter, R.Z., Wampler, D.E., Miller, W.J., Hilleman, M.R., 1984. Human hepatitis B vaccine from recombinant yeast. Nature 307, 178–180. https://doi.org/10.1038/307178a0

McKay, P.F., Hu, K., Blakney, A.K., Samnuan, K., Brown, J.C., Penn, R., Zhou, J., Bouton, C.R., Rogers, P., Polra, K., Lin, P.J.C., Barbosa, C., Tam, Y.K., Barclay, W.S., Shattock, R.J., 2020. Self-amplifying RNA SARS-CoV-2 lipid nanoparticle vaccine candidate induces high neutralizing antibody titers in mice. Nat. Commun. 11, 3523. https://doi.org/10.1038/s41467-020-17409-9

Mencin, N., Štepec, D., Margon, A., Vidič, J., Dolenc, D., Simčič, T., Rotar, S., Sekirnik, R., Štrancar, A., Černigoj, U., 2023. Development and scale-up of oligo-dT monolithic chromatographic column for mRNA capture through understanding of base-pairing interactions. Sep. Purif. Technol. 304, 122320. https://doi.org/10.1016/j.seppur.2022.122320

Milich, D.R., McLachlan, A., Moriarty, A., Thornton, G.B., 1987. A single 10-residue pre-S(1) peptide can prime T cell help for antibody production to multiple epitopes within the pre-S(1), pre-S(2), and S regions of HBsAg. J. Immunol. Baltim. Md 1950 138, 4457–4465.

Mizuguchi, H., Xu, Z., Ishii-Watabe, A., Uchida, E., Hayakawa, T., 2000. IRES-Dependent Second Gene Expression Is Significantly Lower Than Cap-Dependent First Gene Expression in a Bicistronic Vector. Mol. Ther. 1, 376–382. https://doi.org/10.1006/mthe.2000.0050

Nayagam, S., Thursz, M., 2019. Strategies for Global Elimination of Chronic HBV Infection: 2019 Update. Curr. Hepatol. Rep. 18, 300–309. https://doi.org/10.1007/s11901-019-00478-w

Palmer, C.D., Scallan, C.D., Kraemer Tardif, L.D., Kachura, M.A., Rappaport, A.R., Koralek, D.O., Uriel, A., Gitlin, L., Klein, J., Davis, M.J., Venkatraman, H., Hart, M.G., Jaroslavsky, J.R., Kounlavouth, S., Marrali, M., Nganje, C.N., Bae, K., Yan, T., Leodones, K., Egorova, M., Hong, S.-J., Kuan, J., Grappi, S., Garbes, P., Jooss, K., Ustianowski, A., 2023. GRT-R910: a self-amplifying mRNA SARS-CoV-2 vaccine boosts immunity for ≥6 months in previously-vaccinated older adults. Nat. Commun. 14, 3274. https://doi.org/10.1038/s41467-023-39053-9

Passmore, L.A., Coller, J., 2022. Roles of mRNA poly(A) tails in regulation of eukaryotic gene expression. Nat. Rev. Mol. Cell Biol. 23, 93–106. https://doi.org/10.1038/s41580-021-00417-y

Patient, R., Hourioux, C., Sizaret, P.-Y., Trassard, S., Sureau, C., Roingeard, P., 2007. Hepatitis B virus subviral envelope particle morphogenesis and intracellular trafficking. J. Virol. 81, 3842–3851. https://doi.org/10.1128/JVI.02741-06

Persing, D.H., Varmus, H.E., Ganem, D., 1987. The preS1 protein of hepatitis B virus is acylated at its amino terminus with myristic acid. J. Virol. 61, 1672–1677. https://doi.org/10.1128/jvi.61.5.1672-1677.1987

Probst, J., Brechtel, S., Scheel, B., Hoerr, I., Jung, G., Rammensee, H.-G., Pascolo, S., 2006. Characterization of the ribonuclease activity on the skin surface. Genet. Vaccines Ther. 4, 4. https://doi.org/10.1186/1479-0556-4-4

Ramanathan, A., Robb, G.B., Chan, S.-H., 2016. mRNA capping: biological functions and applications. Nucleic Acids Res. 44, 7511–7526. https://doi.org/10.1093/nar/gkw551

Roukens, A.H., Visser, L.G., 2011. Hepatitis B vaccination strategy in vaccine low and non-responders: a matter of quantity of quality? Hum. Vaccin. 7, 654–657. https://doi.org/10.4161/hv.7.6.14986

Rydell, G.E., Prakash, K., Norder, H., Lindh, M., 2017. Hepatitis B surface antigen on subviral particles reduces the neutralizing effect of anti-HBs antibodies on hepatitis B viral particles in vitro. Virology 509, 67–70. https://doi.org/10.1016/j.virol.2017.05.017

Sadler, A.J., Williams, B.R.G., 2008. Interferon-inducible antiviral effectors. Nat. Rev. Immunol. 8, 559–568. https://doi.org/10.1038/nri2314

Samnuan, K., Blakney, A.K., McKay, P.F., Shattock, R.J., 2022. Design-of-experiments in vitro transcription yield optimization of self-amplifying RNA. F1000Research 11, 333. https://doi.org/10.12688/f1000research.75677.1

Schenborn, E.T., Mierendorf, R.C., 1985. A novel transcription property of SP6 and T7 RNA polymerases: dependence on template structure. Nucleic Acids Res. 13, 6223–6236. https://doi.org/10.1093/nar/13.17.6223

Schneider, W.M., Chevillotte, M.D., Rice, C.M., 2014. Interferon-stimulated genes: a complex web of host defenses. Annu. Rev. Immunol. 32, 513–545. https://doi.org/10.1146/annurev-immunol-032713-120231

Sercombe, L., Veerati, T., Moheimani, F., Wu, S.Y., Sood, A.K., Hua, S., 2015. Advances and Challenges of Liposome Assisted Drug Delivery. Front. Pharmacol. 6. https://doi.org/10.3389/fphar.2015.00286

Shapira, M.Y., Zeira, E., Adler, R., Shouval, D., 2001. Rapid seroprotection against hepatitis B following the first dose of a Pre-S1/Pre-S2/S vaccine. J. Hepatol. 34, 123–127. https://doi.org/10.1016/s0168-8278(00)00082-9

Shouval, D., 2003. Hepatitis B vaccines. J. Hepatol. 39 Suppl 1, S70-76. https://doi.org/10.1016/s0168-8278(03)00152-1

Shouval, D., Ilan, Y., Adler, R., Deepen, R., Panet, A., Even-Chen, Z., Gorecki, M., Gerlich, W.H., 1994. Improved immunogenicity in mice of a mammalian cell-derived recombinant hepatitis B vaccine containing pre-S1 and pre-S2 antigens as compared with conventional yeast-derived vaccines. Vaccine 12, 1453–1459. https://doi.org/10.1016/0264-410x(94)90155-4

Shouval, D., Roggendorf, H., Roggendorf, M., 2015. Enhanced immune response to hepatitis B vaccination through immunization with a Pre-S1/Pre-S2/S vaccine. Med. Microbiol. Immunol. (Berl.) 204, 57–68. https://doi.org/10.1007/s00430-014-0374-x

Smedile, A., Dentico, P., Zanetti, A., Sagnelli, E., Nordenfelt, E., Actis, G.C., Rizzetto, M., 1981. Infection with the delta agent in chronic HBsAg carriers. Gastroenterology 81, 992–997.

Smith, G.L., Benfield, C.T.O., Maluquer de Motes, C., Mazzon, M., Ember, S.W.J., Ferguson, B.J., Sumner, R.P., 2013. Vaccinia virus immune evasion: mechanisms, virulence and immunogenicity. J. Gen. Virol. 94, 2367–2392. https://doi.org/10.1099/vir.0.055921-0

Stephenne, J., 1990. Development and production aspects of a recombinant yeast-derived hepatitis B vaccine. Vaccine 8 Suppl, S69-73; discussion S79-80. https://doi.org/10.1016/0264-410x(90)90221-7

Suffner, S., Gerstenberg, N., Patra, M., Ruibal, P., Orabi, A., Schindler, M., Bruss, V., 2018. Domains of the Hepatitis B Virus Small Surface Protein S Mediating Oligomerization. J. Virol. 92, e02232-17. https://doi.org/10.1128/JVI.02232-17

Sureau, C., Salisse, J., 2013. A conformational heparan sulfate binding site essential to infectivity overlaps with the conserved hepatitis B virus A-determinant. Hepatology 57, 985–994. https://doi.org/10.1002/hep.26125

Svetlov, V., Nudler, E., 2013. Basic mechanism of transcription by RNA polymerase II. Biochim. Biophys. Acta 1829, 20–28. https://doi.org/10.1016/j.bbagrm.2012.08.009

Tenchov, R., Bird, R., Curtze, A.E., Zhou, Q., 2021. Lipid Nanoparticles─From Liposomes to mRNA Vaccine Delivery, a Landscape of Research Diversity and Advancement. ACS Nano 15, 16982–17015. https://doi.org/10.1021/acsnano.1c04996

Vogel, A.B., Lambert, L., Kinnear, E., Busse, D., Erbar, S., Reuter, K.C., Wicke, L., Perkovic, M., Beissert, T., Haas, H., Reece, S.T., Sahin, U., Tregoning, J.S., 2018. Self-Amplifying RNA Vaccines Give Equivalent Protection against Influenza to mRNA Vaccines but at Much Lower Doses. Mol. Ther. 26, 446–455. https://doi.org/10.1016/j.ymthe.2017.11.017

Walayat, S., Ahmed, Z., Martin, D., Puli, S., Cashman, M., Dhillon, S., 2015. Recent advances in vaccination of non-responders to standard dose hepatitis B virus vaccine. World J. Hepatol. 7, 2503–2509. https://doi.org/10.4254/wjh.v7.i24.2503

Werr, M., Prange, R., 1998. Role for calnexin and N-linked glycosylation in the assembly and secretion of hepatitis B virus middle envelope protein particles. J. Virol. 72, 778–782. https://doi.org/10.1128/JVI.72.1.778-782.1998

World Health Organisation, 2017. Global Hepatitis Programme, 2017. Global hepatitis report, 2017.

World Health Organisation, 2021. Global progress report on HIV, viral hepatitis and sexually transmitted infections, 2021.

Wounderlich, G., Bruss, V., 1996. Characterization of early hepatitis B virus surface protein oligomers. Arch. Virol. 141, 1191–1205. https://doi.org/10.1007/BF01718824

Wu, M.Z., Asahara, H., Tzertzinis, G., Roy, B., 2020. Synthesis of low immunogenicity RNA with high-temperature in vitro transcription. RNA N. Y. N 26, 345–360. https://doi.org/10.1261/rna.073858.119

Wu, Y., Zhang, H., Meng, L., Li, F., Yu, C., 2022. Comparison of Immune Responses Elicited by SARS-CoV-2 mRNA and Recombinant Protein Vaccine Candidates. Front. Immunol. 13, 906457. https://doi.org/10.3389/fimmu.2022.906457

Xu, Z., Bruss, V., Yen, T.S., 1997. Formation of intracellular particles by hepatitis B virus large surface protein. J. Virol. 71, 5487–5494. https://doi.org/10.1128/JVI.71.7.5487-5494.1997

Yan, H., Zhong, G., Xu, G., He, W., Jing, Z., Gao, Z., Huang, Y., Qi, Y., Peng, B., Wang, H., Fu, L., Song, M., Chen, P., Gao, W., Ren, B., Sun, Y., Cai, T., Feng, X., Sui, J., Li, W., 2012. Sodium taurocholate cotransporting polypeptide is a functional receptor for human hepatitis B and D virus. eLife 1, e00049. https://doi.org/10.7554/eLife.00049

Yato, K., Onodera, T., Matsuda, M., Moriyama, S., Fujimoto, A., Watashi, K., Aizaki, H., Tanaka, T., Moriishi, K., Nishitsuji, H., Shimotohno, K., Tamura, K., Takahashi, Y., Wakita, T., Muramatsu, M., Kato, T., Suzuki, R., 2021. Identification of Two Critical

Neutralizing Epitopes in the Receptor Binding Domain of Hepatitis B Virus preS1. J. Virol. 95, e01680-20, JVI.01680-20. https://doi.org/10.1128/JVI.01680-20

Yoshioka, N., Gros, E., Li, H.-R., Kumar, S., Deacon, D.C., Maron, C., Muotri, A.R., Chi, N.C., Fu, X.-D., Yu, B.D., Dowdy, S.F., 2013. Efficient Generation of Human iPSCs by a Synthetic Self-Replicative RNA. Cell Stem Cell 13, 246–254. https://doi.org/10.1016/j.stem.2013.06.001

Zoulim, F., Durantel, D., 2015. Antiviral Therapies and Prospects for a Cure of Chronic Hepatitis B. Cold Spring Harb. Perspect. Med. 5, a021501–a021501. https://doi.org/10.1101/cshperspect.a021501